UNIVERSITÀ DEGLI STUDI DI NAPOLI

"FEDERICO II"

Dottorato di ricerca in Biologia

XXX CICLO

Study of thermophilic enzymes for biotechnological applications

Dottoranda

Dott. Francesca Anna Fusco

Relatore

Prof. Danila Limauro

Coordinatore del Dottorato

Prof. Salvatore Cozzolino

Anno Accademico 2016-2017

CONTENTS

Riassunto **p.1**

Chapter 1. Introduction **p.6**

1.1 (Hyper)Thermophiles **p.7**

1.2 Biotechnological application of thermozymes **p.8**

1.2.1 Degradation of lignocellulosic biomass **p.10**

1.2.1.1 Biomass composition **p.10**

1.2.1.2 Enzyme involved in biomass degradation **p.13**

1.2.1.3 *Dictyoglomus turgidum* as source of thermophilic Carbohydrate-Active Enzymes **p.16**

1.2.2 Antioxidant enzymes and oxidative stress **p.16**

1.2.2.1 *Sulfolobus solfataricus* as source of robust peroxiredoxins **p.17**

1.3 Aim of the work **p.18**

Chapter 2. Glycoside hydrolases from thermophilic microorganisms **p.24**

2.1 Biochemical characterization of a thermostable endomannanase/endoglucanase from *Dictyoglomus turgidum* **p.26**

2.2 Biochemical characterization of a thermostable β-glucosidase from *D. turgidum* **p.37**

2.3 A synergistic action of a thermophilic α-galactosidase and β-mannanase on galactomannan substrates **p.51**

Chapter 3. Protein-spore system to deliver biological drugs to the human intestinal mucosa **p.62**

3.1 Display of the peroxiredoxin Bcp1 of *Sulfolobus solfataricus* on probiotic spores of *Bacillus megaterium* **p.64**

Chapter 4. General conclusions **p.82**

Appendix I. List of communications and publications **p.85**

Appendix II. Experience in foreign laboratory **p.86**

Qualunque cosa tu possa fare o
sognare di fare, incominciala!
L'audacia ha in sé genio,
potere e magia
Goethe

To my Angel…

Riassunto

I microrganismi termofili/ipertermofili, che vivono a temperature comprese tra 40°C - 120°C, sono stati isolati da una moltitudine di ambienti diversi come aree vulcaniche, fumarole, geyser e sorgenti termali (1). L'interesse biotecnologico per questi microrganismi è focalizzato principalmente sui loro enzimi che esplicano l'attività catalitica ad elevate temperature, mostrano una notevole termoresistenza e sono generalmente in grado di resistere a condizioni estreme di pH, denaturanti e solventi organici; caratteristiche che li rendono particolarmente interessanti rispetto alle controparti mesofile. Nell'era del *bioprospecting*, (ricerca di nuove fonti biologiche per scopi applicativi e commerciali) (2), gli enzimi termofili rappresentano dunque, una fonte interessante per future applicazioni in diversi settori come quello alimentare, farmaceutico, della carta, dei pellami, della detergenza, ma soprattutto nella "green energy" e quindi nelle bioraffinerie (3).

Alla luce di queste considerazioni, il mio studio si è focalizzato sulla caratterizzazione di enzimi da microrganismi ipertermofili, che potrebbero essere utilizzati in due diversi campi: quello della *green energy* mediante degradazione della biomassa e quello farmacologico, mediante l'utilizzo di nuovi sistemi di *drug delivery*. Nel **1**° caso sono stati selezionati, dopo analisi bioinformatica, enzimi appartenenti alla classe delle glicosil idrolasi (GHs), dal microrganismo ipertermofilo *Dictyoglomus turgidum*, che potrebbero essere utilizzati nella degradazione della biomassa; nel **2**° caso si è studiato un nuovo un sistema di *drug delivery* "proteina-spora" in cui l'enzima adsorbito è una perossiredossina di *Sulfolobus solfataricus*, un enzima antiossidante, che potrebbe trovare applicazione nelle patologie infiammatorie gastro-intestinali.

1. Identificazione e caratterizzazione di glicosil idrolasi termofile per la degradazione della biomassa

La biomassa lignocellulosica è costituita principalmente da cellulosa, emicellulosa, lignina e pectina, i cui rapporti possono variare in funzione della tipologia o natura della biomassa. La cellulosa è un polimero lineare costituito da unità di D-glucosio legate tra loro da legami β-1,4 glicosidici; l'emicellulosa è un gruppo di polisaccaridi ramificati di varia struttura, i monomeri della catena principale sono rappresentati da esosi (glucosio, mannosio e galattosio) e pentosi (arabinosio e xilosio) policondensati mediante legami β-1,4. L'emicellulosa predominante in molte pareti cellulari è lo xiloglucano; altre emicellulose sono il glucuronoxilano, l'arabinoxilano, il glucomannano e il galattomannano. La lignina è una molecola complessa, formata da molte unità fenoliche differenti come l'alcool coniferilico, l'alcol cumarinico e l'alcol sinapilico. La pectina è un polisaccaride che contribuisce largamente alla formazione dei tessuti, specialmente dei frutti e delle parti vegetali eduli; esso è costituito da residui di acido D-galatturonico legati mediante legami α-1,4-glicosidici, intervallato da residui di L-ramnosio. La degradazione della biomassa

lignocellulosica è soggetta ad idrolisi enzimatica da parte di differenti classi di enzimi quali: **cellulasi** (endoglucanasi [EC 3.2.1.4], esoglucanasi [EC 3.2.1.91] e β-1,4 glucosidasi [EC 3.2.1.21]), **emicellulasi** (xilanasi [EC 3.2.1.8.], mannanasi [EC 3.2.1.78], arabinasi [EC 3.2.1.99] e galatturonasi [EC 3.2.1.15]), **perossidasi** [EC 1.11.1], **laccasi** [EC 1.10.3.2], **pectinasi** (polimetilgalatturonasi e **poligalatturonasi** [EC 3.2.1.15]), **pectinesterasi** [EC 3.1.1.11] e **pectin liasi** [EC 4.2.2.10].

L'utilizzo di glicosil idrolasi che siano in grado di lavorare in condizioni estreme di pH, temperatura e solventi organici tipici delle bioraffinerie è un punto chiave nella conversione della biomassa, pertanto l'identificazione di nuovi biocatalizzatori ad elevate performance è un campo in continua esplorazione.

La metagenomica o l'analisi bioinformatica possono essere due strategie da utilizzare per l'identificazione di nuovi enzimi. In questo progetto di dottorato l'approccio bioinformatico è stato utilizzato per l'identificazione di nuove putative GHs; in particolare è stata consultata la banca dati CAZy (www.cazy.org) che raccoglie famiglie di enzimi che degradano, modificano o formano legami glicosidici. Sono quindi stati selezionati dal genoma di *Dictyoglomus turgidum*, microrganismo anaerobio ipertermofilo, due geni Dtur_0671 (*DturCelB*) e Dtur_0462 (*Dtur*β*Glu*) che codificano putative GHs appartenenti alle famiglie GH5 e GH1 rispettivamente.

Attraverso produzione dei rispettivi geni sintetici e successivo clonaggio in vettori di espressione pET-30b(+) i due enzimi sono stati prodotti in maniera ricombinante in *E.coli* e successivamente biochimicamente caratterizzati. *Dtur*CelB, analizzata mediante cromatografia ad esclusione molecolare accoppiata al *light scattering*, è risultata essere una proteina monomerica dal peso molecolare di circa 43 kDa. L'attività idrolitica di *Dtur*CelB, verso differenti polimeri quali mannani, carbossimetilcellulosa (CMC) e lichenano, è stata determinata mediante saggio su piastra (*Congo red plate assay*) e successivamente mediante saggio degli zuccheri riducenti (*Nelson-Somogyi (NS) method*). I risultati mostrano che *Dt*urCelB ha più alta attività specifica verso il glucomannano seguita da galattomannani, dalla CMC e dal lichenano. L'ulteriore caratterizzazione di *Dt*urCelB ha mostrato che l'enzima ha valori ottimali di pH e temperatura di 5.4 e 70°C rispettivamente, e possiede una buona resistenza alla temperatura (50% di attività dopo 2 h a 70°C) e al pH (70% di attività a pH 4 e 90% nel range di pH 5-8 dopo 1 ora di incubazione). Saggi condotti in presenza di diversi agenti chimici hanno mostrato che l'attività enzimatica di *Dt*urCelB è moderatamente ridotta in presenza di metalli (~60%) e dei detergenti non ionici Tween-20 e Triton X- 100, mentre è quasi del tutto inibita dall'SDS e all'aumentare della concentrazione salina, infine l'attività enzimatica resta invariata in presenza di EDTA indicando che la proteina non è un metallo enzima.

*Dt*urβGlu, espressa e purificata mediante His-trap, è stata analizzata mediante cromatografia ad esclusione molecolare e risulta essere un tetramero di circa 200 kDa. Saggi condotti su diversi substrati hanno evidenziato che l'enzima ha attività β-glucosidasica, (mostrando la maggiore attività specifica vero il il *p*-Nitrophenyl β-D-glucopyranoside (*p*NPGlu)), ma presenta anche un'ottima attività galattosidasica e xilosidasica ed è inoltre in grado di idrolizzare substrati naturali come la salicina. *Dt*urβGlu presenta un optimum di attività enzimatica a pH 5.4 ed a 80°C, ed ha una buona stabilità a diversi valori di pH (90% di attività nel range di pH 5-8 dopo 1 ora di incubazione), di temperatura (90% di attività dopo 90 min a 70°C) ed in presenza di diversi agenti chimici; infatti i risultati hanno mostrato che l'attività enzimatica resta invariata in presenza di EDTA e LiCl mentre è moderatamente ridotta in presenza di altri metalli analizzati come $CaCl_2$ e $MgCl_2$; contrariamente in presenza dei detergenti non ionici Tween-20 e Triton X-100 l'attività relativa risulta essere addirittura aumentata (~150%), mentre è di circa il 60% in presenza di DMSO e del tutto inibita in presenza di SDS.

1.2 Studi di sinergia tra *Dtur*CelB ed un'α-galattosidasi (*Tt*GalA) di *Thermus thermophilus* su substrati di emicellulosa

Al fine di mettere a punto un cocktail di enzimi da poter utilizzare nella conversione della biomassa, è stato studiato l'effetto sinergico dell'endomannanasi *Dtur*CelB di *Dictyoglomus turgidum* e di un'α-galattosidasi, *Tt*GalA, di *Thermus thermophilus* (4), su diversi galattomannani (*Carob, Guar e Locust bean gum*) che differiscono tra loro per la frequenza dei residui di galattosio legati alla catena principale di unità di mannosio.

Per valutare l'effetto sinergico, i due enzimi sono stati saggiati (mediante saggio degli zuccheri riducenti) contemporaneamente (saggio simultaneo) o in successione (saggio sequenziale) ad 80°C, che rappresenta la media delle temperature ottimali dei due enzimi (70°C per *Dtur*CelB e 90°C *Tt*GalA). I risultati hanno mostrato che i due enzimi operano in maniera sinergica in entrambe le condizioni su tutti i substrati testati; in particolare il più alto grado di sinergia (1.8) è stato ottenuto su *Locust bean gum* con un rapporto *Dtur*CelB:*Tt*GalA di 25:75. Inoltre l'analisi sequenziale ha evidenziato che il maggior grado di sinergia si ottiene quando l'attività α-galattosidasica precede quella endo-mannanasica suggerendo che la rimozione preliminare dei residui di galattosio dal polimero determina una maggiore esposizione dei siti di idrolisi per la successiva azione di *Dtur*CelB.

2. Nuovi sistemi di *drug delivery* costituiti dall'associazione "proteine -spora"

L'uso di spore batteriche come sistema di somministrazione di molecole attive è diventata una strategia sempre più utilizzata in ambito biotecnologico, grazie alla documentata resistenza e sicurezza delle spore. Recentemente, alcuni studi hanno proposto un approccio non ricombinante, basato sull'adsorbimento spontaneo tra spore e proteine eterologhe. Le spore maggiormente utilizzate per questo scopo appartengono alla specie di *Bacillus subtilis* (5), ma studi recenti mostrano un possibile utilizzo anche delle spore di *B. megaterium* (6).

Questi presupposti hanno guidato la seconda parte del progetto di dottorato che è stata focalizzata sullo studio di un possibile sistema di *drug delivery* nella mucosa intestinale umana, costituito da una perossiredossina (Prx) termofila di *Sulfolobus solfataricus,* la Bacterioferritin Comigratory Protein (Bcp1), in associazione con spore di *B. megaterium*.

Le Prxs, sono enzimi ubiquitari identificati in ogni dominio degli organismi viventi che esplicano il loro ruolo antiossidante nelle cellule attraverso la riduzione di perossidi organici ed inorganici (7). Mentre il ruolo di tali enzimi nei procarioti è confinato a quello di antiossidanti, negli organismi eucarioti, le Prxs svolgono anche altri ruoli come quello di chaperon molecolari e nel signaling cellulare (8). Le Prxs procariotiche rispetto a quelle eucariotiche mancano di due motivi strutturali (motivo GGLG e motivo YF) (9) che le rendono meno sensibili all'iperossidazione dei residui catalitici di cisteina coinvolti nella riduzione dei perossidi. Tale caratteristica di maggiore resistenza all'iperossidazione può quindi dimostrarsi vantaggiosa in ambito biotecnologico; per tale motivo è stato deciso di utilizzare come proteina da adsorbire su spore di *B. megaterium*, Bcp1 di *S. solfataricus,* che in recenti studi è risultata essere in grado di proteggere i cardiomioblasti dallo stress ossidativo e quindi di poter agire anche in condizioni fisiologiche ben diverse da quelle endogene (10).

Bcp1 ricombinante è stata espressa in *E. coli*, purificata e successivamente adsorbita, mediante un protocollo di *binding*, a spore del ceppo QM B155 di *B. megaterium*. Esperimenti di western blotting hanno confermato la capacità di Bcp1 di legare le spore (soprattutto a livello dell'esosporio) mentre saggi di attività perossidasica mostrano che Bcp1 conserva la sua attività antiossidante una volta adsorbita. Avendo come obiettivo quello di mettere a punto un sistema di *drug delivery* per la cura di malattie della mucosa intestinale umana (es. Morbo di Chron, colite ulcerosa), causate anche da un'eccessiva produzione di ROS, è stata verificata l'attività di Bcp1 libera e legata a spore di *B. megaterium* in condizioni simulanti il tratto gastro intestinale.

L'enzima libero e adsorbito alle spore è stato testato sia dopo 1 h di incubazione a differenti pH (tipici del tratto gastro-intestinale) che dopo incubazione in presenza di *simulated gastric fluid* (SGF) o *simulated intestinal fluid* (SIF). I risultati hanno mostrato che in tutte le condizioni di pH analizzate, l'attività di Bcp1 adsorbita alle spore è superiore a quella di Bcp1 libera; analogamente

dopo incubazione con SGF e SIF, Bcp1 adsorbita alle spore mostra una maggiore attività rispetto alla Bcp1 libera (40% e 60 % di inibizione in SGF e SIF rispettivamente) confermando quindi, il ruolo protettivo della spora nei confronti di Bcp1.

Bibliografia

1. Demain AL. (2009) **Biosolutions to the energy problem**. *J Ind Microbiol Biotechnol* 36:319-332.

2. Acharya S. et al. (2012) **Bioprospecting thermophiles for cellulase production: a review.** *Braz J Microbiol* 43(3): 844-856.

3. Simmons BA. et al. (2008) **Next-generation biomass feedstocks for biofuel production.** *Genome Biology* 9(12):242.

4. Aulitto M. et al. (2017) ***Thermus thermophilus*** **as source of thermozymes for biotechnological applications: homologous expression and biochemical characterization of an α-galactosidase.** *Microbial cell factories* 13:16-28.

5. Sirec T. et al. (2012) **Adsorption of β-galactosidase of *Alicyclobacillus acidocaldarius* on wild type and mutants spores of *Bacillus subtilis*.** *Microbial cell factories* 3:11-100.

6. Lanzilli M. et al. (2016) **The Exosporium of *Bacillus megaterium* QM B1551 is permeable to the Red Fluorescence Protein of the Coral *Discosoma sp*.** *Frontiers in Microbiology* 7:1752.

7. Limauro D. et al. (2006) **Identification and characterization of 1-Cys peroxiredoxin from *Sulfolobus solfataricus* and its involvement in the response to oxidative stress.** *FEBS J.* 273(4):721-731.

8. Declercq J.P. et al. (2001) **Crystal structure of human peroxiredoxin 5, a novel type of mammalian peroxiredoxin at 1.5 angstrom resolution.** *J. Mol. Biol.* 311:751–759.

9. Pascual MB et al. (2010) **Overoxidation of 2-Cys peroxiredoxin in prokaryotes: cyanobacterial 2-Cys peroxiredoxins sensitive to oxidative stress.** *J Biol Chem.* 285(45):34485-92.

10. Sarcinelli C. et al. (2016) **Discovering Antioxidant Molecules in the Archaea Domain: Peroxiredoxin Bcp1 from *Sulfolobus solfataricus* Protects H9c2 Cardiomyoblasts from Oxidative Stress.** *Archea* 2016:7424870.

Chapter 1

Introduction

1.1 (Hyper)Thermophiles

Extremely hot terrestrial and marine environments are hostile for most living organisms on earth, but these niches represent excellent settings to be inhabited by specialized microorganisms. Thermophiles and hyperthermophiles are defined as microorganisms that not only survive but thrive at high temperatures (1). The first can be found in environments with temperatures over 40°C and the second in environments over 80°C. The first thermophilic microorganisms were isolated in the 1960s by Thomas Brock in the hydrothermal springs of the Yellowstone National Park (2). To date, the highest temperatures known to sustain thermophilic microbial life are 113°C for the chemolithoautotrophic archaeon *Pyrolobus fumarii* (3) and 122°C for the methanogenic hyperthermophile *Methanopyrus kandleri* (4). The ubiquitous nature of the thermophiles is attested by the great variety of sources from which they have been isolated like volcanic area, hot springs, mud pots, fumaroles, geysers, coastal thermal springs, and even deep-sea hydrothermal vents. They are also found in man-made environments, such as heated compost facilities, reactors, and spray dryers. Most thermophilic prokaryotes are classified in the archaeal domain, but several microorganisms, are identified in the bacterial domain (5,6).

Several mechanisms are thought to underlie the adaptation of the thermophiles to their extraordinary growth temperature. There is no simple correlation between the optimal growth temperature (OGT) and genomic features because thermophilicity results from a combination of factors. For example, the high GC genome content is not a good indicator of thermophilicity (7) *e.g Aquifex aeolicus* has a low GC content of 43.4% (8), despite its high OGT of 95 °C.

Actually, several genomic footprints of thermophilic adaptation have been highlighted, in particular the G + C content of helical regions in rRNA secondary structures and small genome size seem to be correlated with the adaptation to higher temperature (9); in fact, thermophiles show less intergenic DNA and slightly shorter genes respect to mesophilic bacteria. Based on comparisons of 1553 prokaryotes, cells that grow below 45 °C have genomes larger than 6 Mbp, while the average genome length is less than 4 Mbp for thermophiles (9).

The second main strategy that thermophiles have adopted for life at high temperatures is about their proteins (10,11), for example the shorter amino acid lengths may reflect the importance of a reduced number of flexible regions in the native protein structures and the frequency of specific aminoacids and nucleotides can be correlate with OTG. In fact, based on 204 complete proteomes of bacteria and archaea, the amino acids Ile, Val, Tyr, Trp, Arg, Glu, and Leu have been found to be correlated with OGT (12). In this genomic era, most scientists search for insights into thermophilicity using the complete annotated genome. It is well established the importance of ORFs encode heat shock proteins (HSPs) (13), chaperones, chaperonins that assist the folding of macromolecules; such as the main role of agmatine (thought to stabilize DNA and RNA),

spermidines (polyamines from ribosomes that maintain membrane potentials), polyamines (needed for growth, possibly as membrane stabilizers), α- and β-subunit prefoldins (protein folding chaperons), SOS regulons (DNA damage responses) and reverse gyrase (a heat-protective DNA chaperone) that is believed to play an important role in genome thermostability (14).

Furthermore, thermophiles also use compatible solutes to stabilize cell components (15-17); negatively charged compatible solutes like mannosylglycerate, di-myo-inositol-phosphate and diglycerol phosphate are identified in hyperthermophilic bacteria and archaea and almost exclusively restricted to them (18).

Previous works suggested that horizontal gene transfer (HGT) is an important process for adaptation of thermophiles. For example, the complete set of genes encoding the flagellar system of *Thermomicrobium roseum* found unusually in the megaplasmid could be the result of HGT. Furthermore, HGT could occur between domains (i.e. hyperthermophilic Bacteria and hyperthermophilic Archaea) or between close genera (i.e. *Thermotoga* and *Aquifex; Anoxybacillus* and *Geobacillus* (19)), as part of survival mechanism under harsh conditions (20).

Finally, complex lipid arrangement and/or type in the cell membrane are known to affect thermostability of microorganisms. Archaeal membranes are heat resistant because of their composition in ether lipids that do not require a regulatory mechanism to adapt lipids to changes in the environmental temperature; on the other side the bacteria have elaborate mechanisms by which they regulate the fatty acid composition at temperatures just above the phase transition temperature (21).

In conclusion these microorganisms are a good source of thermozymes, unique biocatalysts, that work under harsh conditions compared to mesophilic counterparts and represent a great promise in terms of their applications in modern biotechnology.

1.2 Biotechnological application of thermozymes

A great deal of attention is focused on enzymes from hyperthermophiles that have gained always more importance in biotechnological processes. In 1914, the first enzymatic preparation for a commercial application was developed by Otto Rohm. He purified trypsin from animal pancreas and added it to washing detergents to degrade proteins. But only in 1960, enzyme catalysis became an industrial choice with the mass production of proteases from *Bacillus* spp. for use in washing powders and now industrial enzymes have since evolved into a multibillion dollar global market (22). Currently there is a great demand for suitable enzymatic biocatalysts that have high process performances and are ‘greener’ alternatives to chemical synthesis (23-25). It was expected that up to 40% of bulk chemical synthesis processes, that now require environmentally damaging bulk organic solvents and elevated energy inputs, could use enzymatic catalysis by 2030 (26,27).

However, because we have already surpassed the maximum rate of oil extraction (‘peak oil’), we should look for sustainable sources of non-fossil fuel, in the same time we should seek alternative ‘greener’ building blocks for synthesis of biopolymers and biomaterials (28).

Nowadays, the turnover of about USD 5 billion is produced by the application of enzymes in different markets (27), and the World Enzymes to 2017 Report in http://www.rnrmarketresearch.com/world-enzymes-to-2017-market-report.html), and the world enzyme demand is forecasted to rise from USD 6.4 to 6.9 billion p.a. in the future. Accordingly, the demand for biocatalysts in the form of free or immobilized enzymes, whole cell catalysts or cell-free systems, with a high applicability potential in industry is increasing (29, 30).

From an industrial viewpoint, as the vast majority of current processes are performed under harsh conditions, (hyper)thermophilic enzymes possess several advantages: (i) once expressed in mesophilic hosts, thermophilic and hyperthermophilic enzymes are easier to purify by heat treatment, (ii) their thermostability is associated with a higher resistance to chemical denaturants (such as a solvent or guanidinium hydrochloride), and (iii) performing enzymatic reactions at high temperatures allows higher substrate concentrations, lower viscosity, fewer risks of microbial contaminations, and often higher reaction rates. In this context, thermostable enzymes represent the cornerstone for the development of environmentally friendly, efficient, cost-effective and sustainable industrial technologies, and nowadays they are applied in different industrial areas, such as food and beverage, medicine, animal feed, detergents, pulp and paper, leather, textile markets, drugs and in particular in the biorefinery (31). In Fig. 1 are summarized some applications of thermophilic enzymes in different fields.

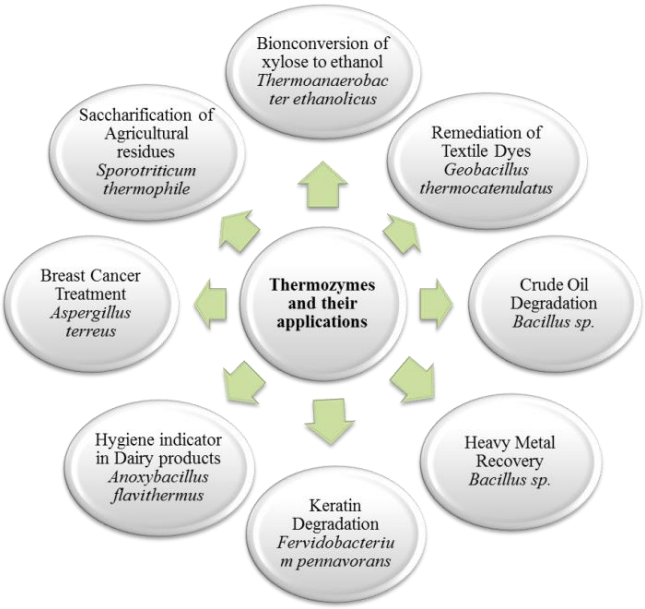

Fig. 1 Applications of enzymes from thermophiles

This PhD-thesis was focused mainly on the study of some thermophilic enzymes for two different types of biotechnological applications. The first concerns the utilization of different Glycoside Hydrolases to convert biomass into sugars for *e.g.* biofuel production and the second regards the application of antioxidant enzyme, peroxiredoxin, for possible therapeutic uses.

1.2.1 Degradation of lignocellulosic biomass

1.2.1.1 Biomass composition

Lignocellulosic materials are the most promising feedstock as natural and renewable resource essential to the functioning of modern industrial societies. A considerable amount of such materials as waste byproducts are being generated through agricultural practices mainly from various agro based industries (32). Lignocelluloses of plant cell walls are composed of cellulose, hemicellulose, pectine and lignin. Cellulose forms a skeleton that is surrounded by hemicellulose and lignin functioning as matrix and encrusting materials, respectively (Fig. 2).

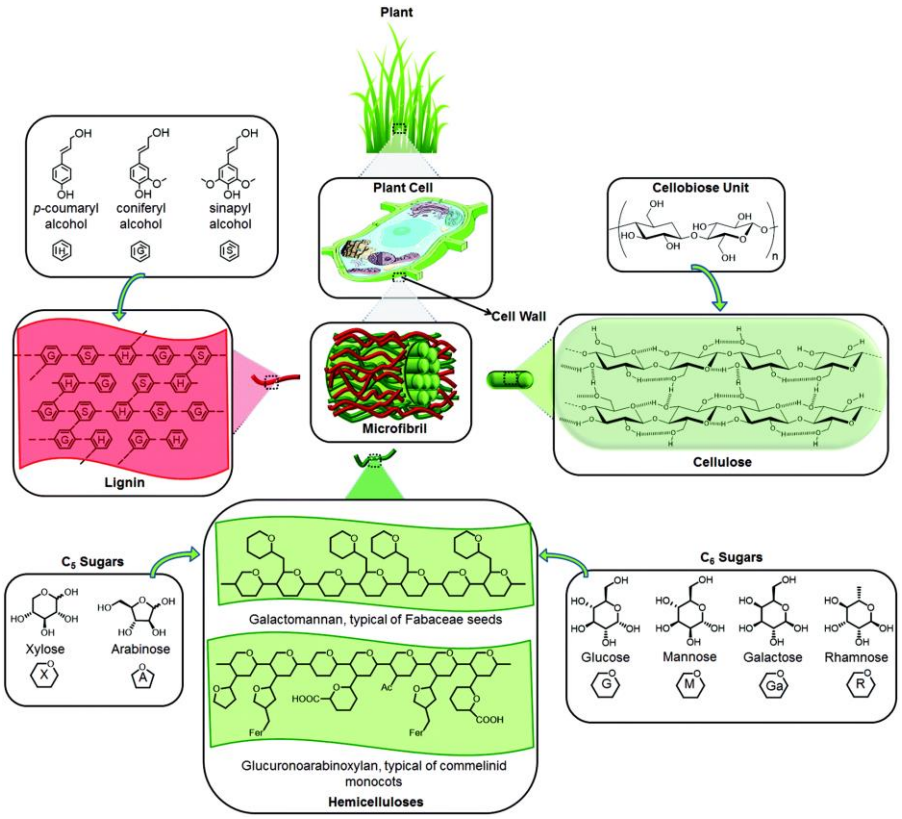

Fig. 2 Lignocellulosic biomass composition

Cellulose is the major structural component in the plant cell wall, is a linear homo-polysaccharide consisting of anhydrous glucose units (500–15000) that are linked by β-1,4-glycosidic bonds, with cellobiose as the smallest repetitive unit. The β-1,4 orientation of the glucosidic bonds results in the potential formation of intramolecular and intermolecular hydrogen bonds, which make native

cellulose highly crystalline, insoluble, and resistant to enzyme attack. The highly crystalline regions of cellulose in the plant cell wall are separated by less ordered amorphous regions (33).

Hemicellulose is a short, highly branched polymer of pentoses (e.g. D-xylose and L-arabinose) and hexoses (e.g.D-manose, D-galactose, and D-glucose) with 50-200 units. Its acetate groups were randomly attached with ester linkages to the hydroxyl groups of the sugar rings. The role of hemicellulose is to provide a linkage between lignin and cellulose (34).

Pectin is a structural heteropolysaccharide that rapresents about 35 % of the primary cell walls; the main backbone is composed by galactouronic acid residues α-(1-4)-linked. Other sugars are rhamnose, arabinose, and galactose. Pectic substances are hydrophillic and therefore have certain adhesive properties (35,36).

Lignin is a heterogeneous, amorphous, and cross-linked aromatic polymer where the main aromatic components are trans-coniferyl, trans-sinapyl and trans-*p*- coumaryl alcohols. Lignin is covalently bound to side groups on different hemicelluloses, forming a complex matrix that surrounds the cellulose micro-fibrils. In plant cell wall it varies from 2 to 40 %. The carbon–carbon (C–C) and ether (C–O–C) linkages in the lignin gives the plant cell wall strength and protection from attack by cellulolytic microorganisms (37). Other polyphenolic compounds are: tannins with high molecular weight (500–3000) composed of either hydroxyflavans, leucoanthocyanidin (flavan-3,4-diol) and catechin (flavan-3-ol) or glucose and phenolic acids that are structural components of the lignin core in plant cell wall. The presence of carboxyl and phenolic groups in phenolic acids enable such compounds to link to lignin and carbohydrates by ether or ester bonds.

All kind of biomass can be used in a biorefinery, a concept today, used in the strategies and visions of many industrial countries, being driven by a combination of environmental (encouraging renewable chemicals and fuels, and discouraging net greenhouse gas), political and economical concerns (38,39). A biorefinery is defined as a system combining necessary technologies between renewable raw materials, industrial intermediates and final products (40). The goal is to produce fuels, power, heat, and value-added chemicals from biomass (Fig. 3). The feedstocks (or their rest products) can be used directly as raw materials for bioprocessing, or be used as cheap substrates for fermentation processes from which products can be extracted (41). Depending on the feedstock available in different countries, biomass of different origins has been suggested as raw materials, and include for example corn (42), wheat (43), sugar cane (44), rape, cotton, sorgo, cassava and lignocellulose (45). The simplest biorefinery systems have in principal fixed processing of one type of feedstock (e.g. grains) to one main product, while the most flexible ones use a mix of biomass feedstock to produce an array of products.

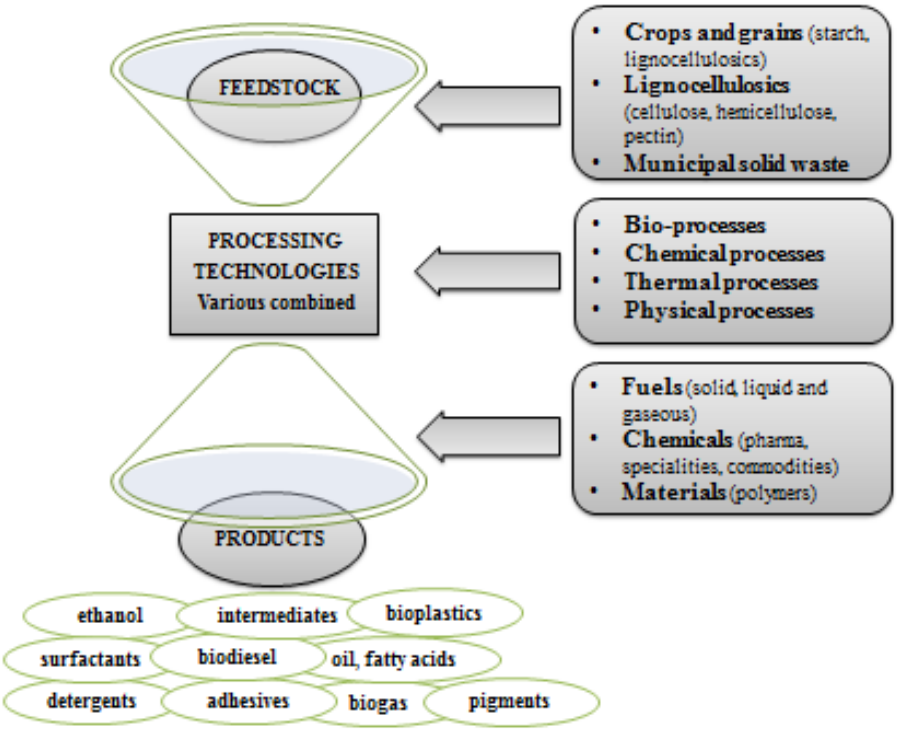

Fig. 3 Schematic overview of the basic principle of a biorefinery

Fuels produced from harvested biomass can be either solid, gas, or liquid. Biosolids, such as wood pellets or forestry waste, and biogas, produced by anaerobic digestion of biomass, are used primarily for electricity generation and heating, whereas liquid biofuels provide drop-in fuels that can be used directly in the transport sector, without a change in infrastructure. In theory, it is possible to convert any biomass feedstock into a liquid or gas fuel using appropriate chemical engineering techniques, but the efficiency of conversion, cost, and scale of demand/supply have led to preferred practices. Generally, liquid biofuels can be classified into "first-generation" and "second generation", where the main distinction is the characteristic of the feedstock used. First-generation bioethanol is made from sugars or starch. The sugar-based ethanol plants are predominantly produced in Brazil from sugarcanes. The starch-based ethanol is generally from corn but also from grains, and is dominated by the US followed by other major ethanol producing countries such as China, Canada, France, Germany, and Sweden. In the global market, ca. 21 million m^3 ethanol is produced from sugarcane, while ca. 60 million m^3 ethanol is produced from corn and grains (46). However, many concerns are still associated to first generation bioethanol such as feedstock insufficiency related to the increased demand; food *versus* fuel conflict, due to the use of edible material for fermentable sugars recovery; greenhouse gas emissions not low as required. Thus, it is needed pushing towards alternative systems, such as second-generation liquid biofuels based on non-food lignocellulosic biomass. Various life cycle analyses (LCAs) have shown

that lignocellulosic ethanol, produced through biochemical conversion, performs significantly better than first-generation, sugarcane/corn-based ethanol, following various environmental and energy security criteria. For instance, second generation ethanol offers a more attractive greenhouse gas emissions profile than other biofuels, with 86 % reduction in comparison to gasoline (47).

The biological process commonly used for the bioconversion of lignocellulose biomass in to bioethanol involves: (i) pre-treatment, (ii) hydrolysis to sugars, (iii) fermentation, (iv) products/co-products recovery. Conventional process currently adopted foresees a chemical/physical pre-treatment of lignocellulose in order to disrupt the fibrous matrix and remove lignin which can be recovered and used as a fuel for heat and electricity. Several techniques have been explored for removing lignin, steam explosion, dilute acid hydrolysis and ammonia fiber expansion (AFEX) being the most studied (48). Once lignin has been removed, saccharification of the free accessible (hemi)cellulose portions of the biomass is carried out. A variety of thermal, chemical and biochemical methods are being developed to carry out it in an efficient and low-cost manner. However, enzymatic hydrolysis has been so far demonstrated to be the best way to achieve (hemi)cellulose depolymerization. The final step is the fermentation of sugars obtained from previous step, which is typically performed by the yeast *Saccharomyces cerevisiae*.

1.2.1.2 Enzyme involved in biomass degradation

The enzymes degrading or modifying plant polysaccharides are classified as carbohydrate-active enzymes (CAZymes) and are divided into families according to their amino acid sequence and structural similarity (49). The CAZy database (http://www.cazy.org/) is organized into families of glycoside hydrolases (GHs), carbohydrate esterases (CEs), polysaccharide lyases (PLs), glycosyltransferases (GTs), and auxiliary activities (AA) Focusing the attention on the GHs, cellulases and hemicellulases are the two major groups involved in the degradation of biomass.

Cellulases are enzymes which able to break down cellulose by hydrolyse β -1-4 glycosidic bonds of cellulose polymer. They are predominantly produced by microorganisms, such as molds, fungi bacteria and archaea (50,51). Three principle cellulases synergistically confer the complete hydrolysis of cellulose: endoglucanases [EC 3.2.1.4], cellobiohydrolases (or–exoglucanases) [3.2.1.91], and β-glucosidases [EC 3.2.1.21] (52,53). The endoglucanases (found in the GH families 5–8, 12, 16, 44, 45, 48, 51, 64, 71, 74, 81, 87, 124 and 128) catalyse random cleavage of internal bonds in the cellulose chain, cellobiohydrolases (GH 5-7, 9 and 48) act at the end of cellulose chains and releasing glucose as well as cellobiose as product and β-glucosidases (GH1, 3, 4, 9, 17, 30 and 116) that are only active on cello-oligosaccharides and cellobiose, releasing glucose (53). The action of β-glucosidases is extremely important for industrial purposes because cellobiose is a

strong inhibitor of cellobiohydrolases, so the presence of β-glucosidases that remove cellobiose by hydrolyzing it, improves the hydrolysis performance of cellulases treatments (54).

Generally, in anaerobic bacteria (*e.g Clostridium thermocellum*) cellulases are present as aggregated structures attached to the cells (55). These extracellular and large enzyme aggregates are known as "cellulosome" that has a scaffolding protein on which enzyme subunits are positioned periodically. The scaffolding protein contains cohesins and dockerins. Each dockerin at one side binds to the enzyme subunit and another side to the cohesin. Cellulosome structure is not uniform in all bacterial species, its heterogeneous nature is due to species specific variation in scaffoldin properties and in the enzyme subunit compositions (56,57). In another way in fungi and in aerobic bacteria, a non-complexed cellulase systems are more common, in fact they usually secrete a set of individual cellulases (six to ten), each of which contains a catalytic domain (CD) that is often linked to other modular accessory domains, including carbohydrate-binding modules (CBMs) (58). CBMs are thought to potentiate the activity of the catalytic modules and they can be N-terminal or C-terminal to the CD (59). Free cellulases are currently most exploited for industrial applications (50); a significant industrial importance for cellulases was reached during the 1990's (60) mainly within textile, food, detergent, paper and pulp industry (*e.g*. in deinking of recycled paper) and biorefinery. Several thermostable enzymes have been characterized and there have been many trials in these areas as thermostability is highly relevant for the performance of the enzymes.

Hemicellulases are key components in the degradation of plant biomass and carbon flow in nature. The variable structure and organization of hemicellulose require the concerted action of many enzymes for its complete degradation. As a large part of the polymers are either insoluble or closely associated with the insoluble cellulose matrix, many of the hemicellulases are also modular proteins, cointaining the CD and the CBM (61). The catalytic modules of hemicellulases are either glycoside hydrolases (GHs) that hydrolyze glycosidic bonds, or carbohydrate esterases (CEs), which hydrolyze ester linkages of acetate or ferulic acid side groups. Hemicellulases belonging to GH families are divided into five major groups:

- **Xylanases (EC 3.2.1.8):** hydrolyze the β-1,4 bond in the xylan backbone, yielding short xylooligomers. Most known xylanases belong to GH families 10 and 11 and about 20 more xylanase genes are distributed between families 5, 8 and 43 (62).
- **β-Mannanases (EC 3.2.1.78):** hydrolyze mannan-based hemicelluloses and liberate short β-1,4-manno-oligomers, which can be further hydrolyzed to mannose by β-mannosidases (EC 3.2.1.25). There are currently about 50 β-mannanase gene sequences in GH families 5 and 26, and about 15 β-mannosidase gene sequences in families 1, 2 and 5 (63).
- **α-L-Arabinofuranosidases (EC 3.2.1.55) and α-L-arabinanases (EC 3.2.1.99):** hydrolyze arabinofuranosyl-containing hemicelluloses and are found in GH families 3, 43, 51, 54 and

62. Some of these enzymes exhibit broad substrate specificity, acting on arabinofuranoside moieties at *O*-5, *O*-2 and/or *O*-3 as a single substituent, as well as from *O*-2 and *O*-3 doubly substituted xylans, xylooligomers and arabinans (64).

- **α-D-Glucuronidases:** cleave the α-1,2-glycosidic bond of the 4-*O*-methyl-D-glucuronic acid sidechain of xylans, and are found exclusively in family 67(65).
- **β-Xylosidases (EC 3.2.1.37):** are exo-type glycosidases that hydrolyze short xylooligomers into single xylose units, and are found in families 3, 39, 43, 52 and 54. The spatial similarity between D-xylopyranose and L-arabinofuranose leads to bifunctional xylosidase–arabinosidase enzymes, found mainly in families 3, 43 and 54 (66,67).

The enzymatic mechanism of the GHs takes place via general acid catalysis that requires two critical residues: a proton donor and a nucleophile/base (68,69) (Fig. 4). This hydrolysis occurs via two major mechanisms giving rise to either an overall retention, or an inversion, of anomeric configuration (68). In both the retaining (Fig. 4a) and the inverting mechanisms (Fig. 4b), the position of the proton donor is identical, in other words it is within hydrogen-bonding distance of the glycosidic oxygen. In retaining enzymes, the nucleophilic catalytic base is in the proximity of the sugar anomeric carbon. This base, however, is more distant in inverting enzymes which must accommodate a water molecule between the base and the sugar. This difference results in an average distance between the two catalytic residues of ~5.5 å in retaining enzymes as opposed to ~10 å in inverting enzymes (70).

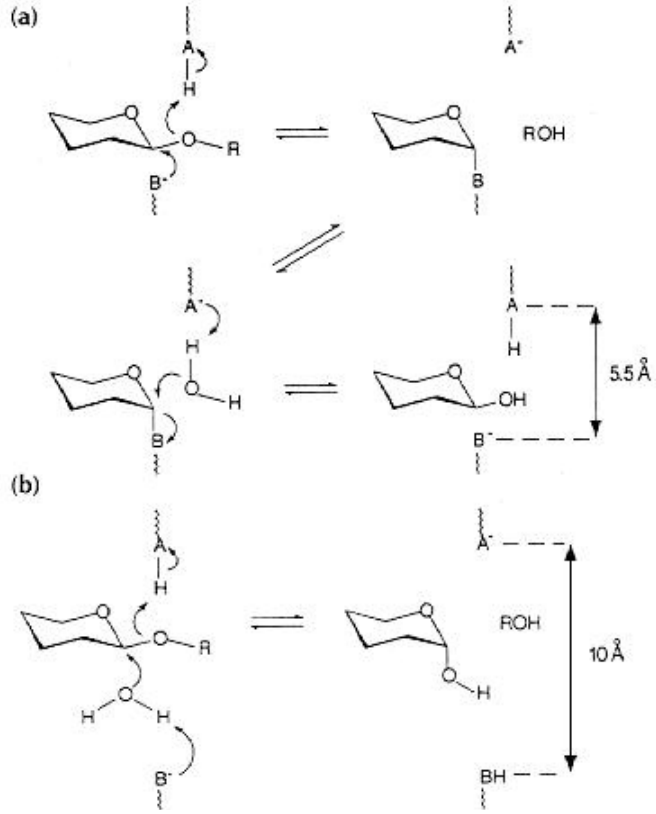

Fig. 4 Mechanisms of enzymatic glycosidic bond hydrolysis. (a) Retaining mechanism (b) Inverting mechanism

1.2.1.3 *Dictyoglomus turgidum* as source of thermophilic Carbohydrate-Active Enzymes

D. turgidum is a hyperthermophilic, anaerobic, Gram-negative bacterium that grow up to 80 °C. It was isolated from a hot spring in the Uzon Caldera, in eastern Kamchatka, Russia (71). *D. turgidum* was reported to grow on a wide range of substrates including starch, cellulose, pectin, carboxymethylcellulose (CMC), lignin, and humic acids, but not on pentose sugars such as xylose and arabinose. Analysis of the *D. turgidum* genome reveals a wide range of genes coding putative enzymes degrading extracellular and intracellular polysaccharide. The CAZy database (49) identifies 57 GHs, 3 PLs and 6 CEs in the *D. turgidum* genome. In particular, based on signal sequence predictions (72), have been identified: 20 extracellular polysaccharide degrading enzymes that can reduce polysaccharides into oligosaccharides and monosaccharide, 18 annotated three-component ABC carbohydrate transporters that bring monosaccharides and oligosaccharides into the cell and about 46 exo-acting and endo-acting enzymes to degrade oligosaccharide into monosaccharides in the cytoplasm (73). Therefore, the information obtained from genomic analysis, make this bacterium a good source to obtain GHs to utilize on biomass for different biotechnological applications.

1.2.2 Antioxidant enzymes and oxidative stress

Reactive oxygen species (ROS), notably, superoxide ($O_2{\cdot}^-$), the hydroxyl radical ($HO\cdot$), and hydrogen peroxide (H_2O_2), are potent oxidants that are generated during aerobic metabolism and in response to external factors (74). At high concentrations ROS can damage all essential biomolecules such as DNA, proteins, and lipids, thereby causing cause cell death (75). They can be classified into oxygen centered radicals (superoxide anion, hydroxyl radicals, alkoxyl radicals, and peroxyl radicals) and oxygen centered non-radicals (hydrogen peroxide and singlet oxygen) (76). The hydrogen peroxide, (H_2O_2) is not only a ROS because in eukaryotic cells plays a key role in cellular metabolism because it functions as a signalling molecule that regulates cell growth, cell adhesion, cell differentiation, and apoptosis (77). Living organisms have evolved different antioxidant defence systems to protect themselves against ROS toxicity. Among the antioxidant enzymes, superoxide dismutase (SOD) convert $O_2{\cdot}^-$ into H_2O_2 that is then converted to H_2O by an array of enzymes, such as catalase, glutathione peroxidase (GPx), and peroxiredoxin (Prx). Recently, much attention has been focused on Prxs, which are ubiquitous thiol peroxidases identified in prokaryotes, including Archaea and Eukaryotes, including humans; they catalyze the reduction of H_2O_2, peroxynitrite, and alkyl hydroperoxides (78-80). Prxs are typically classified as either 1-Cys Prxs or 2-Cys Prxs, depending upon the cysteine residues involved in catalysis. In 2-Cys Prxs, the first cysteine, known as peroxidatic cysteine (C_P), is located at the N-terminus whereas the second cysteine, situated at the C-terminus or in different central positions, is called the

resolving cysteine (CR) (81,82). C_P is oxidized to sulfenic acid (C_P-SOH) by H_2O_2 and condenses with CR to form a disulfide bond. A disulfide reducing system, generally composed of thioredoxin reductase (TrxR)/thioredoxin (Trx), is coupled to Prx for recycling (83) (Fig. 5).

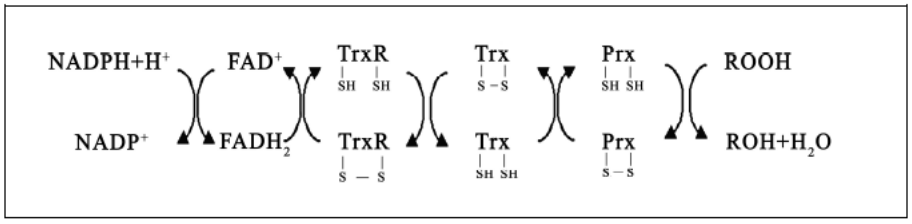

Fig. 5 Disulfide reducing system coupled to Prx rigeneration

In some Prxs, called sensitive Prxs, CP-SOH can be further oxidized to its inactive forms, (the sulfinic (CP-SO_2H) or sulfonic (CP-SO_3H) acids) by H_2O_2, thereby preventing disulfide bond formation and inactivating the enzyme. The reason for this sensitivity is due to specific structural motifs. Specifically, a "GGLG" sequence and a YF C-terminal extension stiffen and stabilize the fully folded (FF) active site, making the enzyme more susceptible to overoxidation (84-86). These structural motifs are mainly present in the eukaryotic Prxs that are therefore more sensitive to the prokaryotic Prxs that in most cases lack these motifs. This structural feature acquired during the evolution endows sensitive Prxs with additional functionality beyond basic antioxidant activity, including the ability to regulate peroxide signalling in eukaryotic cells (87). This difference has inspired the search for new antioxidants from prokaryotic sources that can be used as possible therapeutic biodrugs.

1.2.2.1 *Sulfolobus solfataricus* as source of robust peroxiredoxins

Prxs have also been characterized in the Archaea, particularly in *S. solfataricus* P2, a hyperthermophilic aerobic microorganism that grows at 80 °C. In particular four Prxs called: Bacterioferritin comigratory proteins (Bcps) were identified in this microorganism and characterized: Bcp1 (SSO2071), Bcp2 (SSO2121), Bcp3 (SSO2255) and Bcp4 (SSO2613). Bcp1 and Bcp4 are classified as Prx 2-Cys (82, 88), while Bcp2 and Bcp3 are classified as Prx 1-Cys (88,89).

Archaeal Bcp1 was expressed in *E. coli* and structurally and functionally characterized (82). Bcp1 is regenerated not only by unusual endogenous redox couple formed by TrxR (*Sso*2416) and Protein Disulfide Oxidoreductase (SsPDO) (90,91) that replaces the standard Trx, but it works also with yeast redox system TrxR/Trx at 37°C (92). Furthermore, Bcp1 can protect cardiomyoblasts from oxidative stress *in vitro* and this study is the first report of an archaeal enzyme delivered into mammalian cultured cells that is able to protect cells from oxidative stress by reducing both the

peroxide levels inside the cells and the resulting apoptosis (92). In the light of these results, the second part of this PhD-thesis was focused on the study system Bcp1-spore to be used as a non-recombinant platform to deliver antioxidant enzyme to the human intestinal mucosa.

The use of bacterial spores as a drug/antigen delivery system has been fostered by the remarkable and well-documented resistance of spores (93) that ensures high stability to the delivery system and by the safety record of several species of spore formers (94). Initially, spores of the model organism *Bacillus subtilis* have been used (95), but then also other *Bacillus* species have been tested for the display and mucosal delivery of antigens and enzymes (96). More recently, spores of *Bacillus megaterium* have been used to display a model heterologous protein (97). This species is particularly promising as a delivery vehicle for at least two reasons: the large dimensions of its spore (length up to 3 mm and diameter of 1 mm) (98) and the presence of an exosporium, a protective layer surrounding the spore found only in some spore-forming species (99). The exosporium is essential to allow a high efficiency of display and has been proposed to protect the displayed molecules from degradation (97).

1.3 Aim of the work

The aim of this thesis has been focused on two main objectives:

1. Studies and biochemical characterization of thermophilic GHs for biotechnological applications.

A) Biochemical characterization of a thermostable endomannanase/endoglucanase (*Dtur*CelB) from *Dictyoglomus turgidum.*

B) Biochemical characterization of a thermostable β-glucosidase (*Dtur*βGlu) from *D. turgidum.*

C) A synergistic action of a thermophilic α-galactosidase and β-mannanase on galactomannan substrates.

2. Study of the system protein-spore to be used as a non-recombinant platform to deliver biological drugs to the human intestinal mucosa.

A) Display of the peroxiredoxin Bcp1 of *Sulfolobus solfataricus* on probiotic spores of *Bacillus megaterium.*

References

1. Canganella F, Wiegel J. (2014) **Anaerobic Thermophiles**. *Life* 4(1):77-104.
2. Brock T**. Life at high temperatures**. *Science* 158 (1967), 1012-1019.
3. Cowen DA. (2004). **The upper temperature of life – where do we draw the line?** *Trends in Microbiol*. 12, 58–60.
4. Akai K, Nakamura K, Toki T, Tsunogai U, Miyazaki M, Miyazaki J, et al. (2008). **Cell proliferation at 122 degrees C and isotopically heavy CH4 production by a hyperthermophilic methanogen under high-pressure cultivation.** *Proc. Natl. Acad. Sci. U.S.A.* 105, 10949–10954.
5. Huber R, Eder W, Heldwein S, Wanner G, Huber H, Rachel R, Stetter KO. (1998) ***Thermocrinis ruber*** **gen. nov., sp. nov., A pink-filament-forming hyperthermophilic bacterium isolated from yellowstone national park.** *Appl Environ Microbiol.* 64(10):3576-83.
6. Klenk HP, Spitzer M, Ochsenreiter T, Fuellen G. (2004) **Phylogenomics of hyperthermophilic Archaea and Bacteria.** *Biochem Soc Trans.* 32:175-8.
7. Hickey DA, Singer GA. (2004) **Genomic and proteomic adaptations to growth at high temperature.** *Genome Biol.* 5(10):117.
8. Deckert G, Warren PV, Gaasterland T, Young WG, Lenox AL, et al. (1998) **The complete genome of the hyperthermophilic bacterium *Aquifex aeolicus*.** *Nature* 392:353-8.
9. Sabath N, Ferrada E, Barve A, Wagner A. (2013) **Growth temperature and genome size in bacteria are negatively correlated, suggesting genomic streamlining during thermal adaptation.** *Genome Biol Evol.* 5:966-77.
10. Forterre P. (2002) **A hot story from comparative genomics: reverse gyrase is the only hyperthermophile-specific protein.** *Trends Genet.* 18(5):236-7.
11. Makarova KS, Wolf YI, Koonin EV. (2003) **Potential genomic determinants of hyperthermophily.** *Trends Genet.* 19(4):172-6.
12. Zeldovich KB1, Berezovsky IN, Shakhnovich EI. (2007) **Protein and DNA sequence determinants of thermophilic adaptation.** *PLoS Comput Biol.* 12;3(1):e5.
13. Wang H, Li K, Zhu JY, Fang Q, Ye GY, Wang H, Li K, Zhu JY. (2012) **Cloning and expression pattern of heat shock protein genes from the endoparasitoid wasp, *Pteromalus puparum* in response to environmental stresses.** *Arch Insect Biochem Physiol.* 79(4-5):247-63.
14. Heine M, Chandra SBC. (2009) **The linkage between reverse gyrase and hyperthermophiles: A review of their invariable association.** *The Journal of Microbiol.* 47:229.
15. Borges N1, Matsumi R, Imanaka T, Atomi H, Santos H. (2010) ***Thermococcus kodakarensis*** **mutants deficient in di-myo-inositol phosphate use aspartate to cope with heat stress.** *J Bacteriol.* 192(1):191-7.
16. Empadinhas N, da Costa MS. (2011) **Diversity, biological roles and biosynthetic pathways for sugar-glycerate containing compatible solutes in bacteria and archaea.** *Environ Microbiol*. 13(8):2056-77.
17. Santos, H, da Costa MS. (2002) **Compatible solutes of organisms that live in hot saline environments.** *Environ. Microbiol.* 4:501-509.
18. Santos H, Lamosa P, Borges N. (2006) **Characterization and quantification of compatible solutes in (hyper)thermophilic microorganisms.** *Methods in microbiology: extremophiles.* 171–197.
19. Goh KM, Gan HM, Chan KG, Chan GF, et al. (2014) **Analysis of *Anoxybacillus* genomes from the aspects of lifestyle adaptations, prophage diversity, and carbohydrate metabolism.** *PLoS ONE* 9:e90549.
20. Urbieta MS, Donati ER, Chan KG, Shahar S, Sin LL, Goh KM. (2015) **Thermophiles in the genomic era: Biodiversity, science, and applications.** *Biotechnol Adv* 1;33:633-47.

21. Koga Y. (2012) **Thermal adaptation of the archaeal and bacterial lipid membranes.** *Archaea.* 2012:789652.
22. Dewan S. S. (2014). **Global Markets for Enzymes in Industrial Applications.** *Wellesley, MA: BCC Researc.*
23. Adrio JL, Demain AL. (2014) **Microbial enzymes: tools for biotechnological processes.** *Biomolecules.* 4(1):117–139.
24. Fernández-Arrojo L, Guazzaroni ME, López-Cortés N, Beloqui A, Ferrer M. (2010) **Metagenomic era for biocatalyst identification.** *Curr. Opin. Biotechnol*. 21 725–733.
25. Bornscheuer UT, Huisman GW, Kazlauskas RJ, Lutz S, Moore JC, Robins K. (2012) **Engineering the third wave of biocatalysis**. *Nature*. 485(7397):185-94.
26. Adrio JL, Demain AL. (2003) **Fungal biotechnology**. *Int Microbiol.* 6(3):191-9.
27. Sawaya D, Arundel A. (2010) **La evolución de la bioeconomía hasta 2030: diseño de una agenda políti**c. *Monográfico Nota d'economia* 97-98.
28. Timmis K, de Lorenzo V, Verstraete W, et al. (2014) **Pipelines for New Chemicals: a strategy to create new value chains and stimulate innovation-based economic revival in Southern European countries.** *Environ. Microbiol.* 16,9-18.
29. Schrewe M1, Julsing MK, Bühler B, Schmid A. (2013) **Whole-cell biocatalysis for selective and productive C-O functional group introduction and modification.** *Chem Soc Rev.* 7;42(15):6346-77.
30. You C, Zhang YH. (2013) **Self-assembly of synthetic metabolons through synthetic protein scaffolds: one-step purification, co-immobilization, and substrate channeling.** *ACS Synth Biol.* 15;2(2):102-10.
31. Sarmiento F, Peralta R, Blamey JM. **Cold and Hot Extremozymes: Industrial Relevance and Current Trends.** *Frontiers in Bioengineering and Biotechnology.* 3:148.
32. Pérez J, Muñoz-Dorado de la Rubia T, Martínez J. (2002), **Biodegradation and biological treatments of cellulose, hemicellulose and lignin: an overview.** *Intern. Microbiol.* 53-63.
33. Chesson A, Forsberg CW (1988) **Polysaccharide degradation by rumen microorganisms.** *The Rumen Miciobial Ecosystem* 329-381.
34. Holtzapple MT (1993) **Cellulose.** In: Sadler, M.J., Encyclopedia of food science, food technology, and nutrition. 758-767.
35. Cassab GI, Varner JE. (1988) **Cell wall proteins.** *Annu Rev Plant Physiol Plant Mol Biol.* 39:321–353.
36. Abbott DW, Boraston AB. (2008) **Structural biology of pectin degradation by Enterobacteriaceae.** Microbiol Mol Biol Rev. 72(2):301-16.
37. Abdel-Hamid AM, Solbiati JO, Cann IK. (2013) **Insights into lignin degradation and its potential industrial applications.** *Adv Appl Microbiol.* 82:1-28.
38. Mabee WE, Gregg DJ, Saddler JN. (2005) **Assessing the emerging biorefinery sector in Canada.** *Appl. Biochem. and Biotechnol.* 121:765–778.
39. Pye EK. (2005**) Biorefining; a major opportunity for the sugar cane industry.** *Intern. Sugar Journal.* 107:222.
40. Fernando S, Adhikari S, Chandrapal C, Murali N. (2006**) Biorefineries: Current status, challenges and future direction.** *Energy and Fuels.* 20:1727–1737.
41. Solaiman DKY, Ashby RD, Foglia TA, Marmer WN. **Conversion of agricultural feedstock and coproducts into poly(hydroxyalkanoates)** *Appl. Biochem. and Biotechnol.* 71:783–789.
42. Gaspar M, Juhasz T, Szengyel Z, Reczey K. (2005) **Fractionation and utilisation of corn fibre carbohydrates.** *Process Biochemistry.* 40:1183–1188.
43. Koutinas AA, Wang R, Webb C. (2004) **Restructuring upstream bioprocessing: Technological and economical aspects for production of a generic microbial feedstock from wheat.** *Biotechnology and Bioengineering.* 85:524–538.
44. Edye LA, Doherty WOS, Blinco JA, Bullock GE. (2006) **The sugarcane biorefinery: Energy crops and processes for the production of liquid fuels and renewable commodity chemicals**. *Intern. Sugar Journal.* 108:19–27.

45. Pan X, Kadla JF, Ehara K, Gilkes N, Saddler JN. (2006) **Organosolv ethanol lignin from hybrid poplar as a radical scavenger: relationship between lignin structure, extraction conditions, and antioxidant activity.** *J. Agric. Food. Chem*. 54:5806–5813.

46. Lennartsson PR, Erlandsson P, Taherzadeh MJ. (2014) **Integration of the first and second generation bioethanol processes and the importance of by-products.** *Bioresour Technol.*165:3-8.

47. Kazamia E, Smith AG. (2014) **Assessing the environmental sustainability of biofuels.** *Trends Plant Sci.* 19(10):615-8.

48. Balan V1, Bals B, Chundawat SP, Marshall D, Dale BE. (2009) **Lignocellulosic biomass pretreatment using AFEX.** *Methods Mol Biol.* 581:61-77.

49. Lombard V, Golaconda Ramulu H, Drula E, Coutinho PM, Henrissat B. (2013) **The carbohydrate-active enzymes database (CAZy) in 2013**. *Nucleic Acids Res.* 4:D490-5.

50. Acharya S, Chaudhary A. (2012). **Bioprospecting thermophiles for cellulase production: a review. Acharya S, Chaudhary A. Bioprospecting thermophiles for cellulase production: a review.** *Braz. J. Microbiol.* 43(3):844-856.

51. Bhat M.K, Hazlewood GP. (2001) **Enzymology and other characteristics of cellulases and xylanases.** *Enzymes in farm animal nutrition. CABI, Bradford*: 11–57.

52. Teeri TT. (1997) **Crystalline cellulose degradation: new insight into the function of cellobiohydrolases.** *Trends in Biotechnology.* 15:160–167.

53. Wood TM, Garcia-Campayo V. (1990) **Enzymology of cellulose degradation.** *Biodegradation.* 1:147–161.

54. Teugjas H1, Väljamäe P. (2013) **Selecting β-glucosidases to support cellulases in cellulose saccharification.** *Biotechnol Biofuels.* 24;6(1):105.

55. Hirano K, Kurosaki M, Nihei S, Hasegawa H, Shinoda S, Haruki M, Hirano N. (2016) **Enzymatic diversity of the Clostridium thermocellum cellulosome is crucial for the degradation of crystalline cellulose and plant biomass**. *Sci Rep.* 19;6:35709.

56. Doi RH1, Kosugi A. (2004) **Cellulosomes: plant-cell-wall-degrading enzyme complexes**. *Nat Rev Microbiol.* 2(7):541-51.

57. Mathew GM., Sukumaran RK, Singhania RR, Pandey A. (2008) **Progress in research on fungal cellulases for lignocellulose degradation.** *J. Sci. Indus. Res.* 67:898–907.

58. Várnai A, Mäkelä MR, Djajadi DT, Rahikainen J, Hatakka A, Viikari L. (2014) **Carbohydrate-binding modules of fungal cellulases: occurrence in nature, function, and relevance in industrial biomass conversion.** *Adv Appl Microbiol.* 88:103-65.

59. Wilson DB. (2009) **The first evidence that a single cellulase can be essential for cellulose degradation in a cellulolytic microorganism.** *Mol Microbiol.* 74(6):1287-8.

60. Schulein M. (2000) **Protein engineering of cellulases.** *Biochimica et Biophysica Acta* 1543:239-252.

61. Bourne Y, Henrissat B. (2001), **Glycoside hydrolases and glycosyltransferases: families and functional modules**. *Curr. Opin. Struct. Biol*. 593-600.

62. Van Petegem F, Collins T, Meuwis MA, C et al. (2003) **The structure of a cold-adapted family 8 xylanase at 1.3 Å resolution, structural adaptations to cold and investigation of the active site** *J. Biol. Chem*. 278:7531-7539.

63. Sharma K, Dhillon A, Goyal A. (2016) **Insights into structure and reaction mechanism of β-mannanases.** *Curr Protein Pept Sci.* Oct 13.

64. Saha BC. (2000) **α-l-Arabinofuranosidases: biochemistry, molecular biology and application in biotechnology**. *Biotechnol. Adv*. 403-423.

65. Nurizzo D, Nagy T, Gilbert HJ, Davies GJ. (2002) **The structural basis for catalysis and specificity of the Pseudomonas cellulosa alpha-glucuronidase, GlcA67A.** *Structure* 10:547-556.

66. Mai V, Wiegel J, Lorenz WW. (2000) **Cloning, sequencing, and characterization of the bifunctional xylosidase-arabinosidase from the anaerobic thermophile Thermoanaerobacter ethanolicus** *Gene*, 247:137-143.

67. Lee RC, M Hrmova, Burton RA, Lahnstein J, Fincher GB. (2003) **Bifunctional family 3 glycoside hydrolases from Barley with alpha-l-Arabinofuranosidase and beta-d-Xylosidase activity characterization, primary structures and COOH-terminal processing.** *J. Biol. Chem*. 278:5377-5388.
68. Koshland DE. (1953) **Stereochemistry and the mechanism of enzymatic reactions** *Biol. Rev. Camb. Philos. Soc,* 416-436.
69. Sinnott ML**.** (1990) **Catalytic mechanisms of enzymic glycosyl transfer.** *Chem. Rev*, 1171-1202.
70. McCarter JD, Withers SG. (1994) **Mechanisms of enzymatic glycoside hydrolysis** *Curr. Opin. Struct. Biol*, 885-892 .
71. Svetlichnii, V. A., & Svetlichnii, T. P. (1988). ***Dictyoglomus turgidus*** **sp. nov., a new extremely thermophilic eubacterium isolated from hot springs of the Uzon volcano caldera.** *Mikrobiologiya*, 57, 435–441.
72. Petersen TN, Brunak S, von Heijne G, Nielsen H. (2011). **SignalP 4.0: discriminating signal peptides from transmembrane regions.** *Nat. Methods* 8:785–786.
73. Brumm PJ, Gowda K, Robb FT, Mead DA (2016) **The Complete Genome Sequence of Hyperthermophile *Dictyoglomus turgidum* DSM 6724™ Reveals a Specialized Carbohydrate Fermentor.** *Front Microbiol* 20:1979.
74. Diano S. (2013) **Role of reactive oxygen species in hypothalamic regulation of energy metabolism.** *Endocrinology and metabolism* 28:3–5.
75. Nakamura T, Cho DH, Lipton SA. (2012) **Redox regulation of protein misfolding, mitochondrial dysfunction, synaptic damage, and cell death in neurodegenerative diseases.** *Experimental neurology.* 238:12–21.
76. Phaniendra A, Jestadi DB, Periyasamy L. (2015) **Free radicals: properties, sources, targets, and their implication in various diseases.** *Indian J Clin Biochem*. 30(1):11-26.
77. Declercq JP, Evrard C, Clippe A, Stricht DV, Bernard A, Knoops B. (2001) **Crystal structure of human peroxiredoxin 5, a novel type of mammalian peroxiredoxin at 1.5 A resolution.** *J Mol Biol.* 24;311(4):751-9.
78. Butterfield LH, Merino A, Golub SD, Shau H. (1999) **From cytoprotection to tumor suppression: the multifactorial role of peroxiredoxins.** *Antioxid Redox Signal* 1:385–402.
79. Rhee SG, Kang SW, Chang TS, Jeong W, Kim K. (2001) **Peroxiredoxins, a novel family of peroxidases.** *IUBMB Life* 52:35–41.
80. Fujii J, Ikeda Y. (2002) **Advances in our understanding of peroxiredoxin, a multifunctional, mammalian redox protein.** *Redox Rep* 7:123–130.
81. Hall A, Karplus PA, Poole LB. (2009) **Typical 2-Cys peroxiredoxins—structures, mechanisms and functions.** *FEBS J.* 92469–2477, 2009.
82. D'Ambrosio K, Limauro D, Pedone E et al. (2009) **Insights into the catalytic mechanism of the Bcp family: functional and structural analysis of Bcp1 from *Sulfolobus solfataricus*.** *Proteins: Structure, Function and Bioinformatics,* 995–100.
83. Lu J, Holmgren A. (2014) **The thioredoxin antioxidant system.** *Free Radical Biology and Medicine* 75–87.
84. Wood ZA, Poole LB, Karplus PA. (2003) **Peroxiredoxin evolution and the regulation of hydrogen peroxide signaling.** *Science* 5619:650–653.
85. Kumsta C, Jakob U. (2009) **Redox-regulated chaperones.** *Biochemistry,* 22:4666–4676.
86. Arias DG, Reinoso A, Sasoni N, Hartman MD, Iglesias AA, Guerrero SA. (2014) **Kinetic and structural characterization of a typical two-cysteine peroxiredoxin from Leptospira interrogans exhibiting redox sensitivity**. *Free Radical Biology and Medicine,* 77:30–40.
87. Bang YJ, Oh MH, Choi SH, (2012) **Distinct characteristics of two 2-cys peroxiredoxins of Vibrio vulnificus suggesting differential roles in detoxifying oxidative stress.** *The Journal of Biological Chemistry* 287:42516–42524.
88. Limauro D, Pedone E, Galdi I, Bartolucci S. (2008) **Peroxiredoxins as cellular guardians in *Sulfolobus solfataricus*—characterization of Bcp1, Bcp3 and Bcp4.** *FEBS J* 275:2067–2077.

89. Limauro D, Pedone E, Pirone L and Bartolucci S. (2005) **Identification and characterization of 1-Cys peroxiredoxin from *Sulfolobus solfataricus* and its involvement in the response to oxidative stress.** *FEBS J* 273:721–731.
90. Pedone E, Limauro D, Bartolucci S (2008) **The machinery for oxidative protein folding in thermophiles.** *Antioxid Redox Signal* 10:157–169.
91. Pedone E, Limauro D, D'Alterio R, Rossi M, Bartolucci S. (2006) **Characterization of a multifunctional protein disulfide oxidoreductase from *Sulfolobus solfataricus*.** *FEBS J* 273:5407–5420.
92. Sarcinelli C, Fiorentino G, Pizzo E, Bartolucci S, Limauro D. (2016) **Discovering Antioxidant Molecules in the Archaea Domain: Peroxiredoxin Bcp1 from *Sulfolobus solfataricus* Protects H9c2 Cardiomyoblasts from Oxidative Stress**. *Archea* 2016:7424870.
93. McKenney PT, Driks A, Eskandarian HA, Grabowski P, Guberman J, Wang KH, Gitai Z, Eichenberger P. (2010) **A distance-weighted interaction map reveals a previously uncharacterized layer of the *Bacillus subtilis* spore coat.** *Current Biology* 20:934–938.
94. Cutting SM. (2011) **Bacillus probiotics**. *Food Microbiol.* 28:214-220.
95. Isticato R, Cangiano G, Tran HT, Ciabattini A, Medaglini D, Oggioni MR, De Felice M, Pozzi G, Ricca E. (2001) **Surface display of recombinant proteins on *Bacillus subtilis* spores.** *J. Bacteriol.* 183: 6294-6301.
96. Knecht LD, Pasini P, Daunert S. (2011) **Bacterial spores as platforms for bioanalytical and biomedical applications.** *Anal Bioanal Chem* 400:977-989.
97. Lanzilli M, Donadio G, Addevico R, Saggese A, Cangiano A, Baccigalupi L, Christie G, Ricca E, Isticato R. (2016) **The exosporium of *Bacillus megaterium* QM B1551 is permeable to the red fluorescence protein of the coral *Discosoma sp*.** *Front. Microbiol*. 7:1752.
98. Di Luccia B, D'Apuzzo E, Varriale F, Baccigalupi L, Ricca E, Pollice A. (2016) ***Bacillus megaterium* SF185 induces stress pathways and affects the cell cycle distribution of human intestinal epithelial cells.** *Benef. Microb.* 7:609–620.
99. Koshikawa T, Beaman TC, Pankratz HS, Nakashio S, Corner TR, Gerhardt P. (1984) **Resistance, germination, and permeability correlates of *Bacillus megaterium* spores successively divested of in tegument layers.** *J. Bacteriol*. 159:624–632.

Chapter 2

Glycoside hydrolases from thermophilic microorganisms

2.1 Biochemical characterization of a thermostable endomannanase/endoglucanase from *Dictyoglomus turgidum*.

2.2 Biochemical characterization of a thermostable β-glucosidase from *Dictyoglomus turgidum*.

2.3 A synergistic action of a thermophilic α-galactosidase and β-mannanase on galactomannan substrates.

Summary

Today, alternative energy is an interesting concept to meet global energy demand that no longer counts on the use of fossil fuels and in this contest the lignocellulosic biomass plays a key role for this purpose. From an industrial point of view, the biomass conversion requires a cocktail of highly efficient enzymes; for this reason, enzymes from thermophiles have received more attention because they are in general very stable to harsh conditions and can be recycled with preserving their performance. In the section 2.1 the paper "Biochemical characterization of a thermostable endomannanase/endoglucanase from *Dictyoglomus turgidum*" is focused on the recombinant *Dtur*CelB, a thermophilic enzyme that showed both endomannanase and endoglucanase activity. Until now there are only few enzymes displaying both activities and this feature, together with optimal temperature at 70 °C and a good thermostability, make *Dtur*CelB very interesting for future applications. In the section 2.2 the manuscript "Biochemical characterization of a thermostable β-glucosidase from *Dictyoglomus turgidum*" (manuscript in preparation) is dedicated to the recombinant *Dtur*βGlu, a β-glucosidase belonging to GH 1 family that showed a good activity on various synthetic and natural substrates and in presence of different chemicals. Also in this case the robustness of this enzyme makes it particularly interesting for biotechnological application such as biomass conversion. In the section 2.3 the paper "A synergistic action of a thermophilic α-galactosidase and β-mannanase on galactomannan substrates*"* (submitted to Enzyme and Microbial Technology) is focused on the study of the synergy between *Dtur*CelB, from *D. turgidum* and *Tt*GalA, an α galactosidase from *Thermus thermophilus*. In this study these two enzymes have been tested on different galactomannans both simultaneously and sequentially conditions and it was demonstrated that there is an heterosynergystic association of these two recombinant thermophilic enzymes.

The results highlighted the possibility of these two enzymes to be used in an enzymatic cocktail to pre-hydrolyze the biomass right after the pretreatment and before to the saccharification step.

2.1 Biochemical characterization of a thermostable endomannanase/endoglucanase from *Dictyoglomus turgidum*

Francesca Anna Fusco[1], Raffaele Ronca[1], Gabriella Fiorentino[1], Emilia Pedone[2], Patrizia Contursi[1], Simonetta Bartolucci[1], Danila Limauro[1]*

[1]Dipartimento di Biologia, University of Naples Federico II, Complesso universitario di Monte S. Angelo, Via Cinthia, Naples, Italy

[2]Istituto di Biostrutture e Bioimmagini, CNR, Via Mezzocannone 16, Naples, Italy

*Corresponding author: Danila Limauro, E-mail: limauro@unina.it

Keywords

Endomannanase, endoglucanase, thermophilic enzyme, *Dictyoglomus turgidum*

Extremophiles
https://doi.org/10.1007/s00792-017-0983-6

ORIGINAL PAPER

Biochemical characterization of a thermostable endomannanase/endoglucanase from *Dictyoglomus turgidum*

Francesca Anna Fusco[1] · Raffaele Ronca[1] · Gabriella Fiorentino[1] · Emilia Pedone[2] · Patrizia Contursi[1] · Simonetta Bartolucci[1] · Danila Limauro[1]

Received: 4 September 2017 / Accepted: 20 November 2017

Abstract
Dictyoglomus turgidum is a hyperthermophilic, anaerobic, gram-negative bacterium that shows an array of putative glycoside hydrolases (GHs) encoded by its genome, a feature that makes this microorganism very interesting for biotechnological applications. The aim of this work is the characterization of a hyperthermophilic GH5, Dtur_0671, of *D. turgidum*, annotated as endoglucanase and herein named *Dtur*CelB in agreement to *Dtur*CelA, which was previously characterized. The synthetic gene was expressed in *Escherichia coli*. The purified recombinant enzyme is active as a monomer (40 kDa) and CD structural studies showed a conserved α/β structure at different temperatures (25 and 70 °C) and high thermoresistance (Tm of 88 °C). Interestingly, the enzyme showed high endo-β-1,4-mannanase activity vs various mannans, but low endo-β-1,4 glucanase activity towards carboxymethylcellulose. The K_M and V_{max} of *Dtur*CelB were determined for both glucomannan and CMC: they were 4.70 mg/ml and 473.1 µmol/min mg and 1.83 mg/ml and 1.349 µmol/min mg, respectively. Its optimal activity towards temperature and pH resulted to be 70 °C and pH 5.4, respectively. Further characterization highlighted good thermal stability (~ 50% of enzymatic activity after 2 h at 70 °C) and pH stability over a broad range (> 90% of activity after 1 h in buffer, ranging pH 5–9); resistance to chemicals was also observed.

Keywords Endomannanase · Endoglucanase · Thermophilic enzyme · *Dictyoglomus turgidum*

Introduction

In the last decade, the use of plant biomass polarized the world's interest; in fact, its lignocellulosic component represents a source of renewable and eco-friendly energy that can replace the chemical products of fossil origin (Capolupo and Faraco 2016; Álvarez et al. 2016). The structure of lignocellulosic material, based on the variety of the plants, is characterized by a different proportion of complex polymers represented by cellulose, hemicellulose and lignin. Among these, the cellulose is a linear polymer constituted only by β-1,4 linked D-glucose monomers, where the various chains are closely linked by hydrogen bonds and organized in structures that form microfibrils (Kolpak and Blackwell 1976). Hemicelluloses are linear or branched polysaccharides that are classified in xylans, mannans, arabinogalactans or arabinans based on the main sugar of the polymer backbone (Scheller and Ulvskov 2010). The most representative hemicelluloses are: hetero-1,4 β-xylans, composed by a backbone of 1,4-β-linked D-xylose residues with various appendages attached, and mannans, consisting of a main chain of β-1,4-mannose units that could be differently modified or decorated such as: (1) glucomannans consisting of linear main chains of β-1,4 linked D-glucose and D-mannose residues in 3:1 ratio, (2) galactomannans whose backbone of β-1,4 linked D-mannose residues is decorated by α-1,6-linked galactose, (3) galactoglucomannans that consist of a linear chain of β-1,4 linked D-glucose and D-mannose, with D-galactose residues linked in α-1,6 only to mannose units

Communicated by H. Atomi.

Electronic supplementary material The online version of this article (https://doi.org/10.1007/s00792-017-0983-6) contains supplementary material, which is available to authorized users.

✉ Danila Limauro
limauro@unina.it

[1] Dipartimento di Biologia, University of Naples Federico II, Complesso universitario di Monte S. Angelo, Via Cinthia, Naples, Italy

[2] Istituto di Biostrutture e Bioimmagini, CNR, Via Mezzocannone 16, Naples, Italy

Published online: 25 November 2017

(Yamabhai et al. 2016; Malgas et al. 2015). In the hardwood, the main hemicellulose is composed by glucuronoxylans, while in the softwood, the galactoglucomannans are predominant. The lignin is the most robust polymer to the enzymatic attack that lacks a defined primary structure and is composed by aromatic alcohols known as monolignols (Álvarez et al. 2016).

After suitable chemical/physical pretreatment, the lignocellulosic biomass may be converted to fermentable monosaccharides by the synergic action of multiple enzymes. The biotechnological approach offers strong advantages for the improvement of yields, the decrease of pollutants and waste, and the energy consumption related to less drastic reaction conditions (Aulitto et al. 2017).

Cellulose is hydrolyzed by endo-1,4-β-glucanase (EC 3.2.1.4) that cleaves the polymer producing short oligosaccharides which are hydrolyzed to glucose by the combined action of 1,4 β-cellobiohydrolase (EC 3.2.1.91) and β-glucosidase (EC 3.2.1.21) (Sadhu and Maiti 2013). Due to its heterogeneous structural composition, the hemicellulose is hydrolyzed by an array of enzymes: endo-β-1,4-mannanase (EC 3.2.1.78), exo-β-mannosidase (EC 3.2.1.25), β-glucosidase (EC 3.2.1.21), endo-1,4-β-xylanase (EC 3.2.1.8), endo-1,5-α-L-arabinanase (EC 3.2.1.99) and endo-galacturonase (EC 3.2.1.15) (Srivastava and Kapoor 2017). In particular, endo-mannanases catalyze the cleavage of β-1,4 D-manno-pyranosyl bonds within the main chain releasing linear or branched oligosaccharides of different lengths. The application of mannanases and cellulases is not restricted to the green economy field, because these enzymes are used for several processes in the food and feed, pulp and paper, as well as in oil and textile industries (Dhawan and Kaur 2007; Rytioja et al. 2014; Chauhan et al. 2012).

Nowadays, great efforts are made to discover novel carbohydrases with high activity and stability and capable to hydrolyze efficiently the lignocellulosic biomass (Acharya and Chaudhary 2012). For this reason, enzymes from extremophiles have received more attention, because they are in general very stable to harsh conditions and can be recycled by preserving their performance; in addition, they offer better performance at high temperature than their mesophilic counterparts, such as the reduction of contamination risks, the increase in substrate solubility and shortening of the processing time (Elleuche et al. 2014, 2015; Sarmiento et al. 2015). Thus, the exploration of new thermostable glycoside hydrolases (GHs), active on different polymers, with desired properties is highly required.

In this context, *Dictyoglomus turgidum*, the hyperthermophilic gram-negative anaerobic bacterium, isolated from a hot spring in the Uzon Caldera, in Kamchatka, Russia (Svetlichny and Svetlichnaya 1988), represents a good source of many GHs that can be used for biotechnological purposes. The information obtained from genomic analysis, recently carried out (Kublanov et al. 2009; Brumm et al. 2011a, b, 2016) and the wide range of substrates on which this bacterium grows, ranging from cellulose to lignin (Brumm et al. 2011a, b), make this bacterium a good source to obtain GHs to utilize on biomass for different biotechnological applications. For this reason, we have biochemically characterized Dtur_0671, belonging to GH5 family, that was previously identified (Brumm et al. 2011a, b, 2016). The gene, synthetically produced, was expressed in *Escherichia coli* and successively the recombinant protein was purified. The biochemical structural and functional characterization was performed; in particular, the enzyme was characterized for both endo-β-1,4-mannanase and endo-β-1,4-glucanase activity and it was named *Dtur*CelB in agreement with the nomenclature of the other endoglucanase *Dtur*CelA (Brumm et al. 2011a, b). The results obtained suggest that this enzyme could be a good candidate for employment in industrial applications.

Materials and methods

Gene synthesis

The sequence of *DturcelB* encoding the putative endoglucanase (Dtur_0671, NCBI accession number ACK41956) was synthesized by Eurofins MWG Operon (Ebersberg Germany), inserting *NdeI* and *XhoI* restriction sites at 5′ and 3′, respectively and exploiting *E. coli* codon usage. The coding sequence (1002 bp) was cloned in the vector pET30b (+) to express a fusion protein with a C-terminal histidine tag (LEHHHHHH).

Expression and purification of *Dtur*CelB in *E. coli*

The recombinant plasmid pET30*Dtur*CelB was used to transform the competent *E. coli* BL21(DE3) strain. A single colony was inoculated into the Luria–Bertani (LB) medium supplemented with kanamycin (50 µg/ml) at 37 °C. Cells were grown in an orbital shaker, until 0.8 OD A_{600nm} and induced by 0.5 mM IPTG for 18 h at 25 °C.

The cells cultures (1 l) were then harvested by centrifugation and the pellet was suspended in 25 ml of ice-cold 50 mM Tris–HCl pH 7.5 containing a complete EDTA-free protease inhibitor's cocktail (Roche, IN, USA). After sonication with 5 min pulses at 20 Hz (30″ on and 30″ off), the suspension was clarified by centrifugation at 20000×*g* for 1 h at 4 °C. The cytoplasmic extract was subjected to heat treatment at 70 °C for 15 min and then centrifugated at 20000×*g* for 30 min at 4 °C. The supernatant obtained was loaded on the affinity chromatography (HisTrap HP column GE Healthcare, 1 ml), connected to AKTA system, and equilibrated in 50 mM Tris–HCl pH 7.5, 0.3 M NaCl and

10 mM imidazole. Purification of the protein was carried out as already described in Limauro et al. (2010). The fractions were pooled, analyzed by SDS–PAGE and extensively dialysed against 20 mM Tris–HCl pH 7.5 for the subsequent analyses.

Western blotting and LC/MS/MS analyses

The fractions corresponding to the different purification steps of *Dtur*CelB were separated by SDS–PAGE containing 12% polyacrylamide and transferred to polyvinylidene difluoride (PVDF) membrane (Millipore, MA, USA). The membrane was immunostained with penta-His horseradish peroxidase (HRP) conjugated mAb (Qiagen) (Sarcinelli et al. 2016). Chemiluminescent detection was performed according to the manufacturer's recommendations (Immobilion Western Chemiluninescent HRP substrate, Millipore, MA, USA), using Chemidoc system (Bio-Rad).

LC/MS/MS analysis of tryptic digests of *Dtur*CelB was performed by CHIP LC-ESIQTOF (Agilent Technologies); the identification of the peptides was performed by MASCOT software.

Size-exclusion chromatography and light scattering

Purified *Dtur*CelB protein was analyzed by size-exclusion chromatography connected to a MiniDAWN Treos light scattering system (Wyatt Technology) equipped with a QELS module (quasi-elastic light scattering) for mass value (Del Giudice et al. 2013) 1 mg sample (2 mg/ml) was loaded on Superdex S75 10/30 column (24 ml), equilibrated in 50 mM Tris–HCl pH 8.0, and 150 mM NaCl. A constant flow rate of 0.5 ml/min was applied. Data were analyzed using Astra 5.3.4.14 software (Wyatt Technology).

Circular dichroism spectroscopy

Far-UV and thermal denaturation CD measurements were performed with a J-815 Jasco CD spectrometer, equipped with a Peltier-type temperature control system (model PTC-423S/15), as described (Contursi et al. 2013). CD measurements were carried out using a quartz cell with a path length of 0.1 cm and 7.5 µM *Dtur*CelB in 20 mM Na-phosphate pH 7.5, at 25 °C and 70 °C. Far-UV CD spectra were acquired in 190–260 nm range, with a scan rate continuous, a response of 4 s, 2 nm band width and 0.5 nm data pitch. The signal was averaged over three scans accumulated and corrected by buffer subtraction. CD spectra were analyzed for secondary structure using Dichroweb software (http://dichroweb.cryst.bbk.ac.uk) with the Selecon 3 program (Sreerama et al. 1999, 2000; Sreerama and Woody 2000). Thermal stability profile was obtained by recording the CD signal at 222 nm in 40–100 °C temperature range, with a scan rate of 1.0 °C/min.

Enzyme assays

*Dtur*CelB activity was detected by qualitative gel diffusion assay using Congo red dye. Carboxymethylcellulose (CMC), AVICEL, galactomannan from locust bean gum, glucomannan from konjac, xyloglucan from tamarind, xylan from birchwood, laminarin from *Laminaria digitata*, lichenan from *Cetraria islandica* were the substrates used at 0.1% in a mixture containing 50 mM sodium citrate pH 5.4 and agar 1%. The enzyme (10 µg) was added on the plates that were incubated for 1 h at 70 °C, then shaken gently for 15 min after adding Congo red dye (0.1% w/v) and finally washed with 1 M NaCl.

The mannanase activity of *Dtur*CelB was determined on konjac glucomannan (low viscosity), guar galactomannan (medium viscosity) and carob galactomannan (low viscosity) (Megazyme), adding 0.3 µg of the purified enzyme to the mixture containing various mannans in 50 mM citrate–phosphate pH 5.4 and then incubated at 70 °C for 15 min (optimal condition). The concentration of reducing ends was determined with Nelson–Somogyi (NS) method (Nelson 1944) using mannose as standard.

The endoglucanase activity of *Dtur*CelB was determined adding 2.5 µg of the purified enzyme to the mixture containing CMC in 50 mM citrate–phosphate pH 5.4 and then incubated at 70 °C for 1 h (Limauro et al. 2001). The concentration of reducing ends was determined using glucose as standard. The colored complex between oxidized sugar and arsenomolybdate absorbance was spectrophotometrically measured at 520 nm. One unit of β-1,4 endomannanase/β-1,4 endoglucanase was defined as the amount of enzyme that releases 1 µmol of reducing sugar per min in 50 mM citrate–phosphate pH 5.4 and at 70 °C herein reported as optimal conditions. All the assays were carried out in triplicate and repeated three times. Data are reported as mean ± SD.

Enzyme characterization

All enzyme characterizations were carried out on konjac glucomannan as substrate.

Optimal pH of *Dtur*CelB activity was investigated at 70 °C in a range from pH 4.0 to 8.0 in the following buffers: 50 mM citrate–phosphate (pH 4.0–6.4), 50 mM Hepes (pH 7.0 and 8.0). All the buffers were measured at 70 °C. The enzyme was assayed at 70 °C for 15 min and the concentration of reducing ends was determined with NS method.

pH stability was performed by incubating the enzyme in buffer solutions for 1 h at different pHs ranging from 4.0 to 8.0 at room temperature, then the substrate was added for

15 min at 70 °C and the concentration of reducing ends was estimated under optimal conditions.

Optimal temperature of *Dtur*CelB was measured in the range 30–90 °C at pH 5.4; the thermostability was assessed incubating the enzyme in 50 mM citrate–phosphate pH 5.4 at different temperatures from 60 to 75 °C for different times (0–4 h) and assaying the residual activity at the optimal conditions.

The kinetic parameters of *Dtur*CelB were determined incubating 0.3 µg of *Dtur*CelB at 70 °C for 15 min, in the presence of increasing glucomannan concentration in the range 0.0–5.0 mg/ml, and measuring the activity as reported above. V_{max} and K_M were calculated through the program GraphPad Prism6 using the Michaelis–Menten plot.

The influence on enzyme activity of different chemicals was tested using the following concentrations: 1 mM of metal ions, 1 mM EDTA, 0.5% detergents, 1 mM DTT and NaCl and KCl ranging 0.0–1.0 M. The reaction mix was incubated for 1 h at 37 °C and the enzymatic activity was measured at pH 5.4 at 70 °C as reported above using glucomannan as substrate.

Results and discussion

Bioinformatic analysis

To discover new GHs present in the cellulolytic hyperthermophilic bacterium *D. turgidum*, a careful analysis of carbohydrate-active enzymes database (CAZy) (http://www.cazy.org) was carried out.

The genome of *D. turgidum* DSM 6724 showed different endoglucanases (Lombard et al. 2014); among these, Dtur_0671 (accession number WP_012583041.1) encoding a putative endoglucanase belonging to GH5 family was chosen to be characterized. In addition, bioinformatic analysis revealed: (1) a possible cytoplasmic localization of the protein as suggested by the absence of signal peptide showed by pSORTb analysis; (2) the presence of only one N-glycosylation site (Asn 14) as revealed by NetNGlyc program that could not interfere with the production of an active recombinant protein in *E. coli*. Further analysis on CAZy showed that the putative enzyme does not carry the carbohydrate-binding module (CBM) still confirming that the GH could be intracellular. These features increase the possibility to obtain a soluble protein in *E. coli*.

Multiple sequence alignment and Blast analyses revealed high sequence identity with different endoglucanases from thermophilic and/or cellulolytic bacteria. In detail, the protein shows 90% identity with WP_012547750.1 from *D. thermophilus*, 59% with WP_004082285.1 (Cel5B) from *Thermotoga maritima*, previously characterized (Chhabra et al. 2002), 58% with WP_045165963.1 from *Thermoanaerobacter cellulolyticus*, 50% with WP_010247379.1 from *Acetivibrio cellulolyticus* (Fig. 1). Further bioinformatic analyses were performed with Phyre 2 (http://www.sbg.bio.ic.ac.uk/phyre2) and I-TASSER (http://zhanglab.ccmb.med.umich.edu/I-TASSER/) showed that the residues involved in acid/base catalysis (E141 and E261) are conserved and the protein maintains the classical $(\alpha/\beta)_8$ TIM barrel fold typical of GH5 family.

The genomic environment of Dtur_0671 (Dtur_0664–Dtur_0671) was also analyzed (Fig. S1, Supplementary Materials) and showed a similar organization with respect to the related thermophilic bacteria *T. maritima* (NC_000853.1) (Chhabra et al. 2002) and *Caldanaerobius polysaccharolyticum* (Han et al. 2010). In detail, Dtur_0664 encodes a putative extracellular solute-binding-protein belonging to family 5; Dtur_0665 and Dtur_0666 encode binding-protein-dependent transport system inner membrane proteins; Dtur_0667 and Dtur_0668 encode oligopeptide/dipeptide ABC transporter ATPases, Dtur_0669 encodes a putative cellulase that could have an extracytoplasmic destination (as suggested by the pSORTb and NetNGlyc analyses that indicate the presence of a peptide signal and many glycosylation sites, respectively). Dtur_0670 encodes the endoglucanase *Dtur*CelA that was previously characterized (Brumm et al. 2011a, b); Dtur_0671 encodes a putative protein that we named *Dtur*CelB to maintain the similar nomenclature adopted in other microorganisms.

Expression and purification of *Dtur*CelB

The synthesis of *Dtur_0671* DNA sequence was commissioned to Eurofins MWG Operon using *E. coli* codon usage. The gene was cloned in the expression vector pET30b (+). The recombinant protein with a C-terminal histidine tag was expressed in *E. coli* BL21(DE3). To purify the protein, the soluble fraction obtained after sonication was at first subjected to heat treatment and then to IMAC chromatography. The results of these purification steps are summarized in Table 1. The protein was purified to near homogeneity as revealed by SDS–PAGE analysis (Fig. 2a) showing a single band with a molecular mass of ~ 40 kDa, according with the predicted molecular weight of 40457. The yield of the purified protein was about 3 mg for a liter of culture.

The identity of *Dtur*CelB was confirmed both by Western blot analysis (Fig. 2b) and by liquid chromatography electrospray ionization tandem mass spectrometry (LC/MS/MS) of tryptic digests.

Structural analysis of *Dtur*CelB

To gain insight into the quaternary structure of *Dtur*CelB, the enzyme was analyzed by a size-exclusion chromatography coupled with a quasi-elastic light scattering

Fig. 1 CLUSTAL multiple sequence alignment by MUSCLE (3.8). DturCelB (WP_012583041.1) was aligned with: endoglucanases from: *D. thermophilus* (WP_012547750.1), *Thermotoga maritima* (WP_004082285.1), *Thermoanaerobacter cellulolyticus* (WP_045165963.1), *Acetovibrio cellulolyticus* (WP_010247379.1). The two conserved glutamate residues, catalytic nucleophile (E141) and the general acid/base (E261), involved in acid/base catalysis are highlighted in bold

Table 1 Purification of *Dtur*CelB of *D. turgidum* expressed in *E. coli*

Purification step	Total proteins (mg)	Total activity (U)	Specific activity (U/mg)	Purification factor	Yield (%)
Cellular extract	232.2	3217.53	13.85	1	100
Heat treatment	32.5	3049.40	93.82	6.72	94.7
Affinity chromatography	3	650.9	216.96	15.66	20.2

The enzyme activity was measured using glucomannan as substrate at each purification step

methodology. The results showed in Fig. S2 indicated a homogenous protein with a monomeric structure and a molecular weight of about 43 kDa.

To assess the secondary structure of *Dtur*CelB, far-UV CD spectra in the 190–260 nm region were recorded; α-helical, β turn and random coil content was estimated at both 25 and 70 °C. As showed in Fig. S3a, the CD spectra have similar overall shape and the α/β content is comparable at both the temperatures. The heat stability of the protein was monitored by CD analysis following molar ellipticity per residue at 222 nm from 40 to 100 °C. The thermal midpoint (Tm) of 88 °C (Fig. S3b) indicated that *Dtur*CelB is very stable at high temperatures.

*Dtur*CelB substrate specificity

To first evaluate *Dtur*CelB substrate specificity, a qualitative gel diffusion assay (Fig. 3) was performed using Congo red dye and different substrates such as: (1) carboxymethylcellulose (CMC), (Fig. 3), (2) Avicel (Fig. 3b), (3) xylan (Fig. 3c), (4) xyloglucan (Fig. 3d), lichenan (Fig. 3e), laminarin (Fig. 3f), glucomannan (Fig. 3g), galactomannan (Fig. 3h). As shown, after incubation at 70 °C, the halozone in correspondence of the protein revealed that *Dtur*CelB was able to hydrolyze mainly mannans and CMC similarly to Cel5A of *T. maritima* and *Dtur*CelA of *D. turgidum* (Chhabra et al. 2002; Brumm et al. 2011a, b) and

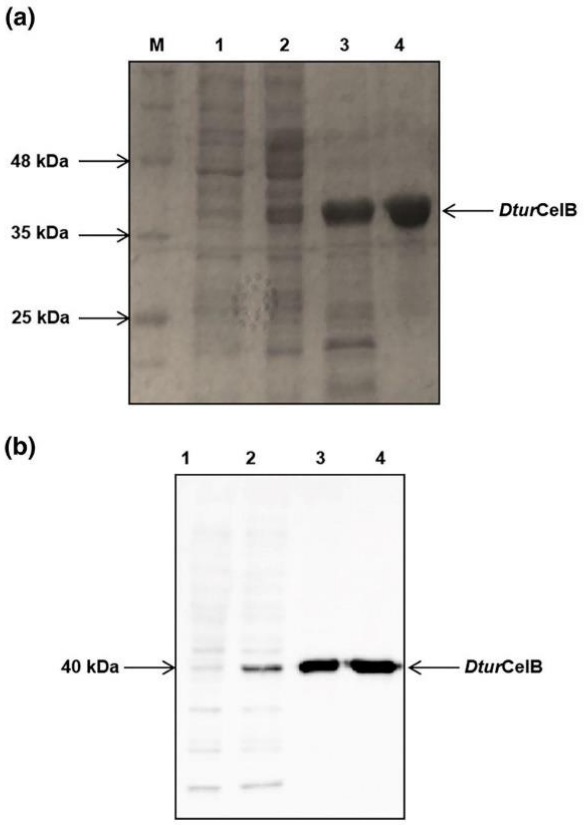

Fig. 2 Purification steps and western blot analysis of *Dtur*CelB. **a** Purification of *Dtur*CelB analyzed by SDS PAGE; lane 1, molecular marker (Applichem); lane 2, *E. coli* BL21DE3 cellular extracts after IPTG induction; lane 3, cellular extracts heat treated; lane 4, IMAC chromatography. **b** Western blot analysis with penta-His HRP conjugated mAb; lane 1, BL21DE3 cell extract not induced; lane 2, BL21DE3 cell extract induced with IPTG; lane 3, cellular extract heat treated; lane 4, fraction purified by IMAC

showing only negligible activity on xyloglucans. The activity on lichenan confirms the β-1,4 endoglucanase activity; furthermore, the absence of enzymatic activity on laminarin and xylan, indicates specificity only towards β-1,4 glucose linkage. The absence of enzymatic activity observed towards Avicel could be explained by the lack of the CBM that is considered responsible for the targeting and hydrolyzing of crystalline cellulose.

With the aim to characterize mannanase and cellulase activities of *Dtur*CelB, we studied the enzymatic activity on different mannans and CMC.

The specific activity of *Dtur*CelB vs glucomannan, galactomannans and CMC was determined using the Nelson–Somogyi (NS) method (Table 2); in fact, this assay is more sensitive for measuring *Dtur*CelB cellulase activity and contemporarily does not overestimate the mannanase activity (Gusakov et al. 2011). *Dtur*CelB exhibits the highest specific activity towards glucomannan from konjac followed by galactomannans from carob and from guar, respectively. The activity on glucomannan is about 200-fold greater than that measured on CMC. In comparison to *Dtur*CelA, *Dtur*CelB shows a higher specific activity on glucomannan (3.2 fold) and galactomannan (14 fold), while it is less active on CMC (Brumm et al. 2011a, b). It is possible that the two enzymes act synergically in the cell to hydrolyze oligosaccharides that are derived from the digestion of hemicellulose and cellulose.

Effect of pH and temperature on *Dtur*CelB

*Dtur*CelB optimal pH was determined on glucomannan. As shown in Fig. 4a, the maximal activity was measured at pH 5.4, while the enzyme retained more than 70% of activity between pH 5.0 and pH 6.4; at a more acidic or basic pH, instead, a greater decrease in the endomannanase activity was detected. Other endomannases belonging to GH5 family can display a different range of optimal pH (Srivastava and Kapoor 2017), suggesting that this feature is not shared by family members. For example, these values are similar to that of the endomannanase of *Clostridium cellulovorans* (pH 5.5–7.0), but very dissimilar with respect to the endomannanase of *Bacillus nealsonii* PN11 (pH 8.8).

To determine the optimal temperature, the endomannanase activity was evaluated in the range from 30 to 90 °C: *Dtur*CelB showed 100% activity at 70 °C, as shown in Fig. 4b. In particular, *Dtur*CelB activity gradually decreased when the assays were performed at lower temperatures, while a sudden drop in enzymatic activity was determined when the temperature was increased up to 90 °C. The same behavior was observed, when the endoglucanase activity was determined on CMC.

The thermostability of the enzyme was functionally determined, assaying the enzyme in optimal conditions after incubation for different times (0–240 min) at different temperatures (60–75 °C) Fig. 4c. The thermal inactivation of the enzyme followed a first-order kinetic with a half-life (T) of 268 min at 60 °C, 241 min at 65 °C, 157 min at 70 °C, 26 min at 75 °C. The discrepancy between optimal temperature and thermal resistance has been verified for other β-1,4 endomannanases (Yang et al. 2015) and the reason could be that the enzyme is stabilized by the presence of the substrate at its optimal temperature.

The pH stability of *Dtur*CelB was measured after 1 h of incubation at room temperature in the different buffers ranging from pH values 3.0 to 9.0 and then *Dtur*CelB was assayed under optimal conditions. The results showed that about 70% of activity was retained at pH 4.00, while more than 90% was conserved in the range 5.0–9.0 (Fig. 4d).

*Dtur*CelB kinetic parameters were also determined on both glucomannan and CMC in optimal conditions, reported

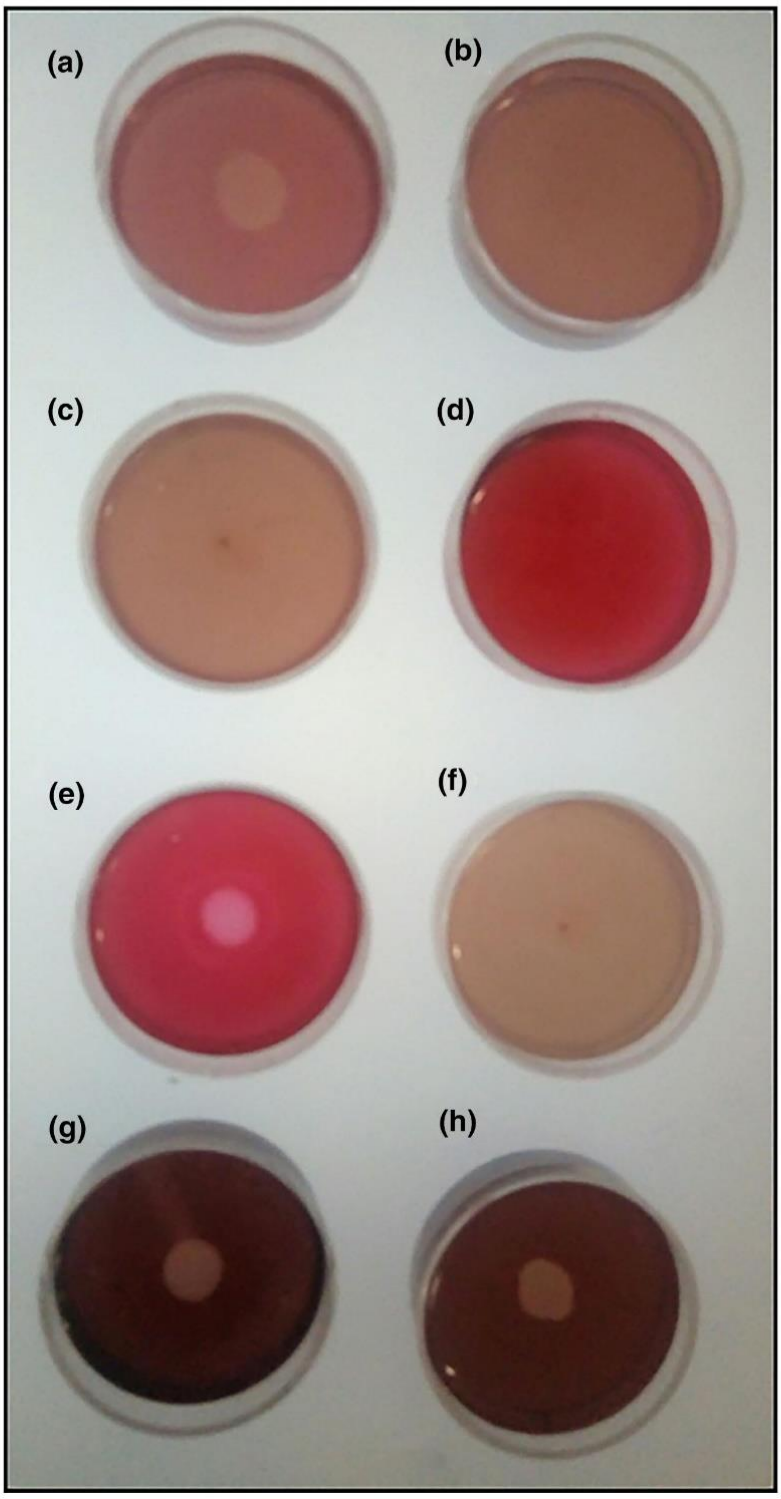

Fig. 3 Gel diffusion assay for glycoside hydrolase activity *Dtur*CelB. Agar plate with 0.1% of different substrates stained with Congo red dye to evaluate the enzymatic activity of *Dtur*CelB. **a** CMC, **b** Avicel, **c** xylan, **d** xyloglucan (β-1,4 glucan backbone with α-1,6 linked xylose sidechains), **e** lichenan (β-1,3 and β-1,4 glucan chain), **f** laminarin (β-1,3 and β-1,6 glucan chain), **g** glucomannan, **h** galactomannan

in "Materials and methods": K_M and V_{max} values on glucomannan were 4.70 mg/ml and 473.1 µmol/min mg, while on CMC they were 1.83 mg/ml and 1.349 µmol/min mg, respectively. The V_{max} value vs glucomannan is higher than that calculated for other thermostable endomannanases (V_{max} = 114 U/mg in *T. petrophila* (Dos Santos et al. 2012),

Table 2 Substrate specificity of *Dtur*CelB vs different mannans, CMC and lichenan

Substrate	Main linkage (monomer)	Sugar ratio	Specific activity (U/mg)	Relative activity (%)
Glucomannan (konjac)	1,4-β-(Mannose)	Glucose: mannose = 40/60	215	100
Galactomannan (carob)	1,4-β-(Mannose)	Galactose: mannose = 22/78	28.7	13.3
Galactomannan (guar)	1,4-β-(Mannose)	Galactose: mannose = 38/62	3.08	1.43
CMC	1,4-β-(Glucose)	Glucose 100%	0.9	0.41
Lichenan	β-1,3: β-1,4 (glucose)	Glucose 100%	0.3	0.33

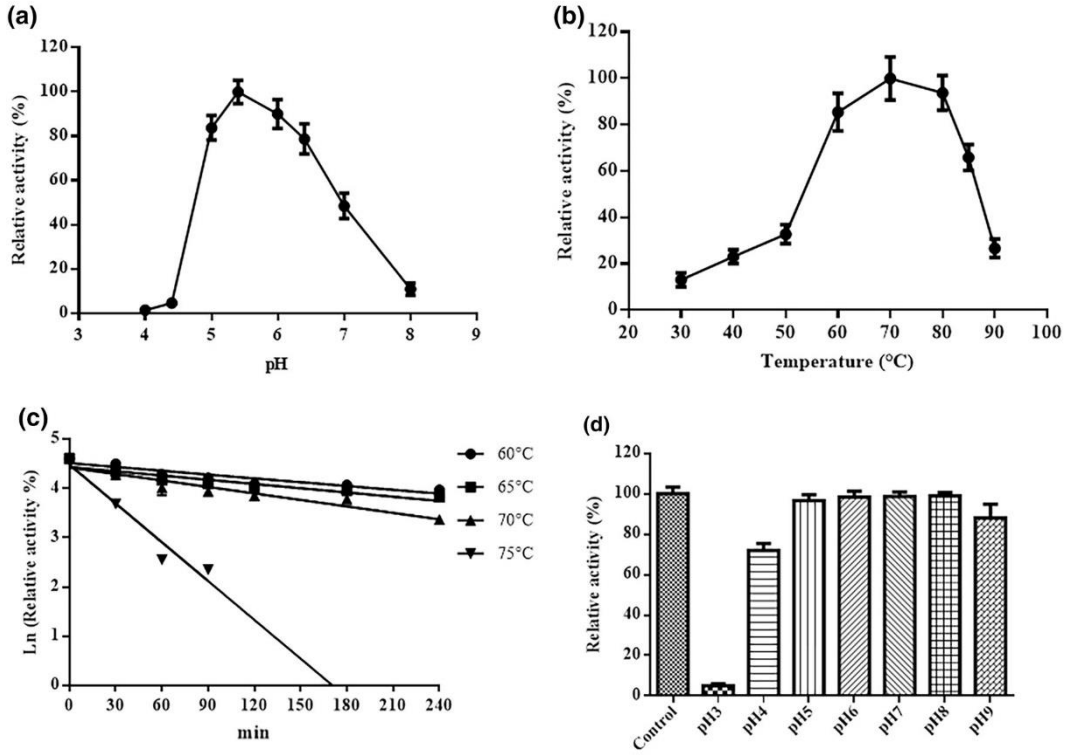

Fig. 4 The effect of pH and temperature on enzymatic activity of *Dtur*CelB. **a** pH optimum was measured in buffers ranging from pH 4.0 to pH 8.0. **b** Temperature optimum was determined in the range 30–90 °C. **c** Thermostability of *Dtur*CelB: the enzyme was incubated at 60, 65, 70, 75 °C for different times and then assayed for residual activity at the optimal conditions. **d** pH stability of *Dtur*CelB: the enzyme was incubated in various buffers (pH 3.0–9.0) for 1 h and assayed for residual activity at the optimal conditions

and V_{max} = 243 U/mg of *Aspergillus niger* BK01 (Do et al. 2009).

Effects of chemical agents on the activity of *Dtur*CelB

The effect of various metal ions, chemicals and detergents on *Dtur*CelB activity was tested and the results are reported in Table 3. Mg^{2+}, Co^{2+}, Fe^{3+}, Zn^{2+}, Mn^{2+} partially inhibited the enzyme, while Cu^{2+} and Ag^{+}, strongly affected *Dtur*CelB activity. On the other hand, Ca^{2+} had a moderate effect on the enzyme which maintained 87% of the activity. As reported for many endomannanases, previously characterized, the metal ion effect varies within different microorganisms (Chen et al. 2016). For example, structural characterization of Cel5A of *T. maritime,* showed that Cd^{2+} metal ions have a strong inhibition effect on the enzymatic activity, because they bind the active site inhibiting substrate recognition (Pereira et al. 2010), while Ag^{+} metal ions are reported to be strong inhibitors of various fungal mannanases (Yang et al. 2015). The influence of various chemicals such as EDTA, DTT was also determined; as shown in Table 3, the enzymatic activity is affected neither by the presence of the chelating agent, suggesting that *Dtur*CelB is not a

Table 3 Effect of metal ions and reagents on *Dtur*CelB activity

Metal ion or chemical agent	Concentration	Relative activity (%)
None	1 mM	100
$CuCl_2$	1 mM	8.71
$FeCl_3$	1 mM	41.6
$AgNO_3$	1 mM	12
$ZnSO_4$	1 mM	48.3
LiCl	1 mM	40
$MgCl_2$	1 mM	34
$CaCl_2$	1 mM	87
$MnCl_2$	1 mM	45.3
$CoSO_4$	1 mM	45
EDTA	1 mM	100
DTT	1 mM	100
SDS	0.5%	1
Triton X-100	0.5%	43.59
Tween 20	0.5%	76.73
ECOR	0.5%	100

metal enzyme, or by the presence of DTT, suggesting that the oxidation state of cysteine is not involved in the catalysis. Regarding surfactants, ionic SDS completely abolished the enzymatic activity, while Tween 20 and Triton X-100 had only a moderate effect; interestingly, for a biotechnological application, a commercial biological detergent (ECOR) did not inactivate all *Dtur*CelB (Table 3). The halotolerance was measured in the presence of increasing concentration of KCl and NaCl in the range 0–1 M. The enzyme retains about 50 and 79% of activity in a mixture containing 0.4 M NaCl or KCl, respectively, while at 1 M of both salts, the activity dropped off drastically (Fig. S4).

Conclusions

In this study, the recombinant *Dtur*CelB was expressed in *E. coli*, purified and biochemically characterized. Enzymes belonging to the family GH5 like *Dtur*CelB with both endomannanase and endoglucanase activity are quite rare; some examples have been found in thermophilic bacteria such as *C. polysaccharolyticus* (Han et al. 2010) and *T. maritima* (Chhabra et al. 2002). Furthermore, different from other endomannanases, *Dtur*CelB showed higher activity on glucomannan than galactomannans (Seesom et al. 2017). Overall, *Dtur*CelB similar to other reported endomannanases is stable in a wide range of pH, but, in addition, shows a much higher thermoresistance (Chauhan et al. 2012; Mendoza et al. 1994; Zakaria et al. 1998; Zhang et al. 2000; Xu et al. 2002; Zhang et al. 2009). In general, most of the endomannanases characterized from mesophilic/thermophilic microorganisms, such as those identified in different *Bacillus* species (Seesom et al. 2017), show an optimum temperature between 45 and 60 °C, lower than *Dtur*CelB. These features make *Dtur*CelB a very interesting enzyme for future applications. In fact, the biotechnological request of endomannanases covers different fields: in the food and feed industries, enzymatic hydrolysis of mannans can produce potentially health-promoting mannan-oligosaccharides (MOSs), prebiotics that stimulate the production of beneficial gut microflora, thus improving the human intestinal microbial balance (Wilson and Whelan 2017). In the production of fruit juices and coffee processing, the endomannanases are useful to reduce the high viscosity of the products that represents a real bottleneck for their commercialization. Of course, regarding the biofuel production, mannans degrading enzymes can be coupled with other GHs to convert lignocellulosic biomass into fermentable sugar to produce bioethanol.

This study also highlights that the genes encoding putative proteins involved in the transport of oligosaccharides (Dtur_0664-0668), the secreted cellulase (Dtur_0669) and intracellular cellulases/endomannanases (*Dtur*CelA and *Dtur*CelB) are clustered in *D. turgidum.* This evidence suggests the existence of an efficient alternative for the cellulosome for the growth of this microorganism on different polysaccharides.

Acknowledgements This work was supported by BIOPOLIS: PON03PE_00107_1 CUP: E48C14000030005.

References

Acharya S, Chaudhary A (2012) Bioprospecting thermophiles for cellulase production: a review. Braz J Microbiol 43:844–856

Álvarez C, Reyes-Sosa FM, Díez B (2016) Enzymatic hydrolysis of biomass from wood. Microb Biotechnol 9:149–156

Aulitto M, Fusco S, Fiorentino G, Limauro D, Pedone E, Bartolucci S, Contursi P (2017) *Thermus thermophilus* as source of thermozymes for biotechnological applications: homologous expression and biochemical characterization of an α-galactosidase. Microb Cell Fact 16:28

Brumm PJ, Hermanson S, Luedtke J, Mead DA (2011a) Identification, cloning and characterization of *Dictyoglomus turgidum* CelA, an endoglucanase with cellulose and mannanase activity. J Life Sci 5:488–496

Brumm PJ, Hermanson S, Hochstein B, Boyum J, Hermersmann N, Gowda K, Mead DA (2011b) Mining *Dictyoglomus turgidum* for enzymatically active carbohydrases. Appl Biochem Biotechnol 163:205–214

Brumm PJ, Gowda K, Robb FT, Mead DA (2016) The complete genome sequence of hyperthermophile *Dictyoglomus turgidum* DSM 6724™ reveals a specialized carbohydrate fermentor. Front Microbiol 20:1979

Capolupo L, Faraco V (2016) Green methods of lignocellulose pretreatment for biorefinery development. Appl Microbiol Biotechnol 100:9451–9467

Chauhan PS, Puri N, Sharma P, Gupta N (2012) Mannanases: microbial sources, production, properties and potential biotechnological applications. Appl Microbiol Biotechnol 93:1817–1830

Chen CY, Huang YC, Yang TY, Jian JY, Chen WL, Yang CH (2016) Degradation of konjac glucomannan by *Thermobifida fusca* thermostable beta-mannanase from yeast transformant. Int J Biol Macromol 82:1–6

Chhabra S, Shockley K, Ward DE, Kelly RM (2002) Regulation of endo-acting glycosyl hydrolases in the hyperthermophilic bacterium *Thermotoga maritima* grown on glucan- and mannan-based polysaccharides. Appl Environ Microbiol 68:545–554

Contursi P, Fusco S, Limauro D, Fiorentino G (2013) Host and viral transcriptional regulators in *Sulfolobus*: an overview. Extremophiles 17:881–895

Del Giudice I, Limauro D, Pedone E, Bartolucci S, Fiorentino G (2013) A novel arsenate reductase from the bacterium *Thermus thermophilus* HB27: its role in arsenic detoxification. Biochim Biophys Acta 1834:2071–2079

Dhawan S, Kaur J (2007) Microbial mannanases: an overview of production and applications. J Crit Rev Biotechnol 27:197–216

Do BC, Dang TT, Berrin JG, Haltrich D, To KA, Sigoillot JC, Yamabhai M (2009) Cloning, expression in *Pichia pastoris*, and characterization of a thermostable GH5 mannan endo-1,4-beta-mannosidase from *Aspergillus niger* BK01. Microb Cell Fact 13:59

Dos Santos CR, Paiva JH, Meza AN, Cota J, Alvarez TM, Ruller R et al (2012) Molecular insights into substrate specificity and thermal stability of a bacterial GH5-CBM27 endo-1,4-β-D-mannanase. J Struct Biol 177:469–476

Elleuche S, Schröder C, Sahm K, Antranikian G (2014) Extremozymes–biocatalysts with unique properties from extremophilic microorganisms. Curr Opin Biotechnol 29:116–123

Elleuche S, Schäfers C, Blank S, Schröder C, Antranikian G (2015) Exploration of extremophiles for high temperature biotechnological processes. Curr Opin Microbiol 25:113–119

Gusakov AV, Kondratyeva EG, Sinitsyn AP (2011) Comparison of two methods for assaying reducing sugars in the determination of carbohydrase activities. Int J Anal Chem 2011:283658

Han Y, Dodd D, Hespen CW, Ohene-Adjei S, Schroeder CM, Mackie RI et al (2010) Comparative analyses of two thermophilic enzymes exhibiting both beta-1,4 mannosidic and beta-1,4 glucosidic cleavage activities from *Caldanaerobius polysaccharolyticus*. J Bacteriol 192:4111–4121

Kolpak FJ, Blackwell J (1976) Determination of the structure of cellulose II. Macromolecules 9:273–278

Kublanov IV, Perevalova AA, Slobodkina GB, Lebedinsky AV, Bidzhieva SK, Kolganova TV et al (2009) Biodiversity of thermophilic prokaryotes with hydrolytic activities in hot springs of Uzon Caldera, Kamchatka (Russia). Appl Environ Microbiol 75:286–291

Limauro D, Cannio R, Fiorentino G, Rossi M, Bartolucci S (2001) Identification and molecular characterization of an endoglucanase gene, celS, from the extremely thermophilic archaeon *Sulfolobus solfataricus*. Extremophiles 5:213–219

Limauro D, D'Ambrosio K, Langella E, De Simone G, Galdi I, Pedone C, Bartolucci S (2010) Exploring the catalytic mechanism of the first dimeric Bcp: functional, structural and docking analyses of Bcp4 from *Sulfolobus solfataricus*. Biochimie 92:1435–1444

Lombard V, Golaconda Ramulu H, Drula E, Coutinho PM, Henrissat B (2014) The carbohydrate-active enzymes database (CAZy) in 2013. Nucleic Acids Res 42:D490–D495

Malgas S, van Dyk JS, Pletshke BI (2015) A review of the enzymatic hydrolysis of mannans and synergic interactions between β-mannanase, β-mannosidase and α-galactosidase. Word J Microbiol Biotechnol 31:1167–1175

Mendoza NS, Arai M, Kawaguchi T, Yoshida T, Joson LM (1994) Purification and properties of mannanase from *Bacillus subtilis*. World J Microbiol Biotechnol 10:551–555

Nelson N (1944) A photometric adaptation of the Somogyi method for the determination of glucose. J Biol Chem 153:376–380

Pereira JH, Chen Z, McAndrew RP, Sapra R, Chhabra SR, Sale KL, Simmons BA, Adams PD (2010) Biochemical characterization and crystal structure of endoglucanase Cel5A from the hyperthermophilic *Thermotoga maritima*. J Struct Biol 172:372–379

Rytioja J, Hildén K, Yuzon J, Hatakka A, De Vries RP, Mäkelä MR (2014) Plant-polysaccharide-degrading enzymes from Basidiomycetes. Microbiol Mol Biol Rev 78:614–649

Sadhu S, Maiti TK (2013) Cellulase Production by Bacteria: a review. Brit Microbiol Res J 3:235–258

Sarcinelli C, Fiorentino G, Pizzo E, Bartolucci S, Limauro D (2016) Discovering antioxidant molecules in the archaea domain: peroxiredoxin Bcp1 from *Sulfolobus solfataricus* Protects H9c2 cardiomyoblasts from oxidative stress. Archaea 2016:7424870

Sarmiento F, Peralta R, Blamey JM (2015) Cold and hot extremozymes: industrial relevance and current trends. Front Bioeng Biotechnol 20:148

Scheller HV, Ulvskov P (2010) Hemicelluloses. Annu Rev Plant Biol 61:263–289

Seesom W, Thongket P, Yamamoto T, Takenaka S, Sakamoto T, Sukhumsirichart W (2017) Purification, characterization, and overexpression of an endo-1,4-β-mannanase from thermotolerant *Bacillus sp.* SWU60. World J Microbiol Biotechnol 33:53

Sreerama N, Woody RW (2000) Estimation of protein secondary structure from circular dichroism spectra: comparison of CONTIN, SELCON, and CDSSTR methods with an expanded reference set. Anal Biochem 287:252–260

Sreerama N, Venyaminov SY, Woody RW (1999) Estimation of the number of α-helical and β-strand segments in proteins using circular dichroism spectroscopy. Protein Sci 8:370–380

Sreerama N, Venyaminov SY, Woody RW (2000) Estimation of protein secondary structure from circular dichroism spectra: inclusion of denatured proteins with native proteins in the analysis. Anal Biochem 287:243–251

Srivastava PK, Kapoor M (2017) Production, properties, and applications of endo-β-mannanases. Biotechnol Adv 35:1–19

Svetlichny VA, Svetlichnaya TP (1988) *Dictyoglomus turgidus* sp. nov., a new extremely thermophilic eubacterium isolated from hot springs of the Uzon volcano caldera. Mikrobiologiia 57:364–369

Wilson B, Whelan K (2017) Prebiotic inulin-type fructans and galactooligosaccharides: definition, specificity, function, and application in gastrointestinal disorders. J Gastroenterol Hepatol 32:64–68

Xu BZ, Hagglund P, Stalbrand H, Janson JC (2002) Endo-beta-1,4-mannanases from blue mussel, Mytilus edulis: purification, characterization, and mode of action. J Biotechnol 92:267–277

Yamabhai M, Sak-Ubol S, Srila W, Haltrich D (2016) Mannan biotechnology: from biofuels to health. Crit Rev Biotechnol 36:32–42

Yang H, Shi P, Lu H, Wang H, Luo H, Huang H et al (2015) A thermophilic β-mannanase from *Neosartorya fischeri* P1 with broad pH stability and significant hydrolysis ability of various mannan polymers. Food Chem 15:283–289

Zakaria MM, Yamamoto S, Yagi T (1998) Purification and characterization of an endo-1,4-β-mannanase from *Bacillus subtilis* KU-1. FEMS Microbiol Lett 158:25–31

Zhang J, He ZM, Hu K (2000) Purification and characterization of beta-mannanase from *Bacillus licheniformis* for industrial use. Biotechnol Lett 22:1375–1378

Zhang M, Chen XL, Zhang ZH, Sun CY, Chen LL, He HL, Zhou BC, Zhang YZ (2009) Purification and functional characterization of endo-beta-mannanase MAN5 and its application in oligosaccharide production from konjac flour. Appl Microbiol Biotechnol 83:865–873

2.2 Biochemical characterization of a thermostable β-glucosidase from *Dictyoglomus turgidum*.

Francesca Anna Fusco, Gabriella Fiorentino, Patrizia Contursi, Simonetta Bartolucci,

Danila Limauro*

Dipartimento di Biologia, University of Naples Federico II, Complesso universitario di Monte S. Angelo, Via Cinthia, Naples, Italy

*Corresponding author: Danila Limauro, E-mail: limauro@unina.it

Keywords

β-glucosidase, thermophilic enzyme, *Dictyoglomus turgidum*

Manuscript in preparation

Abstract

Dtur_0462 gene of the hypertermophilic bacterium *Dictyoglomus turgidum*, encoding a β-glucosidase, was synthetically produced and expressed in *Escherichia coli* BL21(DE3)-RIL strain. *Dtur*βGlu was purified to homogeneity by affinity chromatography and its homoterameric structure was estabilished by gel filtration. The monomer is composed by 418 amino acidic residues and showed high sequence similarity with Glycoside hydrolases (GHs) belonging to GH1 family. The maximum activity of *Dtur*βGlu was observed at 80°C and at pH 5.4. The enzyme is active on *p*-nitrophenyl-β-D-glucopyranoside (*p*NPGlu) and *p*-nitrophenyl- β-D-galactopyranoside (*p*NPGal) with K_M values of 0.82 mM and 1.36 mM respectively. It also exhibits appreciable hydrolytic activity towards salicin and measurable activity towards cellobiose. *Dtur*βGlu was stable in the range of pH 5-8 and after 2 h of incubation at 70°C it retained 70% of its activity. Metal ions and chemical reagents had different influences on the activity of β-glucosidase; metal ions generally affected ~ 50% the *Dtur*βGlu activity; while the supplementation of several monosaccharides reduced the activity by only 10%. Conversely, in presence of non-ionic detergent such as Tween-20 and Triton X-100 the activity of *Dtur*βGlu is increased by 180% and 120% respectively.

The capacity to hydrolyze different substrates, the good thermal resistance, and the ability to be activated in the presence of surfactants make this enzyme a potential candidate for industrial application.

Introduction

β-glucosidases (EC 3.2.1.21) are a heterogeneous group of enzymes that catalyze the hydrolysis of β-D-glycosidic bonds in di- and oligo-glucosaccharides and several other glycoconjugates (1) and often they are also involved in transglycosylation reactions. These enzymes have been classified into six glycoside hydrolase (GH) families (GH1, GH3, GH5, GH9, GH30 and GH116) based on their amino acid sequences (2). β-Glucosidases are widely distributed and have important roles in many biological pathways, such as degradation of structural and storage polysaccharides, cellular signaling, oncogenesis, host-pathogen interactions, as well as in several biotechnological applications (3). In this regard, β-glucosidases are widely used in the biorefinery for biomass conversion, in particular in the final step of cellulose breakdown that produces glucose (4) and in the hydrolysis of different compounds such as aryl-beta-glucosides, flavanoids and isoflavanoid-glucosides. These compounds are commonly found in fruits, vegetables, soy, tea and the release of the aglycone group by β-glucosidases has a powerful biological activity, with different uses in the field of medicine (as antitumor agents or for the treatment and prevention of cardiovascular disease and osteoporosis) (5), in general in biomedical research and in the food industry to enhance the

quality of the beverages and foods (6). In addition to hydrolytic activity, many β-glucosidases can catalyze the formation of glycosidic bonds by or thermodynamically controlled reverse hydrolysis or kinetically controlled transglycosylation. This feature, makes β-glucosidases promising biocatalysts for the synthesis of stereo- and regiospecific glycosides or oligosaccharides which are potentially useful as functional materials, nutraceuticals, or pharmaceuticals because of their various biological properties (7). Currently, the transglycosilation activity by β-glucosidases is the method employed by industry for production of galacto-oligosaccharides (GOS) from lactose (8). Thermostable β-glucosidases are adapted to work in harsh condition, so they offer several advantages, in industrial applications, promoting faster reactions, high solubility of the substrate, a lower risk of contamination, and also lowering the solution viscosity and increasing the miscibility of the solvent (9). *Dictyoglomus turgidum* is an hyperthemophilic and anaerobic microorganism isolated in 1985 from hot springs of the Kamchatka peninsula in Russia (10); it is able to grow on a wide range of substrates including starch, cellulose, pectin, carboxymethylcellulose and lignin. Its genome was sequenced for carbohydrases and contains six annotated β-glucosidases (Dtur_0219; Dtur_0289; Dtur_0321; Dtur_0462; Dtur_1723, and Dtur_1799) (11). With the aim to investigate on new thermostable β-glucosidase we have choosen Dtur_0462 (11) belonging to GH 1 family encoding the enzyme here named *Dtur*βGlu. The gene was synthetically produced and codon-adapted to *Escherichia coli*. The recombinant protein was biochemically characterized also regarding different substrates hydrolysis and physical-chemical parameters.

Materials and methods

Expression of *Dturβ*Glu in *E. coli*

DturβGlu (Dtur_0462) from *D. turgidum* genome (GenBank: NC_011661.1) was synthesized by Genewiz (GENEWIZ LLC 115 Corporate Blvd.South Plainfield, NJ USA) with following changes: 1) the codon usage of the gene was optimized for the expression in *E. coli* 2) at 5' and 3'ends of the gene the *Nde*I and *Xho*I restriction sites respectively was inserted to allow the cloning in pET-30b(+) vector (Novagen). The recombinant vector pET30/*DturβGlu* was used to transform *E. coli* strain BL21(DE3)-RIL. The transformants were selected on LB plates containing ampicillin 50 µg/ml and chloramphenicol 33 µg/ml at 37 °C and grown in same condition in LB until 0.5 OD monitoring absorbance at 600nm. Gene expression was then induced by the addition of 0.25 mM isopropyl-β-D-thiogalactopyranoside (IPTG) and cells were harvested by centrifugation 2 hours later.

Enzyme purification

Pellets from 1 liter cultures were re-suspended in 50 mM Tris-HCl pH 8.0 supplemented with an inhibitor cocktail protease EDTA-FREE (Roche) and disrupted by sonication with 20 min pulses at

20 Hz (Sonicator Ultrasonic liquid processor; HeatSystem Ultrasonics). The suspension was clarified by ultracentrifugation at 16,000xg for 30 min. The soluble fractions of the cell extracts were heated at 70°C for 15 min, and then centrifuged at 16,000xg at 4°C.

Protein was purified almost to homogeneity in a one stage process using affinity chromatography on HisTrapHP column (GE Healthcare) (12). Proteins concentration was determined using BSA as the standard (13) and protein homogeneity was estimated by SDS-PAGE (12%).

β-glucosidase Assay

β-glucosidase assay was performed using *p*-nitrophenyl-β-Dglucopyranoside (*p*NPGlu) as substrate. The reaction mixture (100 µl) containing 4 mM *p*NPGlu, 50 mM citrate phosphate buffer pH 5.4, 0.068 µg of enzyme was incubated at 80ºC for 10 min. The reaction was stopped by addition of 100 µl of cold 0.2 M Na_2CO_3. The concentration of the released *p*-nitrophenol (molar extinction coefficient, 18.5 $mM^{-1}cm^{-1}$) was determined by measuring A_{405nm}, using microplate reader (Synergy H4 Biotek). One unit of β-glucosidase activity was defined as the amount of enzyme required to release 1 µmole of *p*-nitrophenol (*p*NP) in a minute under the assay conditions. All assays were performed in triplicate.

Biochemical characterization

Size-exclusion chromatography

Purified *Dtur*βGlu protein was analyzed by size exclusion chromatography. 100 µg of sample was loaded on BIOsep-SEC-S4000 column (Phenomenex) (300 x 7.8 mm) equilibrated in 50 mM Sodium Phosphate pH 7.2. A constant flow rate of 0.5 ml/min was applied. The column was calibrated with conalbumin (75 kD), aldolase (158 kD), ferritin (440 kD), and thyroglobulin (669 kD).

Effect of pH and temperature on enzyme activity

The optimal pH value was determined at 80°C performing the β-glucosidase assay in the following buffers: 50 mM glycine-HCl for range pH 2.0–3.0, 50 mM citrate phosphate buffer for pH 3.0–6.0, 50 mM phosphate buffer for pH 7–8, and 50 mM glycine-NaOH for pH 9.0.

The pH stability was determined performing the assay after pre-incubation of the enzyme in buffers ranging from pH 3.0 to 9.0 at 37°C for 1 h. The residual enzymatic activity was determined under the standard conditions (pH 5.4, 80°C, 10 min).

The optimal temperature was examined by measuring the enzyme activity ranging from 30°C to 100°C at optimal pH. The thermostability assay was carried out by incubating the enzyme at

temperatures ranging from 70°C to 100°C for different times (30-240 min), in optimal pH conditions. The residual activity was determined under assay conditions reported previously.

Effect of chemicals on enzyme activity

The effects of different chemicals were tested on *Dtur*βGlu activity. Metal ions (Li^{+}, Cu^{2+}, Ca^{2+}, Mn^{2+}, Mg^{2+} Co^{2+}, Zn^{2+},) were added in the reaction mix as LiCl, $CuCl_2$, $CaCl_2$, $MnCl_2$, $MgCl_2$, $CoSO_4$, $ZnSO_4$ at final concentration of 1mM; the EDTA, chelating agent, was added at the same concentration. Non-ionic detergents, (Triton X-100 and Tween-20) ionic detergent (SDS), and Dimethyl sulfoxide (DMSO) were supplemented in the assay mixture at 0.5% concentration. The monosaccharides (glucose, galactose, xylose and arabinose) were added at final concentration of 2,5 5, 10, 50 or 100 mM. The residual activity was determined in the standard conditions.

Substrate specificity and kinetic parameters

The hydrolytic activity of *Dtur*βGlu was determined on several substrates as: *o*NP-β-D-glucopyranoside (*o*NPGlu), *p*NP-β-D-xylopyranoside (*p*NPXyl), *p*NP-β-D-galactopyranoside (*p*NPGal), pNP-α-galactopyrqnoside (*p*NPαGal), *o*NP-β-D-galactopyranoside (*o*NPGal), cellobiose and salicin. Aliquots of *Dtur*βGlu were incubated with saturating concentrations of substrate in 50 mM citrate/phosphate buffer (pH 5.4) for 10 min at 80 °C (standard assay conditions) and the activity was measured by release of *p*NP and *o*-nitrophenol (*o*Np). The concentration of the released *o*NP (molar extinction coefficient, 21.3.$mM^{-1}cm^{-1}$) was determined by measuring A_{420nm}. When cellobiose and salicin were used as substrate, the amount of glucose was determinated with D-Glucose Assay Kit (GOPOD Format) (Megazyme) according to the manufactere's protocol and 1 unit (U) of acivity is defined as the amount of enzyme which is required to release 1 μmol of glucose per minute under the assay conditions.

Different range of concentrations of various substrate were used to determine kinetic parameters of *Dtur*βGlu: 0.1 - 5 mM for *p*NPGlu and *p*NPGal, 0.1 - 6.5 mM for *o*NPGlu and *o*NPGal, 0.5 - 12 mM for *p*NPXyl and 0.5 - 40 mM for salicin. The enzymatic activity was determined as reported above. The enzyme kinetic parameters, Km, Vmax, $k$cat and $k$cat/Km, were calculated by non-linear regression analysis (GraphPad 6.0 Prism software).

Results and discussion

Bioinformatic analysis of *Dtur*βGlu

The genome of *D. turgidum* was recently sequenced (11) and a depth analysis of the carbohydrate-active enzymes (CAZy) database (http://www.cazy.org/) has revealed a great number of potentially

interesting enzymes. We have chosen to study a new β-glucosidase classified as GH1 encoded by Dtur_0462.

Multiple sequence alignment (ClustalW) and Blast analyses revealed high sequence identity with different glycoside hydrolase family 1 protein from thermophilic bacteria. In details, the putative protein shows 88% identity with WP_012547332.1 from *Dictyoglomus thermophilus* (DtGH), 49% with WP_088571012.1 from *Thermoflexus hugenholtzii*, and 46% with WP_012547332.1 from *Thermogemmatispora onikobensis* (Fig. 1). Further bioinformatic analyses performed with Phyre 2 (http://www.sbg.bio.ic.ac.uk/phyre2) showed that the conserved glutamate residue in NEP and ENG (E159 and E324) motifs has been identified as potential active site acid/base catalyst and nucleophile respectively for the GH1 (14).

```
WP_088571012.1      -MVEFAFHFPSGFLWGTATSSHQVEGDNTNNDWWRWEQEPGRIRDGSRSGRACDWWRNAE
WP_069803632.1      MARERTLQFPEGFLWGTASSAHQCEGGNLNNQWYRWEQQ-GRTLTGERSGVAANWWQQAE
WP_012582847.1      ---MVKYKFPEGFLWGTATASHQIEGDNFYNDWWEFEKQ-GKVKNGQVSGKACDSWNRYE
WP_012547332.1      ---MLKYRFPEGFLWGTATASHQIEGDNFYNDWWEFEQK-GKVKNGQISGKACDSWNRYE
                           :**.*******:::** **.*  *:*:.:*:: *:   *. ** *.: *.. *

WP_088571012.1      ADFDRAAAMGQNAHRLSIEWSRIEPREGVFDDAALDRYREMLRGLRERGIEPMVTLHHFT
WP_069803632.1      RDFELAEQMENNALRLSLEWSRIEPEEGRWDESALERYRSLLADLRRRHMTPLVTLHHFT
WP_012582847.1      EDFDLIEKLNNNAYRFSIEWSRIEPEEGRFDESALERYRSMLISLRRRNIEPFVTLHHFT
WP_012547332.1      EDFDLIEKLNNNAYRFSIEWSRVEPEEGRFDQSAIERYRAMLLSLRRRNIEPFVTLHHFT
                     **:    : :** *:*:****:**.** :*::*::*** :* .**.* : *:*******

WP_088571012.1      NPLWLAEQGGWENPLTVERFERYVRHAVGALKDFCRLWCTINEPNVLAYMGWNEGKWPPG
WP_069803632.1      DPLWFADRGGFELEENIRYFVRFVRFVVGQLRDLCSFWLTINEPNVYAFLGYLTGEFPPG
WP_012582847.1      NPLWMAKRGGWLNPDIIDYYLRYVKKIVSEFKDLVNYWMTINEPNAYAFMAYLYGQFPPQ
WP_012547332.1      NPLWIAKKGGWLNSEIIDYYLRYVERIVSEFKDLVNYWMTINEPNAYAFMAYLYGQFPPQ
                     :***:*.:**:     :  : *:*.  *. ::*:   * ******. *:::.  *::**

WP_088571012.1      KRDFGLSMQVLRHLMQAHARAYHAIHEIQPEAQVGIAHNMVVFEPAHPASPLDRMIARLH
WP_069803632.1      ERSALRALRVLRNLMAAHVQAFYAIREWQPEGQIGYCLNYRLLDPFLTYSPLDRVVANLQ
WP_012582847.1      GKSLIKMLRVLNNMAKAHAKAYEVIHQISPDAKVSIAYNVIYFEPKNPNSFIDRKFANFG
WP_012547332.1      KRSLMKMLRVLNNMVKAHAKAYQVIHKISPNSKVGIAYNVIYFEPKNPKSFIDRKLTNFA
                     :.    ::**.::  **.:*: .*:: .*:.::. . *   ::*  . * :** .:.:

WP_088571012.1      DRMFNRLVLDAMAAG--REPGLAAFRTLAALRGTYDFIGLNYYTRRLSAFDRRSPATLFG
WP_069803632.1      DTFFNWLALKLAEGKPVVFPLQVALPALPRAAGARDYHGVNYYTRDLVAFDPRRAGELFG
WP_012582847.1      DRIYNRVFIETLLTG--KFSSPFIKEEIPYAKNTLDYLGINYYTR-----------ILMG
WP_012547332.1      DRIYNRVFIETLTTG--RFSSPFIKEEIPYAKDTLDYLGVNYYTR-----------ILMG
                    * ::* : :.         .       :.   .: *: *:*****           *:*

WP_088571012.1      RTFLNPHGELSD----GEYGEVFPEGLYLLLKRLARYG---KPIYVTENGIPDADDDQRP
WP_069803632.1      RRFPSPGAPMQDPGRAGYFGEIYPEGLYRVLQLVYRRTRGNKPLYVTEHGLNDLEDRLRP
WP_012582847.1      LKMGSPEGETSD-----FGWEIYPEGIYKVVKRFYGLTK--KPIYITENGISDAKDEKRP
WP_012547332.1      LRMTPPSGEKSD-----FGWEIYPEGIYKVVKRFYKLTG--KPIYITENGISDAKDEKRP
                      :  * .  .*        *::***:* ::: .       **:*:**:*: * .*  **

WP_088571012.1      RFLVRHLHAMWRAIQQNVPVRGYFHWSLVDNFEWAEGWTLRFGLIEVDPETQARRPRRSA
WP_069803632.1      RAILEHLAMLHRAIREGLPVRGYFHWTLVDNFEWNEGWGAHFGLVELNPQTQERRPRPSA
WP_012582847.1      KYLISHLIQLHRAIEEGVDVRGYFHWSLMDNFEWAEGFLQRFGLFETDFNTFERKWRESA
WP_012547332.1      KYLISHLIQLHKAIEDGVDIKGYFHWSLVDNFEWAEGFLQRFGLFETDFNNFERKWRKSA
                   : :: **  : :**.:.: ::*****:*:***** **:  :***.* : :.  *: * **

WP_088571012.1       DLYAEVCRANALTSETIIRHTPELLEEMFGISIG---------
WP_069803632.1       SMFGEICRANAITESIVERYAPEAAATIFGSAAATRLGARVLT (88%)
WP_012582847.1       RIYSEIAKNNGITEAMEEKFLK---------------------- (49%)
WP_012547332.1       RIYSEIAKNNGITEEMEKEFLK---------------------- (46%)
```

Fig. 1 Multiple alignment of *Dtur*βGlu with other GH1 protein from *D. thermophilus*, *T. hugenholtzii*, and *T. onikobensis.* The two conserved glutamate residues, catalytic nucleophile (E324) and the general acid/base (E159), involved in the catalysis are highlighted in bold.

Expression and biochemical characterizationof *Dtur*βGlu

Dtur_0462 was synthetically produced and codon-adapted to *E. coli*. The gene was cloned in the expression vector pET30b(+) and the recombinant protein, with His tagged at C-terminal, named *Dtur*βGlu, was expressed in *E. coli* BL21(DE3)-RIL strain. The protein was purified by heat-treatment and His-trap affinity chromatography. The results of these purification steps are summarized in Table 1.

Table 1 Purification of *Dtur*βGlu of *D. turgidum* expressed in *E. coli*

Purification step	Total proteins (mg)	Total activity (U)	Specific activity (U/mg)	Purification factor	Yield
Cellular extract	152.8	3702.6	24.2	1	100%
Heat treatment	54.94	1502.23	40.7	1.68	40.5%
Affinity chromatography	1	160	160	6.61	4.32%

As revealed by SDS-PAGE analysis (Fig. 2), *Dtur*βGlu showed a single band with a molecular mass of ~ 50 kDa, according with the predicted molecular weight of 50615 Da corresponding to the theoretical value. The yield of the purified protein was about 1 mg/L.

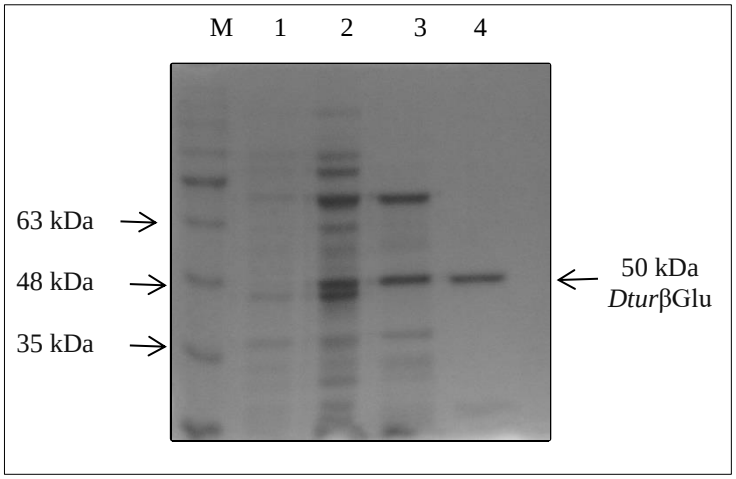

Fig. 2 SDS-PAGE analysis of the recombinant *Dtur*βGlu. M) Protein Marker; 1) Cellular extract from not induced cells; 2) Cellular extract from IPTG-induced cells; 3) Heat-treated sample; 4) Affinity chromatography by His-trap.

To gain insight into the quaternary structure of *Dtur*βGlu, the enzyme was analysed by a size exclusion chromatography. The results showed a molecular weight of about 200 kD, thus indicating that *Dtur*βGlu has a tetrameric structure. This oligomeric structure agrees with the homology-based model (performed with SWISS-MODEL) of *Dtur*βGlu with BGLPf (15), TnBgl1A (16) and Ssβ-Glc1 (17) as templates (Fig. 3).

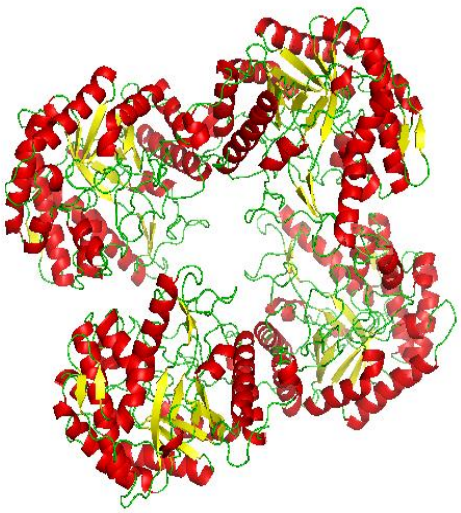

Fig. 3 Homology model of *Dtur*βGlu

Effect of pH and temperature on enzyme activity

The pH optimum for *Dtur*βGlu activity was 5.4 (Fig. 4A) differently by homologous DtGH of *D. thermophilus* that showed pH 7.0 as optimal value, furthermore while *Dtur*βGlu exhibited 90% and 72% activities at pH 5.0 and 7.0 respectively, DtGH activity dropped at pH 5 (18).

Similar pH optima of β-glucosidases have been reported from several thermophilic bacteria such as *Thermus Thermophilus* (19) *Caldicellulosiruptor saccharolyticus* (20) and *Thermoanaerobacter brockii* (21). Moreover, *Dtur*βGlu was fairly stable in the pH range of 5-8, retaining over 90% activity after 1 h of incubation (Fig. 4B). The enzyme displayed maximal activity at 80°C (Fig. 5A), This temperature optimum is slightly higher than that of other thermophilic microorganisms such as *Halothermothrix orenii* (22), *Scytalidium thermophilum* (23), *Talaromyces thermophilus* (24) and *Myceliophthora thermophile* (25).

Thermostability of the enzyme at various temperatures was monitored by measuring its activity after incubation at different time. After 90 min at 80°C the relative activity was about 80% while after 2 h of incubation at 70 or 80°C the residual activity of *Dtur*βGlu was still 70% and 50% respectively (Fig. 5B). This high stability together with an enzymatic activity in a pH range of 5.0-8.0 of about 80%, suggest that the enzyme may have utility in various industrial fields.

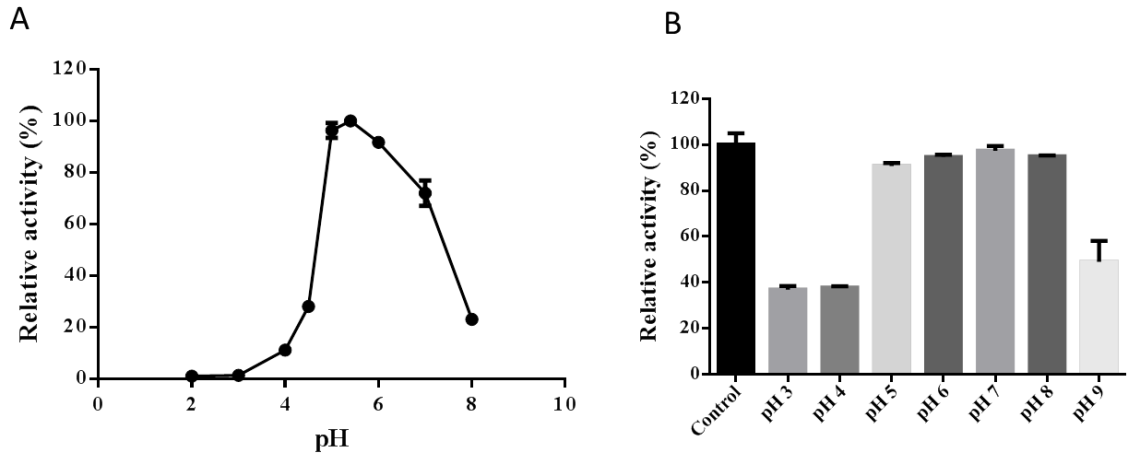

Fig. 4 Effect of pH on enzymatic activity of *Dtur*βGlu. A) pH optimum was measured in buffers ranging from pH 2.00 to pH 8.00. B) The enzyme was incubated in various buffers (pH 3 – 9) for 1 h and assayed for residual activity at the optimal conditions.

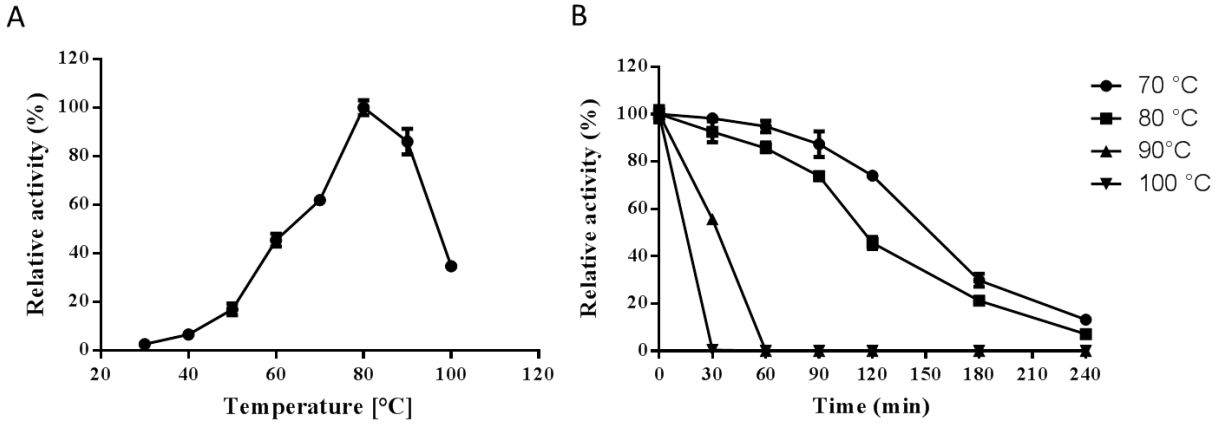

Fig. 5 Effect of temperature on enzymatic activity of *Dtur*βGlu. A) Temperature optimum was determined in the range 30 - 100 °C. B) The enzyme was incubated at 70, 80, 90 and 100°C for different times and then assayed for residual activity at the optimal conditions.

Effect of chemicals on enzyme activity

The effect of various metal ions, chemicals and detergents on *Dtur*βGlu activity were studied and the results are reported in Table 2. Cu^{2+}, Co^{2+}, Mn^{2+}, and Zn^{2+} inhibited ~ 50% the *Dtur*βGlu activity, Ca^{2+} and Mg^{2+} ~ 30%, while Li^{+} didn't affect the enzyme activity. It is probable that the inhibition of the enzymatic activity by salts is caused by an alteration of protein's secondary and tertiary structure. In the presence of EDTA, the enzymatic activity was unchanged, indicating that *Dtur*βGlu is not a metal enzyme.

The influence of various surfactants such as SDS, Tween20 and Triton X-100 was also determined. In presence of Tween-20, Triton X-100, the enzymatic activity was increased (180% and 120% respectively), while SDS affected totally *Dtur*βGlu activity. Other β-glucosidases are reported to be improved by detergents such as the β-glucosidase of *Fervidobacterium islandicum* (26). The addition of non-ionic detergents can play a role in the stability of the enzyme. In several studies, it

has been reported that the addition of surfactant in a catalytic process increased conversion yelds (27, 28). DMSO had only a moderate effect on *Dtur*βGlu activity.

Table 2 Effect of metal ions and reagents on *Dtur*βGlu activity

Metal ion or chemical agent	Concentration	Relative activity
None	1 mM	100%
$CuCl_2$	1 mM	44.23%
$ZnSO_4$	1 mM	46%
LiCl	1 mM	98.5%
$MgCl_2$	1 mM	53.90%
$CaCl_2$	1 mM	56.79%
$MnCl_2$	1 mM	38.23%
$CoSO_4$	1 mM	47.66%
EDTA	1 mM	100%
SDS	0.5%	0.66%
Triton X-100	0.5%	130%
Tween 20	0.5%	173%
DMSO	0.5%	66%

Finally, the influence of four monosaccharides on β-glucosidase activity was investigated. The results showed that supplementation of different concentrations of glucose, galactose, xylose and arabinose in *p*NPGlu hydrolysis did not highlight a strong inhibition, in fact *Dtur*βGlu retained 80% of its activity in presence of 100 mM of glucose, galactose and xylose and the 60% in presence of 100 mM arabinose (Fig. 6).

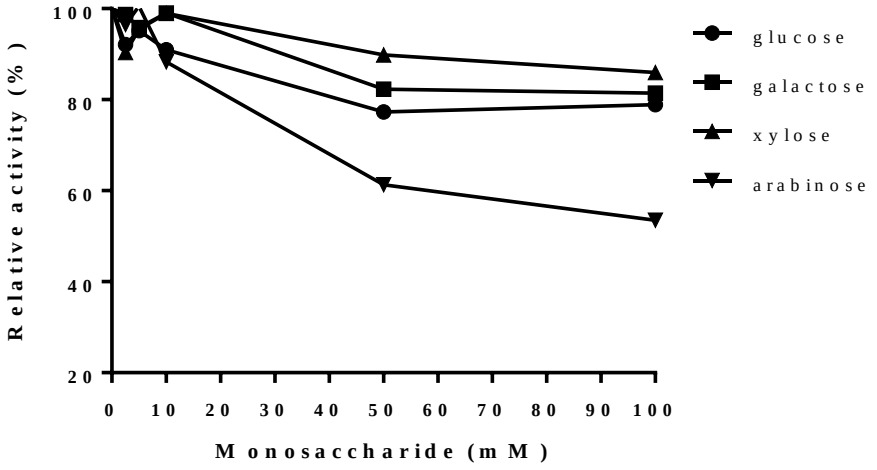

Fig. 6 Effect of monosaccharides on enzymatic activity of DturβGlu. The purified enzyme was assayed in the presence of different concentration of varoius monosaccharides and under the standard condition

Hydrolytic activity and kinetic parameters of *Dtur*βGlu on different substrates

The hydrolitic activity of *Dtur*βGlu was tested on different substrates. The results (Table 3) showed that the enzyme displays the highest specific activity towards *p*NPGlu (160 U/mg) followed by *p*NPGal (155 U/mg) and salicin (67 U/mg). It was less active on *o*NPGal (23 U/mg), *o*NPGlu (21 U/mg), *p*NPXyl (10 U/mg) and cellobiose (2 U/mg), while no activity was detected on *p*NPαGal.

Table 3 Substrate specificity of *Dtur*βGlu

Substrate	Specific activity (U/mg)	Relative activity (%)
***p*NP-β-D-glucopyranoside**	160	100
***o*NP-β-D-glucopyranoside**	21	13
***p*NP-β-D-galattopyranoside**	155	96.87
***o*NP-β-D-galattopyranoside**	23	14
***p*NP-β-D-xylopyranoside**	10	6.2
Salicin	67	42
Cellobiose	2	1.25

The kinetic parameters of *Dtur*βGlu were determined for each substrate (Table 4): the K_M values of *Dtur*βGlu, determined toward *p*NPGlu and salicine, were comparable with Tm-BglA from *T. maritima,* Te-BglA from *T. ethanolicus* (30) and DtGH from *D. thermophilum* (18). On the other hand, K_{cat} value vs *p*NPGlu is about 14 fold higher than Tm-BglA and DtGH and 67 fold higher than Te-BglA, while K_{cat} value vs salicine is about 6 fold and 3,5 fold greater than Te-BglA and TmBglA respectively. In conclusion *Dtur*βglu shows a better catalytic efficiency respect to above reported thermophilic β-glucosidases belonging to GH1.

Table 4 Kinetic parameters of *Dtur*βGlu

Substrate	K_M (mM)	K_{cat} (s^{-1})	K_{cat}/K_M ($mM^{-1}s^{-1}$)
***p*NPDGlu**	0,82	3968	4839
***o*NPGlu**	12,08	3417	282
***p*NPGal**	1,36	9924	7297
***o*NPGal**	1,63	1394	855
***p*NPXyl**	2,79	651	233
Salicin	8,12	659	81

Conclusions

In this study, we have biochemically characterized a novel recombinant thermostable β-glucosidase, *Dtur*βGlu, from the anerobic bacterium *D. turgidum. Dtur*βGlu was expressed in *E.coli* and purified to homogeneity. Gel filtration analysis showed a tetrameric structure of the protein with a molecular mass of about 200 KDa. The enzyme exhibited a good β-glucosidase and β-galactosidase activities on synthetic substrates and it is also able to hydrolize natural substrates as salicin, with a higher catalytic efficiency respect to other thermophilic β-glucosidase. Moreover, *Dtur*βGlu was stable and active at high temperature and in a wide range of pH. The addition of surfactants enhanced the activity of *Dtur*βGlu, while the metal ions did not significantly hinder it. Finally, the enzyme showed a good tolerance to monosaccharides. All these features make this enzyme a good candidate for biotechnological applications, especially in the conversion of biomass to produce fermentable sugars.

Acknowledgements

This work was supported by BIOPOLIS: PON03PE_00107_1 CUP: E48C14000030005

References

1. Shewale JG. (1982) **Beta-Glucosidase: its role in cellulase synthesis and hydrolysis of cellulose.** *Int J Biochem.* 14(6):435-43.
2. Ketudat Cairns JR, Esen A. (2010) **β-Glucosidases.** *Cell Mol Life Sci.* 67(20):3389-405.
3. Bhatia Y, Mishra S, Bisaria VS**. (2002) Microbial beta-glucosidases: cloning, properties, and applications.** *Crit Rev Biotechnol.* 22(4):375-407.
4. Schröder C, Blank S, Antranikian G1. (2015) **First Glycoside Hydrolase Family 2 Enzymes from *Thermus antranikianii* and *Thermus brockianus* with β-Glucosidase Activity.** *Front Bioeng Biotechnol.* 3(3):76.
5. Rimbach G, Boesch-Saadatmandi C, Frank J, Fuchs D, Wenzel U, Daniel H, Hall WL, Weinberg PD. (2008) **Dietary isoflavones in the prevention of cardiovascular disease--a molecular perspective.** *Food Chem Toxicol*. 46(4):1308-19.
6. Schröder C, Elleuche S, Blank S, Antranikian G. (2014) **Characterization of a heat-active archaeal β-glucosidase from a hydrothermal spring metagenome.** *Enzyme Microb Technol.* 10(57):48-54.
7. Uchiyama T, Miyazaki K, Yaoi K. (2013) **Characterization of a novel β-glucosidase from a compost microbial metagenome with strong transglycosylation activity**. *J Biol Chem.* 21;288(25):18325-34.
8. Hassan N, Geiger B, Gandini R, Patel BK, Kittl R, Haltrich D, Nguyen TH, Divne C, Tan TC. (2016) **Engineering a thermostable *Halothermothrix orenii* β-glucosidase for improved galacto-oligosaccharide synthesis.** *Appl Microbiol Biotechnol.* 100(8):3533-43.
9. Dalmaso GZ, Ferreira D, Vermelho AB. (2015) **Marine extremophiles: a source of hydrolases for biotechnological applications.** *Mar Drugs.* 3;13(4):1925-65.
10. Svetlichny VA and Svetlichnaya TP (1988) ***Dictyoglomus turgidus sp. nov*., a new extremely thermophilic eubacterium isolated from hot springs of the Uzon volcano caldera.** *Mikrobiologiia* 57:364-369.

11. Brumm PJ, Gowda K, Robb FT, Mead DA (2016) **The Complete Genome Sequence of Hyperthermophile *Dictyoglomus turgidum* DSM 6724™ Reveals a Specialized Carbohydrate Fermentor.** *Front Microbiol* 20:1979.

12. Sarcinelli C, Fiorentino G, Pizzo E, Bartolucci S, Limauro D (2016) **Discovering Antioxidant Molecules in the Archaea Domain: Peroxiredoxin Bcp1 from *Sulfolobus solfataricus* Protects H9c2 Cardiomyoblasts from Oxidative Stress.** *Archaea* 2016:7424870.

13. Bradford MM. (1976) **A rapid and sensitive method for the quantitation of microgram quantities of protein utilizing the principle of protein-dye binding.** *Anal Biochem.* 7;72:248-54.

14. Bhatia Y, Mishra S, Bisaria VS. (2002) **Microbial beta-glucosidases: cloning, properties, and applications.** *Crit Rev Biotechnol* 22(4):375-407.

15. Kado Y, Inoue T, Ishikawa K. (2011) **Structure of hyperthermophilic β-glucosidase from *Pyrococcus furiosus*.** *Acta Crystallogr Sect F Struct Biol Cryst Commun.* 1;67:1473-9.

16. Kulkarni TS, Khan S, Villagomez R, Mahmood T, Lindahl S Logan DT, Linares-Pastén JA, Nordberg Karlsson E. (2017) **Crystal structure of β-glucosidase 1A from *Thermotoga neapolitana* and comparison of active site mutants for hydrolysis of flavonoid glucosides.** *Proteins.* 85(5):872-884.

17. Gloster TM, Roberts S, Ducros VM, Perugino G, Rossi M, Hoos R, Moracci M, Vasella A, Davies GJ. (2004) **Structural studies of the beta-glycosidase from *Sulfolobus solfataricus* in complex with covalently and noncovalently bound inhibitors.** *Biochemistry* 25;43(20):6101-9.

18. Zou ZZ, Yu HL, Li CX, Zhou XW, Hayashi C, Sun J, Liu BH, Imanaka T, Xu JH. (2012) **A new thermostable β-glucosidase mined from *Dictyoglomus thermophilum*: properties and performance in octyl glucoside synthesis at high temperatures.** *Bioresour Technol.* 118:425-30.

19. Nam ES, Kim MS, Lee HB, Ahn JK. (2010) **Beta-glycosidase of *Thermus thermophilus* KNOUC202: gene and biochemical properties of the enzyme expressed in Escherichia coli.** *Prikl Biokhim Mikrobiol.* 46(5):562-71.

20. Hong MR, Park CS, Oh DK. (2009) **Characterization of a thermostable endo-1,5-α-l-arabinanase from *Caldicellulorsiruptor saccharolyticus.*** *Biotechnol. Lett.* 31(9):1439-43.

21. Breves R, Bronnenmeier K, Wild N, Lottspeich F, Staudenbauer WL, Hofemeister J. (1997) **Genes encoding two different beta-glucosidases of *Thermoanaerobacter brockii* are clustered in a common operon.** *Appl Environ Microbiol*. 63(10):3902-10.

22. Hassan N, Nguyen TH, Intanon M, Kori LD, Patel BK, Haltrich D, Divne C, Tan TC. (2015) **Biochemical and structural characterization of a thermostable β-glucosidase from *Halothermothrix orenii* for galacto-oligosaccharide synthesis.** *Appl Microbiol Biotechnol*. 99(4):1731-44.

23. Zanoelo FF, Polizeli Mde L, Terenzi HF, Jorge JA. (2004) **Beta-glucosidase activity from the thermophilic fungus *Scytalidium thermophilum* is stimulated by glucose and xylose.** *FEMS Microbiol Lett*. 240(2):137-43.

24. Nakkharat P, Haltrich D. (2006) **Purification and characterization of an intracellular enzyme with beta-glucosidase and beta-galactosidase activity from the thermophilic fungus *Talaromyces thermophilus* CBS 236.58.** *J Biotechnol.* 29;123(3):304-13.

25. Zhao J1, Guo C, Tian C, Ma Y. (2015) **Heterologous Expression and Characterization of a GH3 β-Glucosidase from Thermophilic Fungi *Myceliophthora thermophila* in *Pichia pastoris.*** *Appl Biochem Biotechnol*. 177(2):511-27.

26. Jabbour D, Klippel B, Antranikian G. (2012) **A novel thermostable and glucose-tolerant β-glucosidase from *Fervidobacterium islandicum*.** *Appl Microbiol Biotechnol*. 93(5):1947-56.

27. Kaar WE, Holtzapple MT (1998) **Benefits from tween during enzymic hydrolysis of corn stover.** *Biotechnol Bioeng.* 20;59(4):419-27.

28. Kim W, Gamo Y, Sani YM, Wusiman Y, Ogawa S, Karita S, Goto M. (2006) **Effect of Tween 80 on Hydrolytic Activity and Substrate Accessibility of Carbohydrolase I (CBH I) from *Trichoderma viride*.** *Aust. J. Anim. Sci*. 19(5):684-689.
29. Hong MR, Kim YS, Park CS, Lee JK, Kim YS, Oh DK. (2009) **Characterization of a recombinant beta-glucosidase from the thermophilic bacterium *Caldicellulosiruptor saccharolyticus.*** *J Biosci Bioeng.* 108(1):36-40.
30. Song X, Xue Y, Wang Q, Wu X. (2011) **Comparison of three thermostable β-glucosidases for application in the hydrolysis of soybean isoflavone glycosides**. *J Agric Food Chem.* 9;59(5):1954-61.

2.3 A synergistic action of a thermophilic α-galactosidase and β-mannanase on galactomannan substrates

Martina Aulitto[1], Francesca Anna Fusco[1], Gabriella Fiorentino, Simonetta Bartolucci,

Patrizia Contursi*, Danila Limauro

Dipartimento di Biologia, University of Naples Federico II, Complesso universitario di Monte S. Angelo, Via Cinthia, Naples, Italy

[1]Martina Aulitto and Francesca Anna Fusco contributed equally to this work.

*Corresponding author: contursi@unina.it

Keywords: Synergy; Hemicellulose; Thermophiles; enzymatic hydrolysis, α-galactosidase, β–mannanase

Submitted to Enzyme and Microbial Technology

Abstract

The lack of full utilization of hemicellulose sugars (pentose and hexose) present in lignocellulosic material, hinders the development of bio-based fuels and chemicals production. Two recombinant thermophilic enzymes, an endo β−1,4-mannanase from *Dictyoglomus turgidum* (*Dtur*CelB) and an α-galactosidase from *Thermus thermophilus* (*Tt*GalA) were assayed at 80°C, to assess their heterosynergystic association on galactomannans degradation, particularly abundant in hemicellulose. The enzymes were tested under various combinations simultaneously and sequentially, in order to estimate the optimal conditions for the release of reducing sugars. The results showed that the most efficient degree of sinergy was obtained in simultaneous assay with a protein ratio of 25% of *Dtur*CelB and 75% of *Tt*GalA, using locust bean gum as substrate. On the other hand, the mechanism of action was demonstrated through the sequential assays, i.e. when *Tt*GalA acting as first to enhance the subsequent hydrolysis performed by *Dtur*CelB. The synergistic association between the thermophilic enzymes herein described has an high potential application to pre-hydrolyse the biomass right after the pretreatment, prior to the conventional saccharification step.

1. Background

Lignocellulose is the most abundant available feedstock produced every-day on the Earth. The major portion in polymers is represented by cellulose (35-50%), hemicellulose (26-35%) and lignin (14-21%), as well as by other minor components (1). Lignin provides the structural integrity of the plant, encapsulating the microfibrils of hemicellulose and cellulose, to withstand the herbivores and pathogens attacks (2). During the detrital food webs, the natural process for the deconstruction of lignocellulose, the polysaccarides hydrolysis is carried out by saprophytes and detritivores (3). Since lignocellulose-feedstock available in large amount, the biomass is currently used to produce value added-products such as bio-fuels and -chemicals (1, 4). In the industrial processes, the deconstruction is performed using chemical and physical pretreatments (5). During this first step, the lignin is disarrayed and the resulting polysaccharides (i.e. cellulose and hemicellulose) are subsequently hydrolyzed by enzymatic mixture to produce fermentable sugars. This process, also named saccharification, involves (hemi)cellulases and auxiliary enzymes needed to obtain an effective hydrolysis (6). Hemicellulose is the second most abundant biopolymer present in lignocellulosic-feedstocks (2). Unlike cellulose, hemicellulose is a branched heteropolymer composed by pentoses (i.e. xylose and arabinose), hexoses (i.e. glucose, galactose, mannose) and also by sugars in acidified form (glucuronic acid and galacturonic acid) (7).

Mannans are the major source of secondary cell wall found in conifers (softwood) and leguminosae. They are classified on the basis of their sugars components in: mannans, glucomannans,

galactomannans and galactoglucomannans (8). To achieve an efficient hydrolysis of galactoglucomannans, the presence of multiple hydrolases such as β-glucosidases (EC 3.2.1.21), endo-mannanases (EC 3.2.1.78), mannosidases (EC 3.2.1.25) and α-galactosidases (EC 3.2.1.22), is needed (9). Therefore, studies of synergistic association among these enzymes pave the way to establish an efficient enzymatic cocktail to achieve the complete hydrolysis of galactoglucomannans.

Since the pretreatment step is performed at high temperature (90°-120°C), the development of thermophilic enzymatic mixture which could operate at high temperature is needed to reduce the whole process cost (10). Therefore, the main objective of this work has been to study the synergistic effect of the thermophilic endo β-1,4-mannanase (*Dtur*CelB) from *Dictyoglomus turgidum* and the α-1,6-galactosidase (*Tt*GalA) from *Thermus thermophilus* on galactomannan substrates from locust bean, carob tree and guar gum.

2.Methods

2.1 Substrates

Locust bean gum was purchased from Sigma-Aldrich. Carob galactomannan (Low viscosity) and Guar galactomannan (Medium viscosity) were purchased from Megazyme.

2.2 Expression and purification of recombinant enzymes

*Dtur*CelB was expressed in *Escherichia coli* BL21 (DE3), transformed with the recombinant plasmid pET30b-*DturCelB* and purified by nickel affinity chromatography (18). *Thermus thermophilus* HB27::nar strain transformed with the recombinant plasmid pMKE2-*TtGalA* was used for the homologous expression of the α-galactosidase (*Tt*GalA) (11).

2.3 Substrate specificity determination

The *Dtur*CelB and *Tt*GalA activities were determined using as polymeric substrates locust bean gum, carob galactomannan and guar galactomannan. The reaction mixture (1 ml) containing one of the purified enzymes (1 µg) was assayed using 1.0 % galactomannan substrate dissolved in 50 mM citrate-phosphate buffer pH 6.0. The reaction was carried out at 80 °C for 30 min and the concentration of reducing ends was determined following the Nelson-Somogyi (NS) method, using mannose as standard (12). All assays were performed in triplicate. One unit of enzyme activity was defined as the amount of enzyme required to release 1 µmol of product per minute, under the the above assay conditions.

2.4 *Dtur*CelB and *Tt*GalA synergistic action

To evaluate the synergy degree between *Dtur*CelB and *Tt*GalA, the enzymes were tested simultaneously and sequentially using 1% of galactomannans substrates (Locust bean gum, Carob and Guar gum) dissolved in 50 mM citrate-phosphate buffer pH 6.0. For the simultaneous assay, various ratios of *Dtur*CelB and *Tt*GalA were tested for a total amount of 2 μg. The assays were carried out at 80°C for 30 min and the amount of released sugars were quantified by NS (12).

For the sequential assay 1 μg of *Dtur*CelB or *Tt*GalA was incubated in the reaction mix, described above, at 80°C for 30 min , and thenthe enzyme was boiled for 10 min to be inactivate. After ice-cooling, the second enzyme (1 μg) was added to the reaction mixture under the same condition. Reactions containing only one of the heat-inactivated enzyme were used as a negative control. All the samples were analyzed for the concentration of reducing ends by NS method using mannose as standard (12). All enzyme assays were carried out in triplicate.

2.5 Degree of synergy (DS)

To investigate the interaction between two or more enzymes, synergism is calculated as ratio between the observed activity of the enzyme mixture and the theoretical sum of individual specific activity of the same enzymes on a substrate. The calculation of degree of synergy (DS), between *Dtur*CelB and *Tt*GalA, was determined by the following equation:

$$DS = \frac{Y_{1+2}}{(Y_1 + Y_2)}$$

where Y_{1+2}, indicates the yield of reducing sugar achieved by the two enzymes working simultaneously, Y1 and Y2 indicate the yields (μg) of reducing sugars, achieved by each enzyme when working separately.

3. Results and discussion

In nature, plant biomass degradation is accomplished by the complex action of various Glycoside hydrolases (GHs). Therefore, the optimization of enzymatic mixtures to improve the conversion of biomasses into fermentable sugars, is needed for biorefinery purposes. Nevertheless, a major issue in this context is to set up the right reaction conditions to achieve a synergistic interaction among enzymes. The synergic association produces a total effect greater than the sum of individual enzymes and it is present when the degree of synergy (DS) is greater than 1. In particular synergy among different enzymes involved in degradation of galactomanannas can be classified in two types: i) homosynergy between two enzymes cleaving main-chain (i.e β-mannosidase and β-mannanase) or side chain ii) heterosynergy between a side-chain cleaving enzyme and a main-chain cleaving enzymes (i.e α,1-6 galactosidase and β,1-4 mannanase). On the contrary the antisynergic

effect is established when one enzyme inhibits the action of the another because of competition for the same substrate (8).

Nowadays, the knowledge about cocktails of thermophilic enzymes is still limited and it is interesting to study the synergic action of enzymes derived from different *hot* source that hydrolize the biomass in the same harsh industrial conditions.

Determination of specific activity of *Dtur*CelB and *Tt*GalA on different galactomannans.

The endo β-1,4 mannanase, *Dtur*CelB (18) from *D. turgidum* and the α-1,6 galactosidase from *T. thermophilus* (11) were previously characterized for their biochemical features.

We assayed both enzymes on different galactomannans as Locust bean gum, Carob and Guar gum that differ for the frequency of galactose residues (Guar gum > Carob> Locust bean gum) on the mannan backbone (Fig. 1).

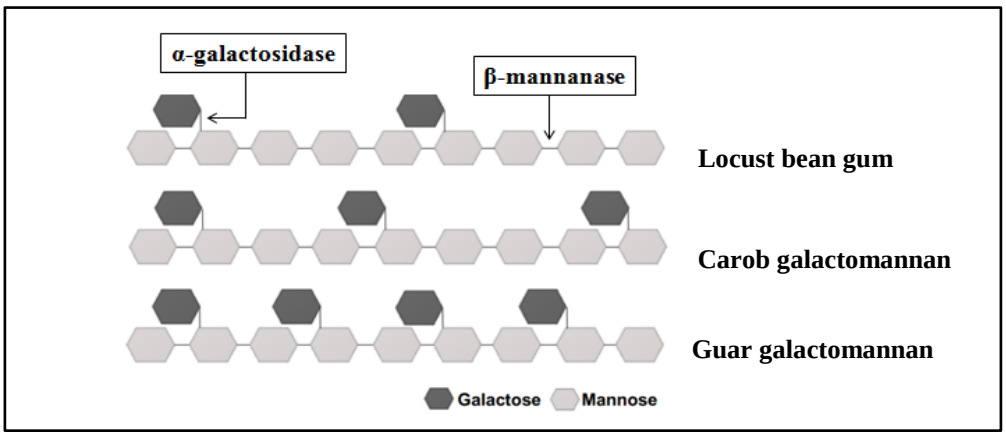

Fig. 1 Graphical representation of different galactomannas (Locust bean gum, Carob galactomanna and Guar galactomannan). β 1,4-endomannanase randomly cleaves mannose backbone.; α 1,6-galactosidase hydrolizes non-reducing terminal galactose units.

*Dtur*CelB showed hydrolytic endo-mannanase activity at 80°C and pH 6.0 towards locust bean gum (44.0 U·mg^{-1}), Carob (40.3 U·mg^{-1}) and Guar gum (2.8 U·mg^{-1}) (Tab.1). The different catalytic efficiency can be explained by the the increasing number of galactose residues branching out from the linear mannan backbones causing steric hindrance to the enzyme. A similar behaviour was also demonstrated for *Clostridium thermocellum* Man5A (13).

*Tt*GalA was chosen as potential partner of *Dtur*CelB for debranching activity to ameliorate the galactomannans hydrolysis. *Tt*GalA showed its highest catalytic activity at 90°C and pH 6.0 on the synthetic substrate, *p*NP-α-D-galattopyranoside (*p*NPgal) (338 U·mg^{-1}) (11) but it retained 98% of its activity at assay condition above reported for *Dtur*CelB. Consequently, in order to test *Tt*GalA in association with *Dtur*CelB, it was assayed at 80°C and pH6, on Locust bean gum (4.4 U·mg^{-1}),

Carob (1.4 U·mg^{-1}) and Guar gum (0.33 U·mg^{-1}) (Table 1). *Tt*GalA catalytic activity on polymeric substrates is not negligible, indeed it is higher if compared to the α-galactosidase AglC from *Aspergillus niger* (1.0 U·mg^{-1}) belonging at the same family GH36 and very similar to a GH27 Aga27A from *Cyamopsis tetragonolobus* (3.7 U·mg^{-1}) (14). Moreover, the different values of specific activity of *Tt*GalA towards *p*NPgal respect to galactose-polysaccaharides are in agreement also with other GH36 members (14).

Therefore the synergistic association between *Tt*GalA and *Dtur*CelB might be functional to improve the hydrolysis of hemicellulose as already demonstrated in other systems (8, 14).

Substrate	***Tt*GalA Specific activity (U·mg^{-1})**	***Dtur*CelB Specific activity (U·mg^{-1})**
Locust bean gum (G/M: 1/4)	4.4	44.0
Carob galactomannan (G/M: 1/3.5)	1.4	40.3
Guar Galactomannan (G/M: 1/2)	0.33	2.8

Table 1 Specificity activity of *Tt*GalA and *Dtur*CelB vs different galactomannanes. Galactose

Synergistic studies of *Tt*GalA and *Dtur*CelB toward three galactomannans

The aim of this study was centred on the setting up of reaction conditions suitable to achieve heterosynergy between *Tt*GalA and *Dtur*CelB to ameliorate the galactomannans hydrolysis. The synergistic interaction between the recombinant enzymes was assessed through the quantification of the reducing sugars released during the degradation of the three galactomannan substrates that contained a different ratio of galactose- versus mannose- residues (Fig. 1). To evaluate how the activity and interactions of *Tt*GalA and *Dtur*CelB, were influenced by the extent of galactose substitution on the mannan backbone, simultaneous and sequenzial assays were performed. In simultaneous assays the enzymes were added to the reaction mixture at the same time varying their relative ratio (50%*Dtur*CelB-50%*Tt*GalA; 75%*Dtur*CelB-25%*Tt*GalA and 25%*Dtur*CelB-75%*Tt*GalA), while in sequential assays the enzymes, used in same ratio (50% *Dtur*CelB-50%*Tt*GalA), were added first one and then the other as described in Materials and methods.

Locust bean gum is the most important galactomannan used as stabilizing agent in food and non-food industries (15), purified from endosperm of seeds of carob tree (16) and it is the lowest galactose containing polymer among the substrates tested (Fig. 1). Using this substrate, in the simultaneous assay, the enzymes exhibited synergism under all combinations with a DS of 1.8, 1.3 and 1.1 using a ratio of 25%*Dtur*CelB-75%*Tt*GalA, 75%*Dtur*CelB-25%*Tt*GalA and 50%*Dtur*CelB-50%*Tt*GalA, respectively (Fig. 2A). To get further insight into the observed synergistic interaction,

we performed sequential assays. When *Dtur*CelB was added as first, the DS (1.1) turned out to be identical to that obtained with simultaneous assays (Fig. 2). Conversely, the DS raised up to 1.4 when *Tt*GalA acted as first (Fig. 2B). These results demonstrate that *Tt*GalA significantly supported *Dtur*CelB activity by removing galactose branches on the polymer that would have sterically hindered *Dtur*CelB.

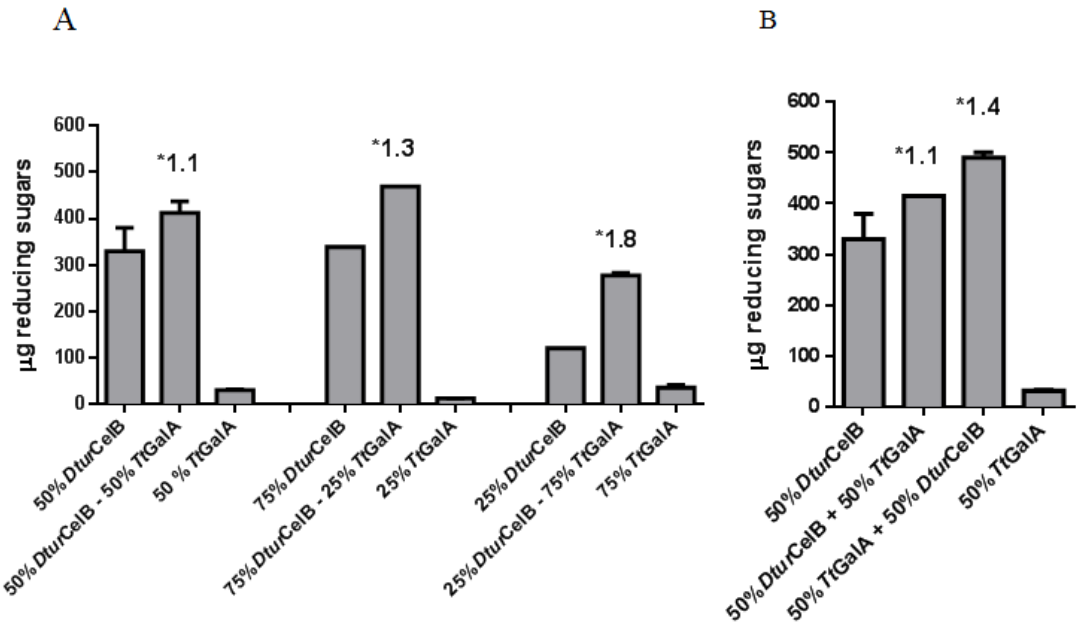

Fig. 2 Simultaneous (A) and sequential (B) assays of *Tt*GalA and *Dtur*CelB on Locust bean gum. Various combinations of recombinant enzymes were tested, and protein ratio was expressed in percentage form. The synergy degree was highlighted with asterisk. Values were presented as mean values ± S.D. (n = 3).

Locust bean gum and Carob galactomannan are both isolated from carob seeds. Nevertheless these galactomannan polymers display different chemical and rheological properties depending on their geographic origin (17). The reported G/M ratio of Carob galactomannan is slightly lower (1/3.5) than Locust bean gum (1:4) and our data indicate that the specific activity of *Tt*GalA on Carob is 30% of that on Locust bean gum thus pointing to a complex nature of this substrate (Table 1). Therefore, we resolved to perform a comparative synergy study of the two thermophilic enzymes also using this second substrate. In fact, when *Dtur*CelB and *Tt*GalA were assayed simultaneously, in combination of 50%-50% no synergy was exhibited (DS =0.8) (Figure 3A). It might be explainable with a complex nature of the Carob substrate (purity degree, extent of galactose ramifications) that renders the binding of *Tt*GalA not completely productive, thus in turn inhibiting the *Dtur*CelB hydrolysis when they are present in the enzymatic mixture in a similar amount. However, a similar degree of synergy (DS=1.4 on Carob vs 1.3 on Locust bean gum) was achieved when the enzymes were assayed simultaneously with a protein ratio of *Dtur*CelB to *Tt*GalA 75%-25% and the total amount of reducing sugars released was also comparable (467 µg vs 454 µg)

(Figure 3A and 2A). However, the highest DS obtained on Carob (DS=1.4) was indeed lower than that measured on Locust bean gum (Figure 2A, DS=1.8), indicating that the two enzymes performed their synergistic catalytic activity, less efficiently on this substrate (Figure 3A). This result can be only explained by the low specific activity of *Tt*GalA on Carob, while the affinity of *Dtur*CelB on Carob and Locust bean gum is almost the same (Table 1). Our data highlighted the role of *Tt*GalA, that plays a major function in enhancing of *Dtur*CelB hydrolysis, improving the linear mannan chain accessibility. Accordingly, results from the sequential assay show clearly that also on Carob the synergistic association, between the two enzymes, greatly benefits (DS=1.5) by the previous action of the debranching enzyme (Fig. 3B).

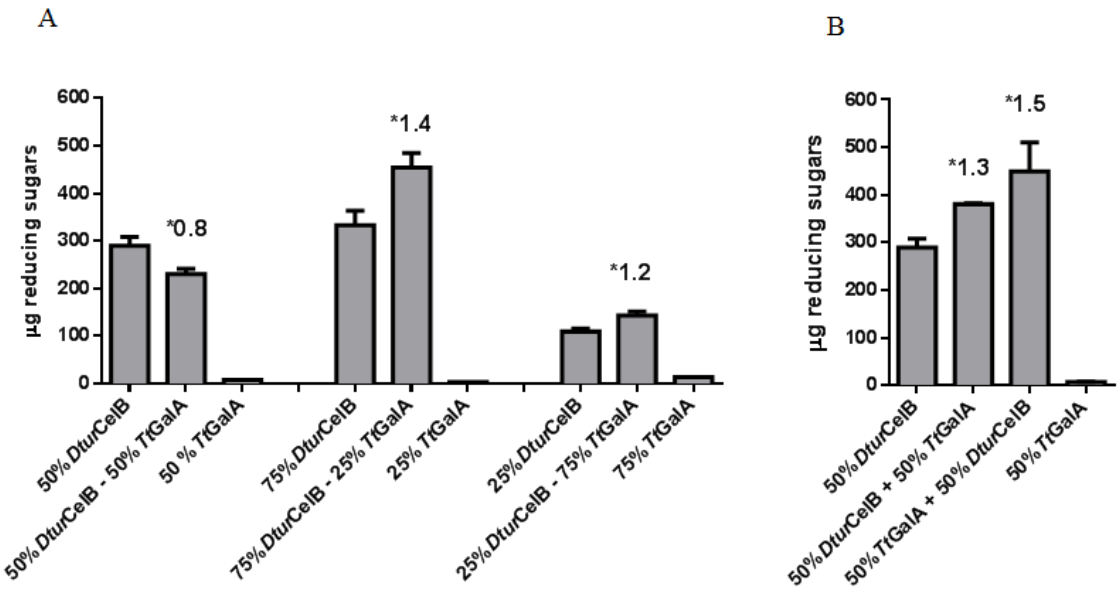

Fig. 3 Simultaneous (A) and sequential (B) assays of *Tt*GalA and *Dtur*CelB on Carob galactomannan. Various combinations of recombinant enzymes were tested, and protein ratio was expressed in percentage form. The degree of synergy was highlighted with asterisk. Values were presented as mean values ± S.D. (n = 3).

The Guar galactomannan backbone is composed of a linear chain of mannose residues, where the galactose side-branches is present at every second mannose residues (Fig.1). The specific activity of *Dtur*CelB and *Tt*GalA on Guar galactomannan was lower than that obtained on Locust bean gum, due to the higher extent of galactose substitutions (Table 1). Accordingly, the total yield of reducing sugars obtained on this substrate was much lower than that on Locust bean gum and Carob galactomannan (Fig. 2, 3 and 4). Nevertheless, in the simultaneous assay our data clearly indicate that the synergistic interaction between the two enzymes occurred also using Guar galactomannan as substrate (i.e DS≥1.0) under all the conditions tested (Fig. 4A). The sequential assays further confirmed that the prior action of *Tt*GalA by removing galactose substituents, increases the *Dtur*CelB reducing sugar release (Fig. 4B).

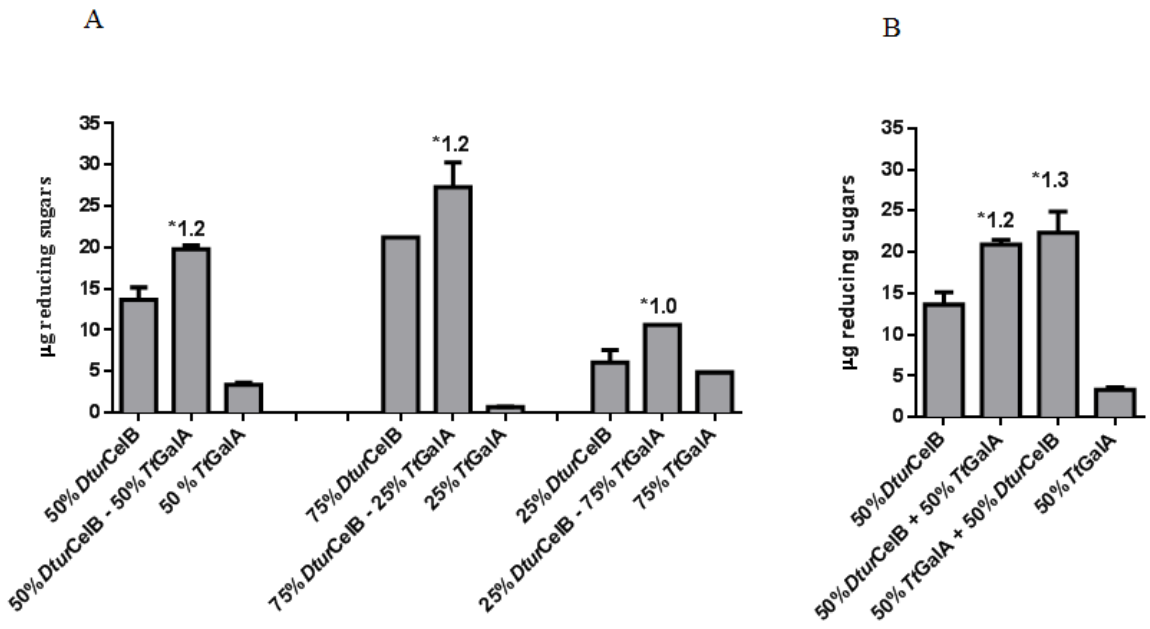

Fig. 4. Simultaneous (A) and sequential (B) assays of *Tt*GalA and *Dtur*CelB on Guar gum. Various combinations of recombinant enzymes were tested, and protein ratio was expressed in percentage form. The degree of synergy was highlighted with asterisk. Values were presented as mean values ± S.D. (n = 3).

Conclusions

One of the major factor contributing to increase the yield of the efficient lignocellulose biomass conversion yield, resides in understanding how different enzymes may cooperate to degrade complex polymeric substrates. Both the new isolated thermophilic *Dtur*CelB and *Tt*GalA enzymes performed a better catalytic activity working in synergy rather than alone, preferring the low galactose-polysaccharides than the highly galactose decorated polymers used in this study. In fact, a good degree of heterosynergy relationship with each other on galactomannan degradation was clearly demonstrated on all the substrate tested at high temperature (80°C) and in a relatively short time (30 min) compared to other studies (14). Based on the sequential assays, the synergy was a result of *Tt*GalA activity, which removes galactose branches from the galactomannan polymers, then improving the accessibility of the linear mannan backbone to *Dtur*CelB. Our finding also revealed that the 75%-25% ratio of *Dtur*CelB and *Tt*GalA is the best combination to attain a compromise between a good degree of synergy and the highest yield of reducing sugar release. The strength point of this enzymatic cocktails resides in the thermophilicity and thermostability of both the enzymes *Tt*GalA (11, 18) that allows to foresee its employment during the gradual cooling right after the pretreatment of lignocellulosic material. The addition of thermophilic enzymes earlier in this step would result in time savings and improved conversion efficiency of the whole process, compared to the use of mesophilic/moderate thermophlic enzyme cocktails.

Acknowledgements

The authors thank prof. Josè Berenguer, Centro de Biologia Molecular Severo Ochoa, Uniniversidad Autonoma de Madrid, Spain, for generously providing *Thermus thermophilus* HB27::nar strain and pMKE2 vector.

This work was supported by BIOPOLIS: PON03PE_00107_1 CUP: E48C14000030005

References

1. Arevalo-Gallegos A, Ahmad Z, Asgher M, Parra-Saldivar R, Iqbal HM: **Lignocellulose: A sustainable material to produce value-added products with a zero waste approach—A review.** *International Journal of Biological Macromolecules* 2017.
2. Pérez J, Munoz-Dorado J, de la Rubia T, Martinez J: **Biodegradation and biological treatments of cellulose, hemicellulose and lignin: an overview.** *International Microbiology* 2002, **5:**53-63.
3. Cragg SM, Beckham GT, Bruce NC, Bugg TD, Distel DL, Dupree P, Etxabe AG, Goodell BS, Jellison J, McGeehan JE: **Lignocellulose degradation mechanisms across the Tree of Life.** *Current Opinion in Chemical Biology* 2015, **29:**108-119.
4. Anwar Z, Gulfraz M, Irshad M: **Agro-industrial lignocellulosic biomass a key to unlock the future bio-energy: a brief review.** *Journal of radiation research and applied sciences* 2014, **7:**163-173.
5. Hu F, Ragauskas A: **Pretreatment and lignocellulosic chemistry.** *Bioenergy Research* 2012, **5:**1043-1066.
6. Keshk SM: **Cellulase Application in Enzymatic Hydrolysis of Biomass.** 2016.
7. Saha BC: **Hemicellulose bioconversion.** *J Ind Microbiol Biotechnol* 2003, **30:**279-291.
8. Malgas S, van Dyk JS, Pletschke BI: **A review of the enzymatic hydrolysis of mannans and synergistic interactions between β-mannanase, β-mannosidase and α-galactosidase.** *World Journal of Microbiology and Biotechnology* 2015, **31:**1167-1175.
9. Malherbe AR, Rose SH, Viljoen-Bloom M, van Zyl WH: **Expression and evaluation of enzymes required for the hydrolysis of galactomannan.** *J Ind Microbiol Biotechnol* 2014, **41:**1201-1209.
10. Van Dyk J, Pletschke B: **A review of lignocellulose bioconversion using enzymatic hydrolysis and synergistic cooperation between enzymes—factors affecting enzymes, conversion and synergy.** *Biotechnology advances* 2012, **30:**1458-1480.
11. Aulitto M, Fusco S, Fiorentino G, Limauro D, Pedone E, Bartolucci S, Contursi P: ***Thermus thermophilus*** **as source of thermozymes for biotechnological applications: homologous expression and biochemical characterization of an α-galactosidase.** *Microbial Cell Factories* 2017, **16:**28.
12. Nelson N: **A photometric adaptation of the Somogyi method for the determination of glucose.** *Journal of biological chemistry* 1944, **153:**375-380.
13. Mizutani K, Fernandes VO, Karita S, Luís AS, Sakka M, Kimura T, Jackson A, Zhang X, Fontes CM, Gilbert HJ: **Influence of a mannan binding family 32 carbohydrate binding module on the activity of the appended mannanase.** *Applied and environmental microbiology* 2012, **78:**4781-4787.
14. Malgas S, van Dyk SJ, Pletschke BI: **β-Mannanase (Man26A) and α-galactosidase (Aga27A) synergism–A key factor for the hydrolysis of galactomannan substrates.** *Enzyme and microbial technology* 2015, **70:**1-8.

15. Wielinga W, Maehall A: **Handbook of Hydrocolloids. Phillips G O, Williams PA, eds.** *Boca Raton: CRC Press* 2000, **200:**137-154.
16. Yousif AK, Alghzawi H: **Processing and characterization of carob powder.** *Food chemistry* 2000, **69:**283-287.
17. Bouzouita N, Khaldi A, Zgoulli S, Chebil L, Chekki R, Chaabouni M, Thonart P: **The analysis of crude and purified locust bean gum: A comparison of samples from different carob tree populations in Tunisia.** *Food chemistry* 2007, **101:**1508-1515.
18. Fusco FA, Ronca R, Fiorentino G, Pedone E, Contursi P, Bartolucci S, Limauro D: **Biochemical characterization of a thermostable endomannanase/endoglucanase from *Dictyoglomus turgidum*.** Extremophiles. 2017 Nov 25. doi: 10.1007/s00792-017-0983-6.

Chapter 3

Protein-spore system to deliver biological drugs to the human intestinal mucosa

3.1 Display of the peroxiredoxin bcp1 of *Sulfolobus solfataricus* on probiotic spores of *Bacillus megaterium*

Summary

Hyperthermophilic microorganisms are a good source of new robust enzymes for various biotechnological applications. Peroxiredoxins (Prxs), are ubiquitous thiol peroxidases involved in reduction of peroxides. Recently an array of Prxs named Bacterioferritin comigratory proteins (Bcps), were characterized from the hyperthermophilc archaeon *Sulfolobus solfataricus* (Bcp1-Bcp4) . They show not only a high thermostabilty, but also a greater structural robustness: in fact as the majority of Prokaryotic Prx, they are less prone to inactivation by over-oxidation. For this reasons in the paper entitled **"**Display of the peroxiredoxin Bcp1 of *sulfolobus solfataricus* on probiotic spores of *Bacillus megaterium***",** submitted to Microbial Cell Factories, we chose Bcp1 to test its antioxidant activity in association with bacterial spores of *Bacillus megaterium* for possible treatment in inflammatory bowel disease (IBD). For this purpose, the conditions to bind the enzyme to the spore surface were set up and then the perossidase activity and stability of system Bcp1-spore in the presence of simulated gastric and intestinal fluids were evaluated. The results showed that Bcp1 can be efficiently adsorbed to spores of *B. megaterium*; in particular the exosporium is essential for the binding of the enzyme. Bcp1 showed peroxidase activity also when it is adsorbed to the spores. In addition, the association protein-spores makes Bcp1 more resistant to degradation in presence of low pH values and proteases typical of gastrointestinal tract. These results represent a potentially useful property for a display platform to be used for the delivery of molecules to animal mucosal surfaces.

3.1 Display of the peroxiredoxin Bcp1 of *Sulfolobus solfataricus* on probiotic spores of *Bacillus megaterium*

Mariamichela Lanzilli, Giuliana Donadio, Francesca Anna Fusco, Danila Limauro, Ezio Ricca, Rachele Isticato*

Dipartimento di Biologia, University of Naples Federico II, Complesso universitario di Monte S. Angelo, Via Cinthia, Naples, Italy

*Corresponding author: Rachele Isticato isticato@unina.it

Manuscript in preparation

Abstract

Background: Bacterial spores displaying heterologous proteins have been proposed as a safe and efficient system to deliver antigens and enzymes to animal mucosal surfaces. Initial studies have been performed using *Bacillus subtilis* spores, but then other spore formers have been also considered. *B. megaterium* spores have been shown able to display large amounts of a model heterologous protein that in part crossed the exosporium localizing in the space between the outer coat layer and the exosporium. We used *B. megaterium* spores to adsorb Bcp1, a peroxiredoxin of the hyperthermophilic archaeon *Sulfolobus solfataricus*, known to have a antioxidant activity. **Results:** We report that purified Bcp1 was adsorbed by spores of *B. megaterium* QM B1551, that the exosporium had an important role in the adsorption and that Bcp1 was more efficiently adsorbed to B. megaterium than to *B. subtilis* spores. Adsorbed Bcp1 localized underneath the exosporium, filling the space between the outer coat and the exosporium. This peculiar localization contributed to the protection of the adsorbed enzyme from degradation in simulated intestinal or gastric conditions. In addition, we observed that *B. megaterium* spores had an endogenous antioxidant activity and that such activity was increased by Bcp1 adsorption, indicating that the adsorbed enzyme retained at least part of its enzymatic activity.

Conclusion: The spore of *B. megaterium* is highly efficient in adsorbing large amounts of the heterologous enzyme Bcp1 that, once adsorbed, retains its activity. In addition, as a delivery platform the spore has an endogenous antioxidant activity and, therefore, has its own potential health beneficial effects. These properties, together with the well-documented safety of *B. megaterium*, propose the spore of this species as a valid system for the mucosal delivery of health beneficial molecules.

Background

The delivery of drugs and antigens by the oral or nasal route offers several advantages over injectable methods and is gaining increasing relevance for the treatment of human and animal diseases. Mucosal routes are promising alternatives to the parenteral delivery also because of the high vascularisation of the mucosal surfaces that allows the direct transfer of molecules to the systemic circulation (1). However, the number of drugs and antigens that can be effectively administered by the oral or nasal route is severely limited by the rapid loss of activity encountered by many of these molecules at mucosal sites. Therefore, the successful development of mucosal therapeutic molecules relies on efficient delivery systems, able to stabilize and protect the molecules from degradation and to reduce or totally avoid the loss of biological activity (2). A

variety of drug delivery systems has been proposed, including live microorganisms, virus particles, synthetic nanoparticles, liposomes, microspheres, gels and cyclodextrins (2, 3) Bacterial spores displaying heterologous proteins have also been proposed as a tool for the delivery of molecules to mucosal surfaces (4, 5). Spores are extremely stable cells and are potentially able to conjugate some advantages of live microrganisms with those of synthetic nanoparticles (4, 5). Bacterial spores are mainly formed by Gram-positives belonging to different genera and including more than 1,000 species (6). The common feature of these organisms is the ability to form a quiescent cell type (the spore) in response to harsh environments. This peculiar cell survives in a dormant state for long periods, resisting to a vast range of stresses such as high temperature, dehydration, absence of nutrients, and presence of toxic chemicals. When the environmental conditions ameliorate, the spore germinates originating a vegetative cell able to grow and sporulate (6). The use of bacterial spores as a drug/antigen delivery system has been fostered by the remarkable and well-documented resistance of spores (7) that ensures high stability to the delivery system and by the safety record of several species of spore formers (8). Initially, spores of the model organism *Bacillus subtilis* have been used (9), but then also other *Bacillus* species have been tested for the display and mucosal delivery of antigens and enzymes (4, 10). More recently, spores of *B. megaterium* have been used to display a model heterologous protein (11). This species is particularly promising as a delivery vehicle for 54 at least two reasons: the large dimensions of its spore (length up to 3 mm and diameter of 1 mm) (12) and the presence of an exosporium, a protective layer surrounding the spore found only in some spore-forming species (13). Also because of their large dimensions, spores of *B. megaterium* were extremely efficient in displaying heterologous proteins and 5.0x108 spores of the QM B1551 strain adsorbed up to 100 μg of the red fluorescence protein of coral *Discosoma sp* (mRFP) that was shown to cross the exosporium of QM B1551 and localize in the inter-coat space (11). The exosporium is essential to allow a high efficiency of display and has been proposed to protect the displayed molecules from degradation (11). The QM B1551 strain of *B. megaterium* is the best-characterized strain of this species, it carries seven indigenous plasmids (14, 15), two of which, pBM500 and pBM600, are strictly required for the formation of the exosporium (16). The protein composition of the exosporium of QM B1551 is poorly characterized and only a few genes encoding orthologues of recognized exosporium proteins in spores of other species have been so far identified by genomic analyses (16). We used a well-characterized archaeal enzyme, the bacterioferritin comigratory protein 1 (Bcp1) of *Sulfolobus solfataricus*, belonging to peroxiredoxin family (17-20), as a model to study enzyme display and delivery by *B. megaterium* spores. Peroxiredoxins are thiol peroxidases commonly found in archaea and eukaryotes, including humans, and known to contribute to the cell protection against reactive oxygen species (ROS) (21). These potent oxidants are normally produced by oxygen metabolism but, when present at elevated

concentrations can cause protein oxidation, lipid peroxidation and DNA damages. ROS accumulation has been associated to neurodegenerative diseases, (22), progression of arteriosclerosis (23), inflammatory bowel diseases and Crohn's disease (24). Therefore, the delivery of enzymes with antioxidant activity can be a strategy to prevent inflammation caused by oxidative stress. Indeed, the high thermostable Bcp1 of *S. solfataricus*, used here as a model enzyme, has been recently found to protect cardiomyoblast cells from oxidative stress in vitro and proposed as a potentially health beneficial molecule with anti-oxidant activity (25).

Results and Discussion

Display of active Bcp1 of *S. solfataricus* on *B. megaterium* spores

To verify whether spores of *B. megaterium* QM B1551 were able to adsorb Bcp1, various amounts of the purified enzyme (Methods) were incubated with 5.0 x 10^8 purified spores. The adsorption reaction was performed in 50 mM sodium citrate at pH 4.0, as previously described (26). After the reaction, spores were extensively washed with 1xPBS pH 4.0, collected by centrifugation and spore surface proteins extracted as described in the Methods section. Extracted proteins were analyzed by western blotting with anti-polyHis-Peroxidase monoclonal antibody (Sigma), which recognizes the his-tagged N terminus of recombinant Bcp1. As shown in Fig. 1A, specific signals of increasing intensity were observed with extracts of spores reacted, respectively, with 20, 50 and 70 μg of purified Bcp1, therefore indicating that Bcp1 was absorbed during the reaction and then released by the extraction treatment.

To evaluate the efficiency of adsorption, we followed a well-established procedure (27, 28, 11) and analyzed the amount of Bcp1 left unbound, i.e., post-adsorbed spores were collected by centrifugation and the supernatant serially diluted and analyzed by dot blotting (Additional Fig. 1). The results of the densitometric analysis of the dot blotting (Additional Table1) are reported in Fig. 1B and showed that when 20 or 50 μg of purified Bcp1 were used in the adsorption reaction almost all molecules were adsorbed to the spore while when 70 μg of enzyme were used about 51 % of Bcp1 was adsorbed. In order to assess whether spore-adsorbed Bcp1 molecules retained their enzymatic activity we assayed the efficiency of H_2O_2 removal by the free and spore-bound enzyme. As a control we also assayed *B. megaterium* QM B1551 spores alone that showed a strong antioxidant activity (grey bar in Fig. 1C). However, spores-adsorbed with 20 or 50 μg of Bcp1 showed antioxidant activity higher than spores alone indicating that the enzyme was, at least in part, active (black bars in Fig. 1C). Although we cannot distinguish between the enzymatic activity due to the adsorbed Bcp1 or to the spore, we noted that spores adsorbed with 20 or 50 μg of Bcp1 (black bars in Fig. 1C) showed an antioxidant activity higher than that of similar amounts of free Bcp1

(white bars in Fig. 1C). Therefore, the activity observed with Bcp1 adsorbed to spores is most likely due to the combination of the activities of the adsorbed enzyme and of spores.

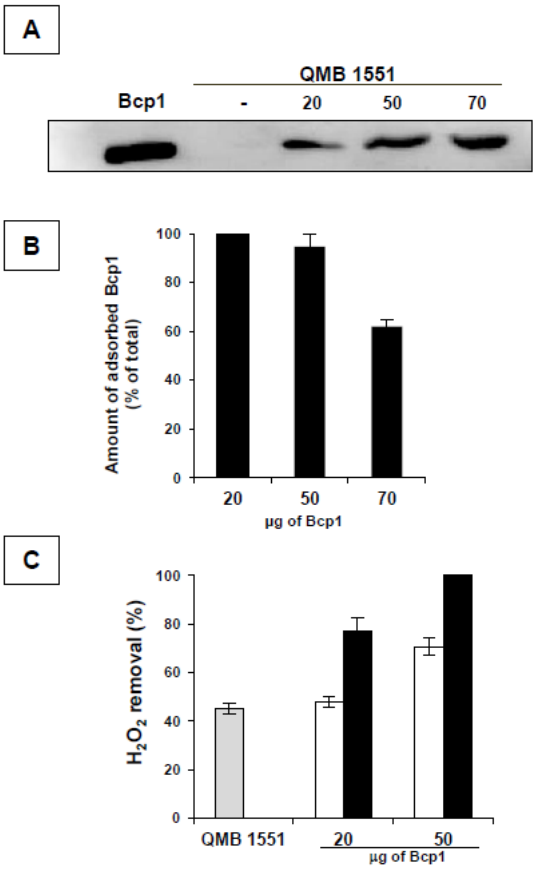

Fig. 1 Adsorption of Bcp1 to *B. megaterium* spores.5 x10^8 spores were incubated with with 20, 50 or 70 µg of Bcp1 and then the samples subject to centrifugation. (A) Spore surface proteins were extracted from the pellet fractions by SDS-DTT treatment and analyzed by Western blot with a Bcp1-recognizing antibody. Free Bcp1 was used as a marker. (B) The percentage of spore-adsorbed Bcp1 was calculated from dot blotting (Additional Fig. 1) of the supernatants fractions containing unbound Bcp1, and relative densitometric analysis (Additional Table 1). (C) Peroxidase activity of QM B1551 spores (grey bars), of 20 and 50 µg of free Bcp1 (white bars) or of the same amounts of enzyme adsorbed to spores (black bars). Error bars show the standard errors of the mean from the three different experiments.

The exosporium of *B. megaterium* is essential for Bcp1 adsorption

Strain QM B1551 of B. megaterium contains seven indigenous plasmids (14, 15), two of which are essential for the formation of the exosporium (16), the outermost spore layer. We used PV361, a QM B1551-cured strain totally lacking the exosporium (16), to analyze the role of the exosporium in Bcp1 adsorption. In parallel, we also used spores of *B. subtilis* PY79 the model organism for spore formers previously used to display a variety of heterologous proteins (5). To compare the adsorption efficiency of spores of *B. megaterium* QM B1551, PV361 and of *B. subtilis* PY79, we adsorbed 50 µg of purified Bcp1 with 5.0x10^8 spores of each of the three strains. After the adsorption reactions spores were collected by centrifugation, proteins extracted by SDS-DTT treatment and analyzed by western blotting with Bcp1-recognizing anti-His antibody. As shown in

Fig. 2A, Bcp1 was apparently extracted in larger amounts from spores of QM B1551 than from spores of the PV361 strain while *B. subtilis* spores adsorbed only minimal amounts of the enzyme. To quantify these apparent differences, unbound Bcp1 from the adsorption reactions was serially diluted and analyzed by dot blotting (Additional Fig. 2). The results of the densitometric analysis of the dot blotting (Additional Table 2) are reported in Fig. 2B and show that QM B1551 spores adsorbed more than 90% of the initial 50 μg of Bcp1 used in the reaction while PV361 and *B. subtilis* spores were less efficient and adsorbed about 70% and less than 50% of the original amount of the enzyme, respectively. Based on the results of Fig. 2 and of Additional Fig 2 and Table 2, we concluded that the exosporium, present in QM B1551 has a relevant role in the adsorption of Bcp1. This conclusion is also supported by a previous analysis in which the exosporium of QM B1551 spores resulted essential for the efficient adsorption of the red fluorescent protein (RFP) of the coral *Discosoma* (11). Spores of both strains of *B. megaterium*, QM B1551 and PV361, appeared more efficient than B. subtilis PY79 spores in adsorbing Bcp1. However, spores of *B. megaterium* are about three times larger than *B. subtilis* spores (12) and this raised the possibility that the different efficiency of adsorption was simply due to the different adsorption volume. Therefore, we repeated the adsorption experiment by using three times more *B. subtilis* spores with the same amount of Bcp1 (50 μg) and analyzed by dot blotting the unbound enzyme (Additional Fig 3). A densitometric analysis of the dot blotting showed that about 65% of the enzyme was adsorbed by $1.5x10^9$ *B. subtilis* spores (Additional Table 3). Therefore, $5.0x10^8$ spores of *B. megaterium* adsorbed at least 25% more Bcp1 than $1.5x10^9$ spores of *B. subtilis*, indicating a higher efficiency of Bcp1 adsorption of *B. megaterium* spores with respect to *B. subtilis* spores.

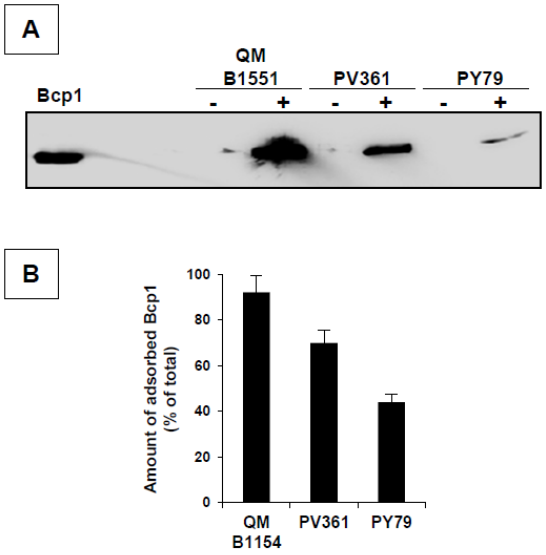

Fig. 2 Adsorption of Bcp1 to *B. megaterium* and *B. subtilis* spores. (A) Western blotting performed with Bcp1-recognizing antibody of free Bcp1 and of proteins extracted from spores of B. subtilis (PY79) or of B. megaterium with I (QM B1551) or PV361 alone (-) or adsorbed (+) with 50 μg of purified Bcp1. (B) Percentage of adsorbed Bcp1 was calculated from dot blotting (Additional Fig. 2) of the supernatants fractions containing unbound Bcp1, and relative densitometric analysis (Additional Table 2)

Bcp1 localizes in the inter-coat space

A previous study has indicated that the heterologous protein mRFP adsorbed to *B. megaterium* spores crossed the exosporium and localized in the space between the exosporium and the outer coat (11). In order to assess whether also Bcp1 was able to cross the exosporium we used an immunofluorescence approach. Bcp1 adsorbed spores were reacted with Bcp1-recognizing antibody and then with a fluorescent secondary antibody. As shown in Fig. 3, when spores were adsorbed with 20 μg of Bcp1 only a weak fluorescence signal was observed. This signal was not all around the spore but localized in a spot. Increasing the amount of Bcp1 used in the adsorption reaction a strong fluorescence signal was observed all around the spore (Fig. 3). Based on previous findings with *B. megaterium* spores and mRFP (11) and on results of Fig. 1 showing that up to 50 μg of Bcp1 can be adsorbed by *B. megaterium* spores, to explain results of Fig. 3 we hypothesized that when 20 μg of Bcp1 were used for the adsorption reaction all molecules of the enzyme crossed the exosporium, localized in the inter coat space and were mainly not available to the Bcp1-recognizing antibody. When the space between outer coat and exosporium was completely filled up by Bcp1 molecules (adsorption with 50 μg of Bcp1), some of them were exposed on the spore surface and available to the Bcp1-recognizing antibody. No differences were observed when 50 or 70 μg of Bcp1 were used. To verify this hypothesis, we used the red fluorescent protein of the coral *Discosoma*, already shown to adsorb to *B. megaterium* QM B1551 spores and to cross the exosporium (11). Spores were reacted either with 5 μg of mRFP or with 50 μg of Bcp1 first and then with 5 μg of mRFP.

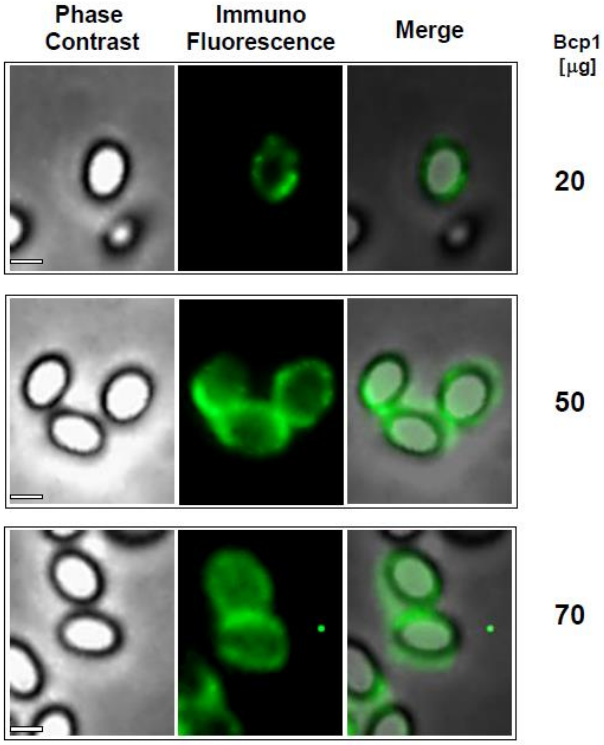

Fig. 3. Immunofluorescence microscopy of *B. megaterium* QM B1551 spores adsorbed with increasing amounts of purified Bcp1. After adsorption reaction, Bcp1-adsorbed spores were reacted with Bcp1-recognizing primary antibody and fluorescein isothiocyanate conjugated secondary antibody. The same microscopy field for phase contrast and immunofluorescence is reported together with the merge panel. The exposure time was 500ms for all images. Scalebar,1 μm.

Spores were then analyzed by fluorescence microscopy and as shown in Fig. 4, the red fluorescence signal was stronger when spores were adsorbed only with mRFP (Fig. 4A) than when were pre-adsorbed with Bcp1 (Fig. 4B), suggesting that Bcp1 filled up the inter-coat space reducing the number of mRFP molecules able to cross the exosporium. In a parallel experiment spores were reacted with 50 μg of Bcp1 or pre-adsorbed with 100 μg of mRFP and then with 50 μg of Bcp1. Spores were then analyzed for their antioxidant activity, and as shown in Fig. 5, the activity of spore pre-adsorbed with mRFP and then adsorbed with Bcp1 (dark grey bar) was significantly lower than that of spores adsorbed only with Bcp1 (black bar) and similar to that of QM B1551 spores alone (light grey bar). Altogether results of Fig. 3, 4 and 5 support the conclusion that, like mRFP (11), also Bcp1 molecules crossed the exosporium of the *B. megaterium* spore, localizing in the inter-coat space and filling the space between outer coat and exosporium.

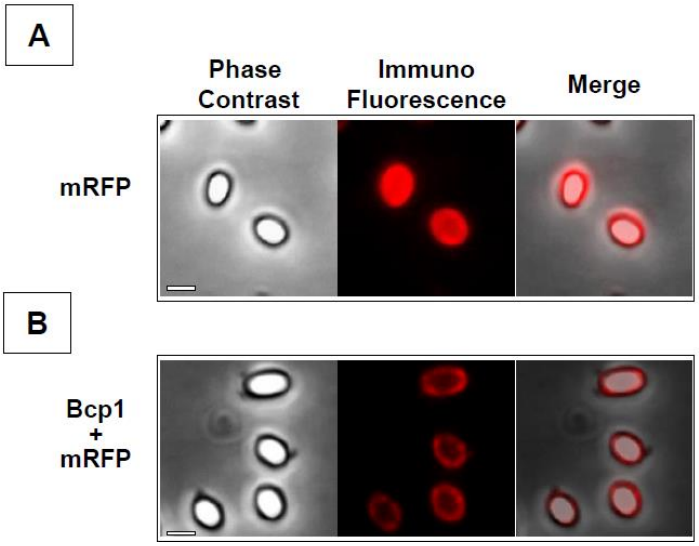

Fig. 4. Fluorescence microscopy of *B. megaterium* QM B1551 spores adsorbed with mRFP and/or Bcp1. *B. megaterium* QM B1551 spores were adsorbed with 5 μg of mRFP (A) or with 50 μg of Bcp1 and then with 5 μg of mRFP (B), washed and analyzed by fluorescence microscopy. The same microscopy field was observed by phase contrast and fluorescence microscopy. The merge panel is reported. The exposure time was 200ms. Scalebar,1 μm.

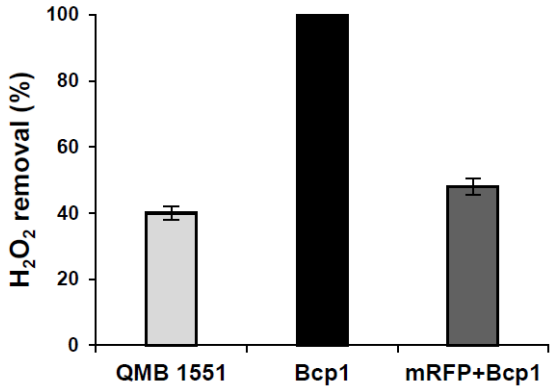

Fig. 5. Antioxidant activity of *B. megaterium* QM B1551 spores adsorbed with Bcp1 and/or mRFP. Peroxidase activity of 5.0x108 spores of QM B1551 alone (light grey bar) or adsorbed with 50 μg of Bcp1 (black symbols) or with 100 μg of mRFP and then with 50 μg of Bcp1 (dark grey bars).

Effects of simulated gastric or intestinal conditions on Bcp1-adsorbed spores

To analyze the effects of intestinal conditions on Bcp1 adsorbed to spores, we treated the free and the spore-adsorbed enzyme with simulated gastric fluid (SGF) or simulated intestinal fluid (SIF) (Methods). $5.0x10^8$ spores adsorbed with 50 μg of Bcp1 were treated with SGF or SIF, washed, used to extract surface proteins and these analyzed by western blotting as above. In parallel, the same amount of free Bcp1 was also treated with SGF or SIF and analyzed by western blotting. As

shown in Fig. 6A, free Bcp1 was totally degraded by SGF treatment and only a minimal amount of the enzyme was still detected after the SIF treatment. Spore-adsorbed Bcp1 molecules were, instead, still extracted and detected after either treatment, indicating that they were only partially affected by SGF or SIF (Fig. 6A). To verify whether the detected enzyme was still active, we analyzed the antioxidant activity of spores, free enzyme and spore-adsorbed enzyme after the treatment with SGF or SIF. As reported in Fig. 6B, the activity of $5.0x10^8$ QM B1551 spores was not affected by either treatment (grey bars), while the activity of the free enzyme (50 μg) was strongly affected by both treatments with a reduction of activity of about 50% with SIF and about 85% with SGF (white bars). The activity of $5.0x10^8$ spores adsorbed with 50 μg of Bcp1was also affected by the treatments but the reduction of activity was about 20 and 30% with SIF and SGF, respectively (Fig. 6B). Both SGF and SIF affected free and spore-bound Bcp1, however the antioxidant activity of spore-bound Bcp1 was slightly higher than the sum of the activities of spores and free enzyme (Fig. 6B), suggesting that part of the adsorbed enzyme was still active after the treatments. It has been previously reported that an enzyme adsorbed to *B. subtilis* spores was somehow protected against acidic conditions (26). Based on this the partial protection of Bcp1 observed in the experiments of Fig. 6 could be explained by a stabilization of the adsorbed enzyme at low pH conditions used at least SGF treatments. To verify this possibility we treated spores, free Bcp1 and spore-adsorbed Bcp1 to various acidic conditions. As shown in Fig. 7A, the activity of Bcp1- spores (black symbols) was higher than that of free Bcp1 (white symbols) at all pHs tested, most likely because of the activity of the spore (grey symbols). However, free and spore-bound Bcp1similarly decreased from pH 7.0 to pH 2.0, suggesting that the interaction with the spore did not protect the enzyme at low pH conditions. Based on this we concluded that: i) the decrease of antioxidant activity of spore-Bcp1 treated with SGF (Fig. 6B) was mostly due to the acidic condition; and ii) the slightly higher activity of spore-bound Bcp1 with respect to free Bcp1 was due to a protection against the proteases present in the SGF. An explanation for the partial protection of adsorbed Bcp1 is that the enzyme is covered by the exosporium (Fig. 3, 4, 5), and not accessible to the degradative enzymes present in SIF or SGF. We hypothesize that these proteases would not be able to cross the exosporium and degrade Bcp1 because, as shown for mRFP (Fig. 4), when QM B1551 spores were adsorbed with 50 μg of Bcp1 the space between outer coat and exosporium was almost completely full. To verify this hypothesis, we repeated the experiment of Fig. 6B, but adsorbing QM B1551 spores with 20 μg of Bcp1. As shown in Fig. 7B, the activity of spores adsorbed with 20 μg of Bcp1 was strongly reduced by SIF and almost completely eliminated by the SGF. The antioxidant activity of spore bound Bcp1 was slightly higher than or identical to that of spores alone after the SIF or SGF treatment, respectively (Fig. 7B), indicating that the enzyme was

almost completely degraded. We infer that in these conditions, some of the protease molecules contained in SGF and SIF crossed the exosporium and degraded Bcp1. Therefore, results of Fig. 7B supported the idea that the proteases of SIF and SGF could not enter the inter-coat space when it was already filled up with other molecules.

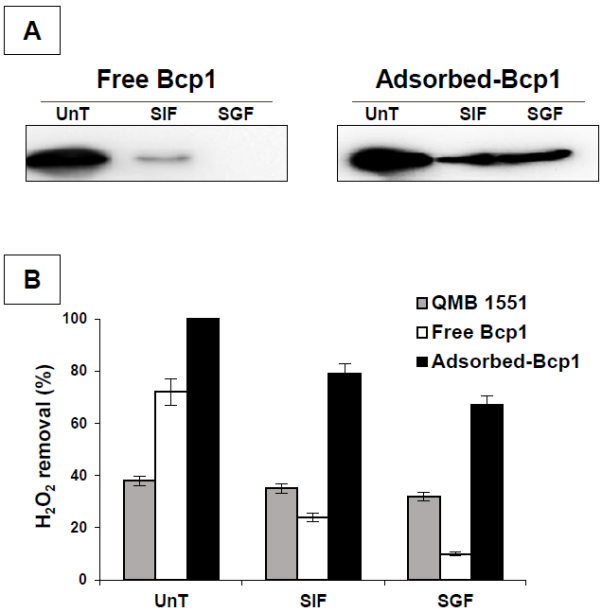

Fig. 6. Effect of SIF and SGF on spore adsorption. (A) Western blotting performed with Bcp1-recognizing antibody of free Bcp1 and of proteins extracted from spores of *B. megaterium* QM B1551 adsorbed with 50 μg of purified Bcp1. Free and spore-adsorbed enzyme was not treated (UnT) or treated with SIF or SGF as described in Methods section. (B) Peroxidase activity of $5.0x10^8$ spores of QM B1551 (grey bars), of 50 μg of free Bcp1 (white bars) or of the same amount of enzyme adsorbed to spores (black bars) without (UnT) or with SIF or SGF treatment. *Error bars* show the standard errors of the mean from three independent experiments ($P < 0.05$).

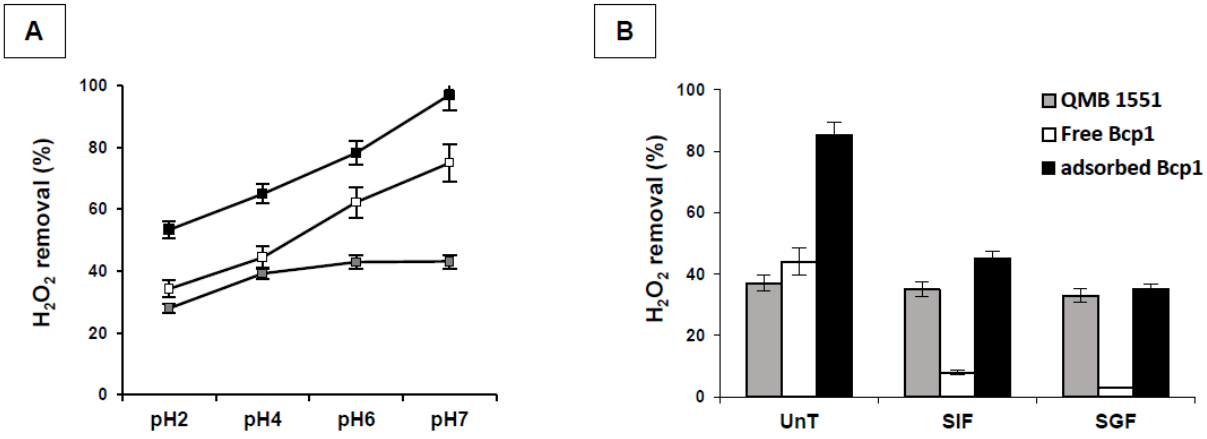

Fig. 7 Effect of pH or protease on spore adsorption (A) Effect of low pH conditions on the Peroxidase activity of free Bcp1 (white symbols), spores (grey symbols) and spore-adsorbed Bcp1 (black symbols). (B) Antioxidant activity of $5.0x10^8$ spores of QM B1551 (grey bars), of 20 μg of free Bcp1 (white bars) or of the same amount of enzyme adsorbed to spores (black bars) without (UnT) or with SIF or SGF treatment.

Conclusions

Main conclusion of this report is that the thermoacidophylic enzyme Bcp1 of *S. solfataricus* can be efficiently adsorbed to spores of *B. megaterium*, with about 50 μg of enzyme adsorbed by $5.0x10^8$ spores. The adsorption is more efficient than with *B. subtilis* spores and is in part due to the presence of the exosporium. Adsorbed Bcp1 localized the space between the outer coat and the exosporium and this peculiar localization contributes to the protection of the enzymes from degradation by treatments with SIF or SGF. An additional interesting observation highlighted by this report is that *B. megaterium* spores have an endogenous antioxidant activity. This endogenous antioxidant activity of *B. megaterium* spores is also stable at low pH conditions and represents a potentially useful property for a display platform to be used for the delivery of molecules to animal mucosal surfaces.

Methods

Bacterial strains and spore purification

B. megaterium strains QM B1551 and PV361 (14) and B. subtilis strain PY79 (27) were used in this study. Sporulation was induced by the exhaustion method. After 30 h of growth in Difco Sporulation medium (DSM) at 37 °C with vigorous shaking, spores were collected, washed three times with distilled water and incubated overnight in distilled water in H_2O at 4°C to lyse residual sporangial cells as described before (11). Spore counts were determined by direct counting with a Bürker chamber under an optical microscope (Olympus BH-2 with 40× lens)

Expression and purification of Bcp1

BL21 DE3 RIL/ pET30Bcp1 strain was grown up to 0.8 OD600nm in Luria-Bertani (LB) medium supplemented with kanamycin (10 μg mL-1) and chloramphenicol (34 μg mL-1) at 37 °C. The expression of the recombinant enzyme was induced by 1 mM isopropyl-β-D-thiogalactoside (IPTG) for 6 h at 37 °C (28). The cells were harvested by centrifugation, resuspended in 20mM Tris-HCl pH 8.0 containing complete EDTA-free protease inhibitors cocktail and disrupted by sonication. Purification of protein was carried out by two steps: heat treated cell extract at 80°C for 15 min and affinity chromatography by His Trap HP (21).

Adsorption reaction

Different amounts of Purified Bcp1 were incubated with $5x10^8$ spores in 200 μl of 50 mM Sodium Citrate pH 4.0 at 25°C (26). After 1 h of incubation, the binding mixture was centrifuged (10 min at 13,000xg) to fractionate Bcp1 adsorbed-spores in the pellet from free Bcp1 in the supernatant (29).

Western and Dot-Blotting Analysis

Extraction of proteins from spores and Bcp1-adsorbed spores was performed with treatment at 65°C in 40 µl of SDS-DTT extraction buffer (10mM tris pH 8.0, 1%SDS, 50 mM DTT, 10 mM EDTA, mM Tris–HCl, pH 8.0). 20 µl of extracted proteins were then electrotransferred to nitrocellulose filters (Amersham Pharmacia Biotech) and analysed by Western blot using monoclonal Bcp1-recognizing anti-His antibody (Sigma), as previously reported (29). A quantitative determination of the amount of Bcp1 was obtained by dot blot experiments comparing serial dilutions of purified Bcp1 and binding assay supernatant. Filters were then visualized by the ECL-substrates method (Clarity, Bio-rad) and subjected to densitometric analysis by Quantity One 1-D Analysis Software (Bio-Rad) (29). Dot blot and relative densitometric analyses were performed three times to verify the significance of the results.

Fluorescence and immunofluorescence microscopy

Samples for Immunofluorescence microscopy were prepared as described by Lanzilli et al. (2016) and observed with an Olympus BX51 fluorescence microscope (11). mRFP-adsorbed spores were resuspended in 50 µl of 1xPBS pH 4.0 and 5 µl of the suspension observed at fluorescence microscope. Exposure times were in the range between 200 and 5000ms. Images were captured using an Olympus DP70 digital camera and processed with Image Analysis Software (Olympus) for minor adjustments of brightness, contrast and color balance (30).

Assays of peroxidase activity

The ability to remove peroxide of the spores and of free or spore-adsorbed Bcp1 was tested by an in vitro non-enzymatic assay (28). The reaction was started adding H_2O_2 at a final concentration of 0.2 mM to the reaction mixture containing 50 mM Hepes (pH 7.0) and 10 mM DTT in presence of different concentration of Bcp1, spores or Bcp1-adsorbed spores in a final volume of 0.1 mL. The reaction was incubated at 37 °C for 5 min and stopped by adding 0.9 mL of trichloroacetic acid solution (10%, w⁄v), as previously described (25). Peroxidase activity was determined from the amount of H_2O_2 remaining, which was detected by measurement at A_{490nm} of the purple-colored ferrithiocyanate complex developed after the addition of 0.2 mL of 10 mm $Fe(NH4)_2(SO4)_2$ and 0.1 mL of 2.5 M KSCN, using H_2O_2 as a standard.

Treatments with simulated gastric and intestinal fluids

Free Bcp1, spores and Bcp1-adsorbed spores were incubated for 1 h at 37°C in 100 µl of simulated gastric juice (SGF) (1 mg of pepsin (porcine stomach mucosa; Sigma) per ml of 10 mM HCl; pH 2.0) or small intestine fluid (SIF) (1 mg of pancreatin (porcine pancreas; Sigma) per ml and 0.2%

bile salts (50% sodium cholate-50% sodium deoxycholate; Sigma); pH 6.8). To remove the proteases contained in SIF and SGF After incubation, the samples containing free Bcp1 were treated at 90°C for 15 min while samples containing spores were centrifuged 10 min at 13000xg. For the pH-stability assay, free Bcp1, spores and Bcp1-adsorbed spores were incubated at 37°C for 1h in following buffers: 0.1 M Glycine-HCl pH 2.0; 0.1 M citrate-phosphate pH 4.0 and pH 6.0, or 0.1 M HEPES pH 7.0. After incubation, the peroxidase activity of the samples was measured following the protocol described above.

Statistical Analysis

Results of peroxidase activity analysis are the averages from three independent experiments. The error bars reported in the figures show the standard errors of the mean from the three experiments. Statistical significance was determined by the Student t-test, and the significance level was set at $P < 0.05$.

Competing interests

The authors declare that they have no competing interests.

Acknowledgments

This work was supported by a grant (Star - 2014) from the Federico II University to R.I. and by a 8 grant of the Agenzia Spaziale Italiana to E.R.

Supplementary material

Additional Figure 1

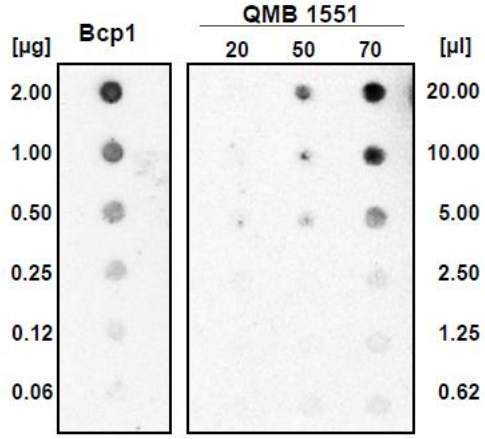

Additional Figure 1. Dot blot of serial dilutions of unbound Bcp1 after adsorption reactions with 5.0 x 108 B. megaterium QM B1551 spores and different amounts of Bcp1 (20, 50 or 70 µg). The amount of purified Bcp1 (µg) and the volume of supernatant (µl) loaded are indicated. Immuno reactions were performed with with Bcp1-recognizing antibody conjugated with the horseradish peroxidase ("Methods" section).

Additional Table 1. Densitometric analysis of dot blot experiments reported in Add. Fig 1.

Bcp1 source	Amount of sample used	Density (OD/mm2) [a]	Amount of Bcp1 (µg) [b]	Average Bcp1 µg (% total)
Purified	2.00 µg	1543.80	N/A	N/A
	1.00 µg	683.31	N/A	N/A
	0.50 µg	292.54	N/A	N/A
	0.25 µg	155.80		
Unbound				
20 µg		N/A	N/A	N/A
50 µg	20µl	223.55	0.30	2.6 (5.2%)
	10µl	88.01	0.11	
70 µg	10µl	767.33	1.19	28.2 (40%)
	5µl	310.69	0.57	
	2.5µl	112.51	0.19	

[a] Density measured by optical density (OD) per square millimeter and obtained by ChemiDocXRS apparatus with Quantity-One software (Bio-Rad).
[b] Calculated from signals (density OD/mm2) obtained with purified Bcp1. NA, not applicable

Additional Figure 2

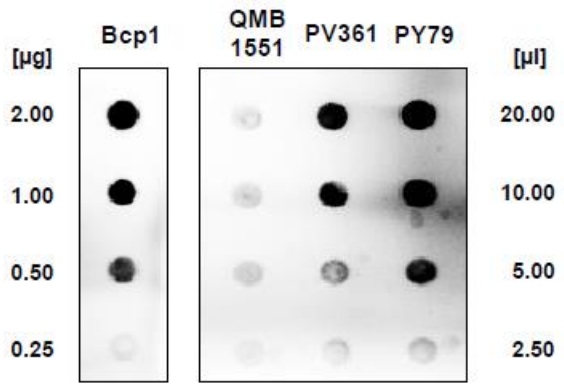

Additional Figure 2. Dot blot analysis of serial dilutions of unbound Bcp1 after adsorption reactions with 5.0 x 108 *B. subtilis* PY79 or with *B. megaterium* QM B1551 or PV361 spores and 50 µg of Bcp1. The amount of purified Bcp1 (µg) and the volume of supernatant (µl) loaded are indicated. Immuno reactions were performed with with Bcp1-recognizing antibody conjugated with the horseradish peroxidase ("Methods" section).

Additional Table 2. Densitometric analysis of dot blot experiments reported in Add. Fig 2.

Bcp1 source	Amount of sample used	Density (OD/mm2) [a]	Amount of Bcp1 (µg) [b]	Bcp1 µg (% total)
Purified Bcp1				
	2.00 µg	2641.90	N/A	N/A
	1.00 µg	1352.54	N/A	N/A
	0.50 µg	568.23	N/A	N/A
	0.25 µg	218.69	N/A	N/A
Unbound Bcp1				
QM B1551	20.µl	377.55	0.39	3.92
	10µl	N/A	N/A	(7.8%)
	5µl	N/A	N/A	
PV361	20.µl	1513.84	1.55	15.00
	10µl	788.01	0.85	(30%)
	5µl	533.13	0.31	
PY79	10µl	1585.63	1.63	27.90
	5µl	776.51	0.68	(56%)
	2.5µl	295.45	0.298	

[a] Density measured by optical density (OD) per square millimeter and obtained by ChemiDocXRS apparatus with Quantity-One software (Bio-Rad).
[b] Calculated from signals (density OD/mm2) obtained with purified Bcp1.
NA, not applicable

Additional Figure 3

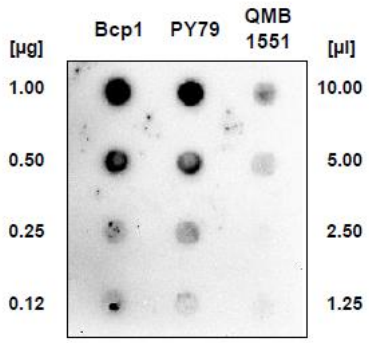

Additional Figure 3. Dot blot analysis of the supernatants of adsorption reactions of 1.5 x 109*B. subtilis* spores (PY79) and 5.0 x 108 or of *B. megaterium* spores (QM B1551) with 50 µg of Bcp1. The amount of purified Bcp1 (µg) and the volume of supernatant (µl) loaded are indicated.

Additional Table 3. Densitometric analysis of dot blot experiments reported in Add. Fig 3.

Bcp1 source	Amount of sample used	Density (OD/mm2) [a]	Amount of Bcp1 (µg) [b]	Bcp1 µg (% total)
Purified Bcp1				
	1.00 µg	1771.91	N/A	N/A
	0.50 µg	774.41	N/A	N/A
	0.25 µg	332.35	N/A	N/A
	0.12 µg	115.55	N/A	N/A
Unbound Bcp1				
PY79	10µl	1529.85	0.71	17.28
(1.5x10^9 spores)	5µl	652.53	0.42	(33%)
	2.5µl	343.83	0.26	
QM B1551	10µl	347.58	0.26	5.0
(5x10^8 spores)	5µl	118.36	0.12	(10%)

[a] Density measured by optical density (OD) per square millimeter and obtained by ChemiDocXRS apparatus with Quantity-One software (Bio-Rad).
[b] Calculated from signals (density OD/mm2) obtained with purified Bcp1.
NA, not applicable

References

1. Zhang H, Zhang J, Streisand JB. **Oral mucosal drug delivery: clinical pharmacokinetics and therapeutic applications.** *Clin. Pharmacokinet*. 2002. 41:661-680.
2. Tiwari G, Tiwari R, Sriwastawa B, Bhati L, Pandey S, Pandey P, Bannerjee S. **Drug delivery systems: an updated review.** *Int. J. Pharm. Investig*. 2012. 2:2-11.
3. Wells J. **Mucosal vaccination and therapy with genetically modified lactic acid bacteria.** *Annu. Rev. Food Sci. Technol*. 2011. 2:423-45.
4. Isticato R, Ricca E. **Spore surface display.** *Microbiol.Spectr*. 2014. 2:351–366.
5. Ricca E, Baccigalupi L, Cangiano G, De Felice M, Isticato R. **Mucosal vaccine delivery by non-recombinant spores of *Bacillus subtilis*.** *Microb. Cell Fact.* 2014. 13: 115.
6. Cutting SM, Hong HA, Baccigalupi L, Ricca E. **Oral Vaccine Delivery by Recombinant Spore Probiotics.** *Intern. Rev. Immunol*. 2009, 28:487-505.
7. McKenney PT, Driks A, Eskandarian HA, Grabowski P, Guberman J, Wang KH, Gitai Z, Eichenberger P. **A distance-weighted interaction map reveals a previously uncharacterized layer of the *Bacillus subtilis* spore coat.** *Current Biology* 2010, 20:934–938.
8. Cutting SM. ***Bacillus* probiotics.** *Food Microbiol*. 2011, 28:214-220.
9. Isticato R, Cangiano G, Tran HT, Ciabattini A, Medaglini D, Oggioni MR, De Felice M, Pozzi G, Ricca E. **Surface display of recombinant proteins on *Bacillus subtilis* spores.** *J. Bacteriol.* 2001, 183: 6294-6301.
10. Knecht LD, Pasini P, Daunert S. **Bacterial spores as platforms for bioanalytical and biomedical applications.** *Anal. Bioanal. Chem.* 2011, 400:977-989.
11. Lanzilli M, Donadio G, Addevico R, Saggese A, Cangiano A, Baccigalupi L, Christie G, Ricca E, Isticato R. **The exosporium of *Bacillus megaterium* QM B1551 is permeable to the red fluorescence protein of the coral *Discosoma sp.*** *Front. Microbiol*. 2016. 7:1752.
12. Di Luccia B, D'Apuzzo E, Varriale F, Baccigalupi L, Ricca E, Pollice A. ***Bacillus megaterium* SF185 induces stress pathways and affects the cell cycle distribution of human intestinal epithelial cells.** *Benef.Microb*. 2016. 7:609–620.

13. Koshikawa T, Beaman TC, Pankratz HS, Nakashio S, Corner TR, Gerhardt P. **Resistance, germination, and permeability correlates of *Bacillus megaterium* spores successively divested of in tegument layers.** *J. Bacteriol*. 1984. 159:624–632.
14. Rosso ML, Vary PS. **Distribution of *Bacillus megaterium* QM B1551 plasmids among other *B. megaterium* strains and *Bacillus* species.** *Plasmid* 2005. 53: 205–217.
15. Eppinger M, Bunk B, Johns MA, Edirisinghe JN, Kutumbaka KK, Koenig S S, et al. **Genome sequences of the biotechnologically important *Bacillus megaterium* strains QMB1551 and DSM319.** *J. Bacteriol*. 2011. 193:4199– 4213.
16. Manetsberger J, Hall EAH, Christie G. **Plasmid-encoded genes influence exosporium assembly and morphology in *Bacillus megaterium* QM B1551 spores.** *FEMS Microbiol.Lett.* 2015. 362:fnv210.
17. Limauro D, Pedone E, Pirone L, Bartolucci S. **Identification and characterization of 1-Cys peroxiredoxin from *Sulfolobus solfataricus* and its involvement in the response to oxidative stress**. *FEBS J*. 2006. 273:721–731.
18. Limauro D, Pedone E., Galdi I, Bartolucci S. **Peroxiredoxins as cellular guardians in *Sulfolobus solfataricus*: characterization of Bcp1, Bcp3 and Bcp4.** *FEBS J*. 2008. 275:2067–2077.
19. Pedone E, Limauro D, Bartolucci S. **The machinery for oxidative protein folding in thermophiles.** *Antioxidants and Redox Signaling* 2008. 10:157–169.
20. Limauro D, Saviano M, Galdi I, Rossi M, Bartolucci S, Pedone E. ***Sulfolobus solfataricus* protein disulphide oxidoreductase: insight into the roles of its redox sites.** *Protein Eng Des Sel.* 2009 22(1):19-26.
21. Pedone E, Limauro D, D'Ambrosio K, De Simone G, Bartolucci S. **Multiple catalytically active thioredoxin folds: a winning strategy for many functions.** *Cell. Mol. Life Sci.* 2010. 67:3797–3814.
22. Westfall S, Lomis N, Kahouli I, Dia SY, Singh SP, Prakash S. **Microbiome, probiotics and neurodegenerative diseases: deciphering the gut brain axis.** *Cell Mol Life Sci.* 2017 Jun
23. Guo H, Callaway JB, Ting JP-Y. **Inflammasomes: mechanism of action, role in disease, and therapeutics.** *Nature Medicine* 2015. 21: 677–687
24. LeBlanc JG, Laiño JE, del Valle MJ, Vannini V, van Sinderen D, Taranto MP, de Valdez GF, de Giori GS, Sesma F. B**-group vitamin production by lactic acid bacteria—current knowledge and potential applications.** *J Appl Microbiol*. 2011. 111:1297-309.
25. Sarcinelli C, Fiorentino G, Pizzo E, Bartolucci S, Limauro D. **Discovering Antioxidant Molecules in the Archaea Domain: Peroxiredoxin Bcp1 from *Sulfolobus solfataricus* Protects H9c2 Cardiomyoblasts from Oxidative Stress.** *Archea.* 2016.
26. Sirec T, Strazzulli A, Isticato R, De Felice M, Moracci M, Ricca E. **Adsorption of betagalactosidase of *Alicyclobacillus acidocaldarius* on wild type and mutants spores of *Bacillus subtilis*.** *Microb Cell Fact* 2012. 11:100.
27. Youngman P, Perkins JB, Losick R. **A novel method for the rapid cloning in *Escherichia coli* of *Bacillus subtilis* chromosomal DNA adjacent to Tn917.** *Mol. Gen. Genet.* 1984 195: 424–433.
28. Limauro D, D'Ambrosio K, Langella E, De Simone G, Galdi I, Pedone C, Pedone E, Bartolucci S. **Exploring the catalytic mechanism of the first dimeric Bcp: Functional, structural and docking analyses of Bcp4 from *Sulfolobus solfataricus*.** *Biochimie.* 2010 92 :1435-44
29. Isticato R, Sirec T, Treppiccione L, Maurano F, De Felice M, Rossi M, Ricca E. **Nonrecombinant display of the B subunit of the heat labile toxin of *Escherichia coli* on wild type and mutant spores of *Bacillus subtilis*.** *Microb. Cell Fact.* 2013. 12:98.
30. Donadio G, Lanzilli M, Sirec T, Ricca E, Isticato R. **Localization of a red fluorescence protein adsorbed on wild type and mutant spores of *Bacillus subtilis*.** *Microb. Cell Fact.* 2016. 15:153.

Chapter 4

General conclusions

Industrial biotechnology aims to replace the current chemical synthesis processes of useful compounds with low environmental impact methods based on (micro)organisms, plants and enzymes, for a "Green Chemistry". Thermophilic biocatalysts for their robustness and ability to work in extreme conditions make them particularly advantageous in various biotechnology sectors (1). This PhD project has been focused on the study of thermophilic biocatalysts to be used in two different applications: one concerning the “green energy” by degradation of biomass and the other one regarding possible pharmacological application by the use of new drug delivery systems (2). In the first part of this project, two glycosyde hydrolases (GH), from the hyperthermophilic bacterium *Dictyoglomus turgidum*, were identified: Dtur_0671 (*Dtur*CelB) belonging to the GH5 family and Dtur_0462 (*Dtur*βGlu) belonging to the GH1 family (3). Through the production of the respective synthetic genes and subsequent cloning into pET vectors, they were recombinantly produced in *E. coli* and subsequently biochemically characterized.

*Dtur*CelB can be classified as endoglucanase/ endomannanase because showed high hydrolytic activity on glucomannan and different galactomannans and slight but appreciable activity on carboxymethylcellulose; moreover, *Dtur*CelB showed optimal activity values at pH and temperature of 5.4 and 70 °C respectively and a good stability to temperature (50% activity after 2 h at 70), to pH (70% activity at pH 4 and 90% in range of pH 5-8 after 1 hour of incubation), to metals and non-ionic detergents.

*Dtur*βGlu is a β-glucosidase with a tetrameric structure; the enzyme showed optimal activity values at 80°C and at pH 5.4, a good stability at high temperature and in a wide range of pH, moreover it was enhanced by the addition of non-ionic detergents such as triton X-100 and Tween-20. *Dtur*βGlu displayed also an optimal β-galactosidase activity and the ability to hydrolyse aromatic β-glucosides, such as salicin with a higher catalytic efficiency respect to others thermophilic β-glucosidases.

The features of these two enzymes take them good candidate for biotechnological applications, especially in the conversion of biomass to produce fermentable sugars (4).

In order to create a cocktail of hemicellulases to be tested on biomass, the synergistic effect of *Dtur*CelB from D. turgidum and *Tt*GalA, an α galactosidase from *Thermus thermophilus* (5) has been studied. These two enzymes have been assayed on different galactomannans both simultaneously and sequentially conditions and it was demonstrated that there is an heterosynergystic association of these two recombinant thermophilic enzymes on all the substrate tested at high temperature (80°C) and in a relatively short time (30 min). In particular, results highlighted that *Tt*GalA, removing galactose branches from the galactomannan polymers improve the accessibility of the linear mannan backbone to *Dtur*CelB.

In the second part of this project a protein-spore antioxidant system has been studied for a possible treatment in inflammatory bowel disease. The recombinant bacterioferritin comigratory protein 1 (Bcp1) from Sulfolobus solfataricus (6) was efficiently adsorbed on spores of Bacillus megaterium and this system was tested in different condition simulating the intestinal gastric tract. Results showed that the system retain a higher antioxidant activity respect to Bcp1 alone in this harsh condition, highlighting the protective role of the spore towards the protein and the ability to use this system as a display platform for the delivery of molecules to animal mucosal surfaces.

References

1. Dalmaso GZ, Ferreira D, Vermelho AB. (2015) **Marine extremophiles: a source of hydrolases for biotechnological applications.** *Mar Drugs.* 3;13(4):1925-65.
2. Isticato R, Cangiano G, Tran HT, Ciabattini A, Medaglini D, Oggioni MR, De Felice M, Pozzi G, Ricca E. (2001) **Surface display of recombinant proteins on *Bacillus subtilis* spores.** *J. Bacteriol.* 183: 6294-6301.
3. Brumm PJ, Gowda K, Robb FT, Mead DA (2016) **The Complete Genome Sequence of Hyperthermophile *Dictyoglomus turgidum* DSM 6724™ Reveals a Specialized Carbohydrate Fermentor.** *Front Microbiol* 20:1979.
4. Simmons BA. et al. (2008) **Next-generation biomass feedstocks for biofuel production.** *Genome Biology* 9(12)**:**242.
5. Aulitto M, Fusco S, Fiorentino G, Limauro D, Pedone E, Bartolucci S, Contursi P: ***Thermus thermophilus* as source of thermozymes for biotechnological applications: homologous expression and biochemical characterization of an α-galactosidase.** *Microbial Cell Factories* 2017, **16:**28.
6. Sarcinelli C, Fiorentino G, Pizzo E, Bartolucci S, Limauro D (2016) **Discovering Antioxidant Molecules in the Archaea Domain: Peroxiredoxin Bcp1 from *Sulfolobus solfataricus* Protects H9c2 Cardiomyoblasts from Oxidative Stress.** *Archaea* 2016:7424870.

List of communications

Limauro D**, Fusco FA,** Lanzilli M, Donadio G, Bartolucci S, Isticato R. A new antioxidant system for the human intestinal mucosa: the archaeal peroxiredoxin Bcp1 adsorbed to spore of *Bacillus megaterium*. ***59TH*** **Congresso Società italiana di biochimica e biologia molecolare, Caserta Settembre 20-22, 2017**

Lanzilli M, Donadio G, **Fusco FA**, Limauro D, Ricca E. Isticato R. Adsorption of a thermoacidophilic peroxiredoxin of *Sulfolobus solfataricus* on *Bacillus megaterium* spores. Microbiology 2017, XXXII SIMGBM Congress, Palermo September 17-20, 2017

Fusco FA, Fiorentino G, Contursi P, Bartolucci S, Limauro D. Characterization of a new thermophilic β-glucosidase from *Dictyoglomus turgidum*. **7TH Congress of European microbiologist FEMS 2017, Valencia Luglio 9-13, 2017**

Fusco FA, Ronca R, Aulitto M, Contursi P, Bartolucci S, Limauro D. Biochemical characterization of a new endoglucanase from *Dyctioglomus turgidum*. **SOLID URBAN WASTE MANAGEMENT; XXI IUPAC CHEMRAWN CONFERENCE, Rome April 6-8, 2016.**

Aulitto M, Fusco S, **Fusco FA**, Limauro D, Bartolucci S, Contursi P. A thermophilic *Bacillus coagulans* strain isolated from beans-waste is promising for cellulosic biomass saccharification. **SOLID URBAN WASTE MANAGEMENT; XXI IUPAC CHEMRAWN CONFERENCE, Rome April 6-8, 2016.**

Fusco FA, Sarcinelli C, Bartolucci S, Limauro D. New cellulase from the hyperthermophilc bacterium *Dyctioglomus turgidum*. **58TH National Meeting of the Italian Society of Biochemistry and Molecular Biology Urbino, September 14-16, 2015.**

Antonucci I, **Fusco FA**, Limauro D, Del Giudice I, Berenguer J, Bartolucci S, Fiorentino G. Exploiting the arsenic resistance of the thermophilic bacterium *Thermus thermophilus*. **58TH National Meeting of the Italian Society of Biochemistry and Molecular Biology Urbino, September 14-16, 2015.**

List of publications

Fusco FA, Ronca R, Fiorentino G, Pedone E, Contursi P, Bartolucci S, Limauro D. ***Biochemical characterization of a thermostable endomannanase/endoglucanase from Dictyoglomus turgidum.*** Extremophiles. 2017 Nov 25. doi: 10.1007/s00792-017-0983-6.

Fusco FA, Fiorentino G, Contursi P, Bartolucci S, Limauro D. **Biochemical characterization of a thermostable β-glucosidase from *Dictyoglomus turgidum*.**
Manuscript in preparation

Aulitto M[1], **Fusco FA[1]**, Fiorentino G, Bartolucci S, Contursi P, Limauro D. **A synergistic action of a thermophilic α-galactosidase and β-mannanase on galactomannan substrates.**
[1]Martina Aulitto and Francesca Anna Fusco contributed equally to this work.
Submitted to Enzyme and Microbial Technology

Lanzilli M, Donadio G, **Fusco FA**, Limauro D, Ricca E, Isticato R. **Display of the peroxiredoxin Bcp1 of *Sulfolobus solfataricus* on probiotic spores of *Bacillus megaterium.***
Manuscript in preparation

Experience in foreingn laboratory

CONSEJO SUPERIOR
DE INVESTIGACIONES
CIENTÍFICAS
CSIC
UNIVERSIDAD AUTÓNOMA
DE MADRID
UAM
CENTRO DE BIOLOGÍA MOLECULAR
"SEVERO OCHOA"

December 15th, 2016

To whom it may concern,

This letter is to **certify** that Francesca Anna Fusco, Ph. D. student from the Università Degli Studi di Napoli Federico II (Naples, Italy) carried out experimental works in my laboratory at the Centro de Biología Molecular Severo Ochoa (Madrid) from September 15 to December 15, 2016. Her work in this priod was focussed on the recombinant expression in *Thermus thermophilus* of thermostable enzymes from heterologous origin in the framework her Ph. D. Thesis project.

Signed: José Berenguer
Professor of Microbiology